NOTICE

The quality of this microform is heavily dependent upon the quality of the original thesis submitted for microfilming. Every effort has been made to ensure the highest quality of reproduction possible.

If pages are missing, contact the university which granted the degree.

Some pages may have indistinct print especially if the original pages were typed with a poor typewriter ribbon or if the university sent us an inferior photocopy.

Reproduction in full or in part of this microform is governed by the Canadian Copyright Act, R.S.C. 1970, c. C-30, and subsequent amendments.

AVIS

La qualité de cette microforme dépend grandement de la qualité de la thèse soumise au microfilmage. Nous avons tout fait pour assurer une qualité supérieure de reproduction.

S'il manque des pages, veuillez communiquer avec l'université qui a conféré le grade.

La qualité d'impression de certaines pages peut laisser à désirer, surtout si les pages originales ont été dactylographiées à l'aide d'un ruban usé ou si l'université nous a fait parvenir une photocopie de qualité inférieure.

La reproduction, même partielle, de cette microforme est soumise à la Loi canadienne sur le droit d'auteur, SRC 1970, c. C-30, et ses amendements subséquents.

Canada

A Study of an Air-Conditioning Control System Using A Variable Speed Compressor and A Variable Speed Evaporator Fan

Zhao-Shu Zeng

A Thesis

in

The Department

of

Mechanical Engineering

Presented in Partial Fulfilment of the Requirements

for the Degree of Master of Applied Science at

Concordia University

Montreal, Quebec, Canada

June 1993

National Library
of Canada

Acquisitions and
Bibliographic Services Branch

395 Wellington Street
Ottawa, Ontario
K1A 0N4

Bibliothèque nationale
du Canada

Direction des acquisitions et
des services bibliographiques

395, rue Wellington
Ottawa (Ontario)
K1A 0N4

Your file Votre référence

Our file Notre référence

ISBN 0-315-87295-0

Canada

ABSTRACT

A Study of An Air-Conditioning Control System Using A Variable Speed Compressor and A Variable Speed Evaporator Fan

Zhao-Shu Zeng

Relative humidity and temperature are the two essential parameters to be controlled in air-conditioning practice. In this research, a Proportional-Integral-Derivative (PID) control system to simultaneously control space air temperature and space relative humidity was studied. This system employed two PID control loops. One loop controlled evaporator fan motor speed, which varied the evaporator air flow rate, in order to control space relative humidity. The other loop was utilized to control the compressor motor speed, thus varying the compressor volumetric displacement rate, in order to control space air temperature. The experimental results show the system maintained space temperature within ±0.5°F from its set-point value and space relative humidity within ±0.01 of its set-point value. The space sensible loads during the experiment is estimated to range from 7000 to 14000 BTU/hr. The space latent loads is estimated to range from 2200 to 5600

BTU/hr.

A numerical air-conditioning system model, which is derived from the Krakow and Lin [1986] heat pump model, was developed in this work. The model employed three-region evaporator model by Oskarsson et al. [1989]. The model was utilized to study the air-conditioning system performance characteristics and to create performance maps. The performance maps were utilized to determine the range of sensible and latent system capacities over which the system may be controlled by varying the evaporator air flow rate and compressor volumetric displacement rate.

ACKNOWLEDGEMENTS

The author wishes to express his gratitude and appreciation to his supervisors, Professor K. I. Krakow and Dr. S. Lin, for initiating this project and providing continued guidance and support throughout the research. Without their ideas, suggestion, encouraging guidance, and insight into the problem, this work would be impossible to be successfully concluded. This research was sponsored by NSERCC grant Numbers OGP0001656 and OGP0007929. The author would like to thank the sponsor.

The author would also like to express his indebtedness to his parents C. L. Zeng and S. Z. Deng, his wife Z. Zhu and his daughter Cheng, his cousin Mr. and Mrs. J. Chow, his brother Z. C. Zeng, and family and friends for their encouragement and support before and throughout the author's academical year.

TABLE OF CONTENTS

LIST OF FIGURES

CHAPTER 1

INTRODUCTION

The purpose of an air-conditioning system is to provide a specific set of environmental conditions to a space. A system is designed to satisfy the various space conditions required, whether it is for human comfort or for industrial processes. In order to provide complete air-conditioning, a year-round system must have the following functions: heating, cooling, dehumidification, humidification, ventilation, filtration, and air circulation. In many air-conditioning applications, an air-conditioning system often needs to provide only a few of the above seven functions.

This thesis reports on research done in a study of a controlling method of an air-conditioning system. The study is focused on the cooling and dehumidification functions only, but it is worth to consider that the methods which were used in this research may be expanded to other functions.

There are many methods to implement air-conditioning, such as the vapour compression refrigerating process and the absorption refrigeration system. The most common method in practice is the vapour compression refrigerating process. In this process, warm air is forced to pass though an evaporator coil where air is cooled by a low-temperature two-phase

refrigerant in the coil. If the evaporator surface temperature is lower than the air dew-point temperature, the air is dehumidified by the coil. The heat, which is transferred from warm air, changes the refrigerant from liquid to vapour. The compressor removes the low temperature and low pressure refrigerant vapour from the evaporator coil and discharges that vapour at a high temperature and high pressure to a condenser. In the condenser, the heat of the refrigerant is removed by a coolant, which often is water or air, causing the refrigerant to return to a liquid state at that high pressure. The high pressure liquid refrigerant passes through a throttling device and becomes a low pressure and low temperature two-phase, vapour plus liquid, state refrigerant. The refrigerant then passes into the evaporator to cool and to dehumidify warm air. After heat and mass are transferred, the lower temperature and lower humidity air is sent to the air conditioned space to balance heat and humidity load of the air conditioned space.

There are many types of air-conditioning systems, utilizing a diverse range of equipment, presently available. Each attempts to provide and control a specific set of environmental conditions to the air conditioned space with varying degrees of success. However, a recurring problem in air-conditioning installations is that not all the predetermined space conditions of an air-conditioning system are matched by actual system performance. This problem is a

very complicated one because many factors are interrelated to create the problem. Of all the factors, two have significant influence. The first factor is the performance of the equipment over the range of cooling loads of an air conditioned space. The second factor is the lack of precision control methods.

This thesis studies air-conditioning systems with respect to two objectives. The first is to determine the performance of the systems over a range of space cooling loads. The second one is to study air-conditioning control systems by using proportional-integral-derivative (PID) control methods. The output signal of a PID controller is a function of three terms. The first term is proportional to the error between a sensed value and a set point value. The second term is related to the sum of the error over a period of time. The third term is related to the time rate of change of the error.

In order to determine the performance of systems over a range of cooling loads, a numerical model of air-conditioning systems, which is derived from the Krakow and Lin [1987] heat pump model, has been developed. The model is based on the models of the system components: evaporator, condenser, compressor, expansion valve, and suction line heat exchangers. A component model is a series of equations that govern the component's performance. An air- conditioning system model is based on the component models and is then used to study and to predict the performance of the air-conditioning system over a

range of cooling loads. This is accomplished by 1), maintaining the space air temperature and the space air relative humidity constant with varying evaporator air flow rate and varying compressor volumetric displacement rate, and 2), by maintaining the evaporator air flow rate and the compressor volumetric displacement rate constant with varying space air temperature and varying space air relative humidity. In the system studied, the evaporator air flow rate was equal to space air flow rate. The evaporator air inlet temperature and relative humidity were equal to space air temperature and relative humidity respectively.

The evaporator model for the air-conditioning system, which is derived from the Oskarsson, Krakow and Lin [1989] "three-region" evaporator model. The model divides the evaporator coil into three regions based on their refrigerant states. The three regions are the two-phase region, the transition region, and the superheated region. Two evaporator coils were utilized for experimental research. The geometry of their construction varies with respect to rows, columns, fin density, face area, and circuit arrangement. The experimental results were then used to verify the evaporator model and the air conditioning system model. Based on the verifications, two sets of system performance maps, which were used to describe and predict an air-conditioning system performance over a range of cooling and dehumidifying loads, were developed.

In this thesis, an air-conditioning control system was

developed. The control system uses two PID control systems to control space conditions. The first PID control system uses space temperature as the signal to control compressor speed in order to control compressor volumetric displacement rate to maintain space temperature at its predetermined set point value. At the same time, the second PID control system uses space relative humidity as a signal to control evaporator fan speed in order to control space air flow rate so that the space relative humidity could remain at its predetermined set point value.

Traditionally an on-off method is utilized to control the compressor in order to control the space temperature. To control the space relative humidity, the conventional method is to cool the air to the desired specific humidity value and then reheat the air to the desired temperature.

The advantage of the developed dual PID control system is that this control system provides more precision and smooth operating conditions. It uses two PIDs to control both space temperature and space relative humidity. Because the space temperature and space relative humidity are two essential items to be controlled by any air conditioning system, this dual PID control system should be interesting to other researchers and designers in the air-conditioning field.

The result of this research has many applications in industrial processing. It can be applied to a space where both accurate temperature and relative humidity are required. Both

textile industry and paper industry processes require accurate temperature and relative humidity to maintain the high quality of their products. In the food industry, vegetable and fruits need to be stored in environments having accurate temperatures and relative humidities. These are a few of the possible applications of results presented in this research.

The conventional unit system (i.e., ft, lb_m, lb_f, and BTU) is utilized because the majority of literature on this subject in North America is still in this format. Refrigerant and psychrometric subroutines available make use of the conventional unit system. Instrumentation calibrations were done in conventional units. A conversion table is presented in the Appendix I to help the readers transfer conventional units into SI units.

CHAPTER 2

LITERATURE SURVEY

2.1 Introduction

This research project involves two major parts: 1) simulating air-conditioning system, and 2) controlling air-conditioning systems by using the proportional-integral-derivative (PID) method. There are two basic parts in the PID controlling system: the PID control method and an air conditioning system using PID control systems. Thus the survey of literature can be divided into three parts:

1) air-conditioning system simulation,
2) PID control theory, and
3) air-conditioning control systems using PID control methods.

Additional papers of interest are listed in the bibliography.

2.2 Air-conditioning system simulation

There is extensive documentation of research done on air-conditioning system simulation which utilize two basic approaches: first principle modelling and functional fit modelling. First principle modelling gives components and system detail but requires time consuming calculations. Most literature on simulations of air-conditioning or heat pump systems or components use first principle modelling.

Functional fit modelling uses experimental or catalog data to maintain accuracy. The work that was done in this research utilizes the first principle modelling method, so the literature surveyed in this project focuses on this method.

2.2.1 Krakow and Lin Heat Pump Model

Krakow and Lin [1987] did an analytical investigation of heat pump systems. In their research, the equations governing the performance of the heat pump components are solved simultaneously in order to get the steady-state performance characteristics of a heat pump. The steady-state performance characteristics of a heat pump are also determined by the equations of the state of the refrigerant, by the specified temperatures of the source and the sink, and by parameters specifying the capacities of the components. These steady-state performance characteristics are: the condition of the refrigerant at the key points in the heat pump, the heat transfer rates for the heat exchangers, the power input to the compressor, and the leaving temperatures of the source and sink fluids.

Krakow and Lin [1987] present a heat pump performance map by using a speed variable compressor. The performance map of a heat pump, which shows the performance characteristics for a range of source temperatures, may be determined by varying the parameters specifying the operating point. The compressor volumetric displacement rate may be varied by varying the

compressor speed. To determine the steady-state performance at an operating point, the compressor speed is constant; to determine the performance map, the compressor speed is a variable.

Krakow and Lin [1987] also present models of each component of the heat pump. Evaporator and condenser models were derived with the concept of heat exchanger effectiveness. The interchanger is modelled for dry and wet heat exchanger effectiveness. There are three types of throttling devices models. A superheat controlled expansion valve, a capillary tube, and an evaporation pressure controlled expansion valve, are considered and presented.

The model which was developed by Krakow and Lin [1987] has been validated with experiment data. The deviation between model predictions and experimental results are within a quite satisfactory range.

2.2.2 Oskarsson, Krakow and Lin Evaporator Simulation

Oskarsson, Krakow and Lin [1989] did research to simulate evaporators suitable for heat pump applications for operation with dry, wet, and frosted finned surfaces. In their research they developed three evaporator models, a parametric model, a finite element model, and a three regions model.

The three regions model divided the evaporator into three regions depending on the refrigerant state inside the evaporator. Those three regions are two-phase region,

transition region, and superheated region. The two-phase region is the region in which refrigerant quality ranges from that of the inlet state to 0.75. The refrigerant quality in the transition region is from 0.75 to 1.0. The superheated region extends from the point at which the refrigerant quality is from 1.0 to the evaporator outlet.

In this evaporator model, the number of rows are equal to the number of refrigerant circuits. The direction of air is normal to the direction of refrigerant. The evaporator was constructed as a multi-row coil.

In their research, the computer predictions of the three region model are compared with experimental data on the six row coil for dry and wet surface conditions. It has been found that the deviations between simulation results and experimental data for total cooling capacity are within 15%. Many of those deviations are within 10%.

2.2.3 Other Air-Conditioning System Simulation

Hamilton and Miller [1990] presented a method of modelling an air-conditioning system. In their simulation, they use functional fits of individual component manufactures' catalog data along with thermodynamic relationships to mathematically model the air-conditioning system. They consider that each component in an air-conditioning system consists of an energy balance and a mass balance at steady-state conditions. In the modelling, each component

mathematical model has been individually constructed. The air-conditioning system model then uses continuity of mass and energy flow at each component.

Cecchini and Marchal [1991] developed a simulation model of refrigerating and air-conditioning systems. The simulation aims at characterizing systems with a limited number of parameters deduced from experimental data. The system includes a compressor, a condenser, an evaporator, and a thermostatic expansion valve. The simulation has been divided into two steps. The first step uses equations to describe the thermodynamic cycle of the refrigerant. Then heat transfer rates at the evaporator and at the condenser were simulated. Cecchini and Marchal [1991] also give a comparison between computed results and experimental data. The validation shows the uncertainty of the performances is about ±5% for water heat-source equipment ranging between 5kW and 20kW heat output. The uncertainty of the capacity for air-to-air conditioners, ranging between 2kW and 12kW, is about ±10%.

2.3 Proportional-Integral-Derivative (PID) Control Methods

Ziegler and Nichols [1942] give the guidelines for digital control. In their research, they first discussed the three simple control effects: proportional, integral, and derivative responses. The proportional response gives a movement of the controlling object proportional to the controlling signal. The integral response is used to clean up

offsets. It detects deviations between the signal and the set point and then gives a slow and continuous movement of the controlling object to correct the offset. The derivative response provides an additional controlling object movement proportional to the rate of the signal movement. Ziegler and Nichols [1942] discussed the tuning method to get optimum controller settings in the research. They discovered that the proper tuning for proportional control is to let the sensitivity or "throttling range" equal to 25 percent of "amplitude ratio" or "peak overshoots". The procedure they recommended is to measure the response of a signal to a step-change in control input, and plot the response of the process variable, as a function of time.

Goff [1966] investigated a direct digital control (DDC) and a control algorithm. The control algorithm consists of three parts, the proportional part, the integral part, and derivative part. The paper discusses the outputting operation of the control system. Goff [1966] studied the actuation methods and concluded that the full speed actuation method offers the minimum delay in the control loop for a given actuator speed which is the preferred approach. Goff [1966] also pointed out that the ratio of the process delay time over the process time constant is the key in order to control the control loop. The smaller this ratio is, the easier the control loop can be adjusted.

Fertik and Ross [1967] studied direct digital control.

The study focused on the design and application of the DDC algorithm. In the research, they studied the PI and PID controlling method and noticed that when the derivative term is added to proportional-integral terms, computation and memory will increase. Due to this reason PID control equations should be examined by frequency response analysis and simulation in order to have the derivative term effectively differentiate at lower sample frequencies. The derivative term is filtered to reduce the sensitivity of the derivative action and the noise attenuation. Determining the control sample period depends on the knowledge of the process characteristics and the control parameters of an analog controller. The paper defines and suggests solutions of the PID control problem which is the windup problem. The possible causes of the windup problem are the control algorithm being used, the feedback from the actuator, and the economic considerations so the computation time and memory requirements may not be suitable. Fertik and Ross [1967] point out that the actuator speed selection is important due to the fact that the inability of the actuator to respond to the output demands of the control equation causes the controller windup. The inability of the response happens when large, fast disturbances occur, causing the controller information to be lost which results in a windup response. The actuator speed can be decided for an individual application by the process dynamics and the control equation and the nature and magnitude of the disturbance.

2.4 Air-Conditioning System Control

ASHRAE [1991] and Stoecker et al. [1989] present general theory of automatic control of air-conditioning systems. The PID control method is among the control methods discussed. Most air-conditioning system controller use only the PI control method because the PID controller is harder to tune than the PI controller and the derivative term is more sensitive to noisy signals.

2.4.1 Part-Load Performance of Air-Conditioning System

Howell, Ganesh and Sauer [1987] made a comparison of two control techniques to simulate part-load performance of an air-conditioning system. These two control strategies are: (1) adjusting the chilled water flow rate and (2) varying the percentage of bypass air. There are also two ways to operate the bypass control system: the room air bypass method and mixed-air method (return and outside mixed air). In earlier research, Howell [1986] studied these two types of bypass control systems and noticed the problem that the relative humidity deviates from the design condition in certain situations. During the study made by Howell et al. [1987], conditions of the air leaving the cooling coil are fixed. Changing the percentage of bypass air will result in a change in the room's relative humidity. Howell et al. [1987] found that when the design sensible load is reduced and design latent load remains unchanged, the mixed air bypass control

system is better than a chilled-water control system to maintain the room's relative humidity. The results also show that the chilled-water control system consumes less energy at part-load operation of the coil than bypass air control.

Shaw and Luxton [1988] studied the part-load air-conditioning variable air volume (VAV) system performance. The system uses three series connected chilled water coil to cool and to dehumidify the air passing through the coil. Three valves, which were parallel connected, were used to control the coolant flow rate. At the peak load working condition, the three coils are all in active. There are two coils in active when works at the 60 per cent of the peak load condition. There is only one coil active when systems operates works at 40 per cent peak loads. A low face velocity VAV system was used in the research. In order to lower the face velocity when maintaining the same mass flow rate of the air through the coil, the coil depth was reduced and the coil face area was increased. The conditions (dry and wet bulb temperatures) of leaving air from the air handle unit are varied when varying the system cooling load during the research. The results show that both space temperature and relative humidity were kept unchanged for 100%, 60%, and 40% peak load.

2.4.2 Air-Conditioning System Control Using the Proportional-Integral Method

Nesler and Stoecker [1984] studied the proportional-

integral (PI) control of discharge air temperature. In their previous research, Stoecker et al. [1978] developed a heating coil discharge air temperature control system model in order to match the experimental results. The method is to use the simplest models for the components and then compare the results with the experimental data to make the necessary adjustment.

Based on the work of Stoecker et al. [1978], Nesler and Stoecker [1984] built a PI control system to control the discharge air temperature. The system uses hot water coil to transfer heating loads to air, a centrifugal fan to force air though coil, and pneumatic three-way bypass valves to adjust water flow rate. In the research the coil inlet air temperature, which is room temperature, the inlet water temperature, and the inlet air flow rate were kept constant. In the controlling system four temperature transducers were used to sense the discharge air temperature, a computer was programmed to be used as controller, and an electric-to-pneumatic transducer was used as an actuator to control system hot water flow rate. During the research, proportional control and proportional-integral control were studied. The proportional controller output control signal equals the deviation from a set point multiplied by the proportional gain constant and added to the integral mode. The integral mode sums the error over time and adds the result to the output. Nesler and Stoecker [1984] discussed the tuning of

proportional and PI controller problems. The aim of tuning proportional controller is to achieve the Ziegler-Nichols' quarter-wave damped response. Quarter-wave damping refers to settings which have a ratio of 1:4 as the successive peak overshoots or undershoots. The proportional term of a PI controller is used to determine the desired transient response of the controller and the integral term of the PI controller is used to centre that response at the set point.

May, Borresen and Hurley [1982] did research using a proportional-integral controlling system to control the leaving air temperature of a large air handling unit. A temperature transducer was used as a sensor to monitor the leaving air temperature from the air handling unit. The transducer output was proportional to air leaving temperature changes. A microcomputer was used to as the controller to process the data collected from transducers and to send controlling commands to actuate valve of chill water. The air handling unit consist of three fluid-to-air heat exchanger coils, two of which use steam to heat air, and the third one uses chill water to cool air. The air discharge temperature is controlled by controlling a cooling water valve position which varied the cooling water flow rate. During the research the system air flow rate and the temperature of the chilled water which is supplied to the air handle unit are kept constant. The air discharge temperature is successfully controlled by the PI controlling loop.

Shavit and Brandt [1982] modeled and analyzed the dynamic performance of a discharge air temperature system with proportional and proportional-integral (PI) controller methods. The system consisted of a hot water coil to heat air, a sensor in the downstream side of the coil to sense coil discharge temperature, a controller to analyze the sensed value from the sensor and to send controlling commands, and a valve acting as an actuator.

Four ordinary differential equations and a set of algebraic relations describing the static behaviour of the system's components were developed to build their system's mathematical model to simulate the sensor, the actuator, the controller, and the heating coil. The proportional gain, K_p, is a function of the static characteristics of the controlling system, which can be determined from the maximum range of the output and the maximum deviation signal. The integral gain, K_I, is a function of the dynamic characteristics of the controller system, which can be determined by the maximum rate of change of the controller output and the corresponding deviation signal. The static response of the coil is a function of the water flow rate while the dynamic response of the coil is a function of the air temperature leaving the coil.

Shavit and Brandt [1982] discovered that when the throttling range is at its maximum values, the proportional controller is in its most stable operating condition but has the largest deviation from its set point. Also when the

optimum integral gain is used, the response of the system with a PI controller is similar to the response with a proportional controller.

Spitler et al. [1986] presented a comparison of the fan power consumption between constant air volume system and variable air volume (VAV) system. In the constant air volume system, a proportional-integral (PI) controller is used to control the cold-deck temperature at a constant value. In the VAV system, the proportional-integral (PI) control methods were used to control the fan motor speed in order to vary air flow rate and to control the cold-deck temperature at a constant value. The results indicate that approximately 18% fan power consumption can be saved by varying fan motor speed instead of constant volume method. The range varied from 16% to 49% for the different buildings analyzed. The higher savings occurred for the buildings in which the load varied more.

Brothers and Warren [1986] present a quantitative analysis of fan energy consumption for variable air volume air-conditioning systems. Two kinds of comparisons are presented in their study. The first kind is to compare the energy consumption of the following flow control techniques: system dampers, inlet vanes, and variable speed motors. The study shows the significant savings by utilizing variable speed motors. The average energy saving is 36% compared to inlet vane control. The average energy saving is even more

compared with system dampers control. By using the variable speed motor, the minimum air flow rate can be reduced to about 25 percent of full flow compare with 40% to 50% by using other two flow control techniques. The second comparison is between proportional control and proportional-integral control methods. Brothers and Warren [1986] find significantly less energy was used under PI control than under P control and ranged from 15% to 50% with different location.

2.4.3 Tuning Method for PID Controller

A number of papers introduced the tuning methods for the PID controllers. There are two kinds of tuning methods, the self tuning method and trial-and-error process, available. The self tuning process is a complex one and involves complex mathematics to model the process. Because these reasons, the self tuning process was not used in the research.

Nesler and Stoecker [1984], Nesler [1986], and Stoecker and Stoecker [1989] suggested a trial-and-error tuning process of PI and PID controller to control heating, ventilation, and air-conditioning system. This method first sets the controller to the proportional-only controller in order to determine the proportional gain. The proportional gain should be adjusted until the controlled parameter reaches a slight overshoot steady state operating condition. The next step is to set the controller as a PI or PID controller to determine the integral gain and derivative gain. The integral gain and the

derivative gain should be adjusted until the controller has a same response as proportional-only control, but with the response centred at the set point.

CHAPTER 3

AIR-CONDITIONING SYSTEM MODELLING

3.1 Air-Conditioning System Model

The air-conditioning system model, which was derived from the Krakow and Lin [1987] heat pump model, predicts the steady state performance of conventional vapour compression electrically driven air-conditioning systems. The steady-state performance characteristics of the air-conditioning system are determined by the following three sections:

1. by the simultaneous solution of the equations governing the performance of the components of the air-conditioning system for specified temperatures and relative humidity of the source and temperature of the sink,
2. by the equation of the state of the refrigerant, and
3. by the parameters for each component which specify its capacity.

The model is based on the Krakow and Lin [1987] heat pump model, with the following changes:

1. In the Krakow and Lin [1987] heat pump model, the evaporator was modelled by using the concept of heat exchanger effectiveness to determine the heat

transfer rate of the evaporator. The evaporator model of the heat pump model assumes dry air passing though coil. In the present research, the three region model by Oskarsson, Krakow, and Lin [1989] is used to simulate the evaporator. The evaporator model of the present air-conditioning system model assumes the coil works with moist air as well as dry air and operates at dehumidifying conditions.

2. The Krakow and Lin [1987] heat pump model was restructured by deleting the reversing valve portion from the model in order to use the model only for the air-conditioning application.
3. In the Krakow and Lin [1987] heat pump model, three kinds of throttling device models are discussed. In this study, only the expansion valve is used.

The model, which is used in this research, is based on the components of the air-conditioning system. The approach used here is to mathematically model each component and then combine these individual models to form an air-conditioning system model.

The air-conditioning system configuration used in this study is shown schematically in Figure 3.1. The system consists of an air source evaporator, a compressor, a water cooled condenser, a thermostatic expansion valve, and two interchangers (suction line liquid sub-cooling heat

exchangers). A water valve was used to control the condensing pressure. Because the air-conditioning system cannot be formulated as a set of linear simultaneous equations, the solution of the system has to be determined by using an algorithm involving an iteration method. Figure 3.2 is the pressure-enthalpy diagram of the air-conditioning system. Both Figure 3.1 and Figure 3.2 show the key points of the air-conditioning system.

In the superheated region are points 3, 4 and 5. State point 3 is between the two interchangers where the refrigerant is on the low pressure side. State point 4 is between the second interchanger refrigerant outlet at low pressure side and the compressor inlet. State point 5 is between the compressor outlet and the condenser refrigerant inlet. The compression process from state 4 to state 5 is non-isentropic.

In the subcooled region are points 6, 7, 8, and 9. State 6 is between the condenser refrigerant outlet and the receiver inlet. State 7 is between the receiver refrigerant outlet and the second interchanger inlet at high pressure side. State 8 is between two interchangers where the refrigerant is on the high pressure side. State 9 is between the first interchanger refrigerant outlet at high pressure side and the expansion valve inlet.

At state point 1, which is between the expansion valve refrigerant outlet and the evaporator inlet, the refrigerant is generally in a two-phase region. The refrigerant state at

point 2, between the evaporator refrigerant outlet and the first interchanger inlet at low pressure side, may be in superheat region, or in two-phase saturated region depend on system operating conditions. Finally, the process from state 9 to state 1 through the expansion valve is assumed to be an adiabatic and constant enthalpy device.

The steady state performance characteristics to be determined include the condition of the refrigerant at the key points in the air-conditioning system. These performance characteristics are the heat transfer rates of heat exchangers (including evaporator, condenser, and suction line heat exchangers), the power input to the compressor motor and fan motor, the leaving temperature and relative humidity of the source, and the leaving temperature and flow rate of the sink fluid. The basic air-conditioning system model determines the performance characteristics for an operating point, which is specified by the temperature and relative humidity of the source and the temperature of the sink, compressor displacement rate, source air flow rate.

The evaporator model used in this study was derived from the Oskarsson, Krakow and Lin [1989] evaporator model. The present model calculates the heat transfer rate based on the rates from the three flow regions in the heat exchanger. These three regions are the two-phase region, the transition region, and the superheated region. The average temperature of the outlet air is the weighted average of the temperature of the

air exiting each region. The amount of air dehumidification is determined independently in each region.

The models of condenser and interchangers use the concept of heat exchanger effectiveness (which is the ratio of the actual heat transfer rate to the maximum possible heat transfer rate) to determine the heat transfer rate. The heat exchanger effectiveness, which depends on the type of heat exchanger and flow patten, is a function of the number of heat transfer units.

The refrigeration property subroutines used for the system model are based on those developed by Kartsonnes and Erth [1971]. The psychrometric property subroutines are based on ASHRAE Fundamentals [1989].

The input data required to build the air-conditioning system model are:

- type of the refrigerant,
- source and sink fluids (air and/or water),
- source conditions (temperature and relative humidity),
- source flow rate,
- sink temperature,
- component capacities, geometric efficiencies, and
- condensing pressure control set point or sink flow rate.

3.1.1 Evaporator Model

The evaporator model discussed here uses a three-region model which was derived from the Oskarsson, Krakow and Lin [1989] evaporator model. The three following changes have been made in order to use the Oskarsson et al. [1989] model for this research.

1. The model was shortened by deleting the frosting part in order to use the model in the air-conditioning application.
2. In the Oskarsson et.al. [1989] evaporator model, the number of the rows are equal to the number of refrigerant circuits. The evaporator model is formulated for multi-row coils which assumed that each row is one refrigerant circuit. A multi-row coil is a cross-flow heat exchanger where the direction of air is normal to the direction of the refrigerant. In this research, the use range of their model is extended to a number of rows which are not only equal to but also greater than the number of refrigerant circuits.
3. In the Oskarsson et.al. [1989] evaporator model, all rows from every circuits were "lumped" together to formulate the evaporator. In this thesis the evaporator model was constructed by two methods. The first one uses the above "lumped" together formulating method. The second one divides the

evaporator into coil sections, according to numbers of circuits, and then calculates the overall evaporator performance as a series of individual coil sections.

The model considers that the evaporator coil can be divided into three regions, depending on the refrigerant state in the coil. The three regions are the two-phase region, the transition region, and the superheated region.

The two-phase region is the region from the refrigerant inlet state of the evaporator until the refrigerant quality equals a selected value, e.g., 0.75. The transition region is the region at which refrigerant quality ranges from that selected value to 1.0. The superheated region extends from a state at which the refrigerant quality is 1.0 to the outlet plane.

In the transition region the heat transfer coefficient is different from the two-phase region. The inlet point of refrigerant of the transition region is variable for a particular evaporator. The outlet point of refrigerant of the transition region is saturated leaving condition. The transition region is added in the model instead of only having a two region model. The reason for using transition region is due to the fact that the equation which is used to calculate heat transfer coefficient for the two-phase region is not applicable when refrigerant qualities are high. The refrigerant heat transfer coefficient in the transition region

is proportional between the coefficient for a quality of 0.75 and the heat transfer coefficient for the vapour refrigerant according to quality. In the three-region model, the air leaving condition and the percentage area of each region which is required.

The following are the assumptions for simulating the model.

1. There is no pressure drop on the refrigerant side.
2. There is a constant air mass flux along the face of the coil.
3. In the superheated region, the coil is dry.
4. A fouling conductance applies on inside tube only.

In the two-phase region and the transition region there is condensation on the air side. The heat transfer rate in the two-phase region and the transition region are described as functions of the air temperature, the refrigerant temperature and overall heat transfer coefficient which can be written as the following:

$$q_{WR} = U \cdot A \cdot \Delta T_{WR} \qquad (3.1)$$

where **U** is the overall heat transfer coefficient, **A** is the area, and ΔT is the temperature difference between air and refrigerant.

The procedure for determine heat transfer coefficients for condensing moisture (required to evaluate U) and the procedure for determining the latent heat transfer from the air and the amount of condensation are detailed in Oskarsson

et al. [1989].

In the superheated region there is no condensation on the air side. The superheated region is analyzed by using the ε-NTU method which was suggested by Kays and London [1984] for the cross-flow heat exchangers. The coil heat exchanger effectiveness, ε, is a function of the number of transfer units (NTU),

$$\varepsilon = f\left(NTU, \left(\frac{C_{min}}{C_{max}} \right) \right) \tag{3.2}$$

where **NTU** is defined as follows:

$$NTU = \frac{U \bullet A}{C_{min}} \tag{3.3}$$

C_{min} is the smaller value of heat capacity rate of the hot and cold fluid. When one fluid is a refrigerant, this smaller value of heat capacity rate is the heat capacity rate value of the other fluid. For air to refrigerant heat transfer, the smaller value of heat capacity rate is the air heat capacity rate value.

The heat transferred to the superheated region is a function of the heat exchanger effectiveness and the inlet temperature difference between the air and refrigerant.

$$q_{SR} = \varepsilon \bullet C_{min} \bullet \Delta T_{SR} \tag{3.4}$$

The leaving condition of air from evaporator is then calculated by mixing the air leaving conditions from the above

three region.

The detail calculation steps for the evaporator can be found in the Oskarsson, Krakow and Lin [1989] evaporator model.

The specified data for the evaporator model are:

- the geometric parameters of the evaporator,
- the inlet refrigerant condition, temperature, pressure and quality,
- the inlet air temperature and relative humidity,
- the air flow rate,
- the refrigerant flow rate, and
- the option of the calculation method: lumped or divided into sections.

The evaporator model is used to calculate:

- the total heat transfer rate,
- the sensible heat factor (SHF_{ev}),
- the outlet refrigerant conditions, and
- the outlet air temperature and relative humidity.

3.1.2 Condenser Model

The following equations relate the condenser heat transfer rate to the sink from the refrigerant. The heat capacity rate of the sink is the limiting factor to determine maximum heat transfer rate. The heat transfer rate from the

refrigerant to the sink is described as a function of the heat exchanger effectiveness, the heat capacity rate of the sink, the condensation temperature of the refrigerant, and the inlet temperature of the sink. The condenser performance is represented as:

$$Q_{cd} = \varepsilon_{cd} \cdot C_{snk,1} \cdot (T_c - T_{snk,1}) \tag{3.5}$$

where

$$\varepsilon_{cd} = \frac{T_{snk,2} - T_{snk,1}}{T_c - T_{snk,1}} \tag{3.6}$$

and

$$C_{snk} = C_{p,snk} \cdot \dot{m}_{snk} \tag{3.7}$$

The condenser heat exchanger effectiveness is a weak function of the refrigerant mass flow rate at a constant sink flow rate situation, i.e.,

$$\varepsilon_{cd} = \varepsilon_{c0} + \varepsilon_{c1} \cdot \frac{\dot{m}_r - \dot{m}_{r,0}}{\dot{m}_{r,0}} \tag{3.8}$$

The following specified values are required to determine the capacity of the condenser.

- the sink (water) inlet temperature,
- the heat capacity rate of the sink, and
- the condenser heat exchanger effectiveness coefficients.

The model is used to calculate:

- the sink outlet temperature, and

- condenser heat transfer rate.

3.1.3 Compressor Model

In this study, a reciprocating compressor is utilized in the air-conditioning system modelling. The ideal volumetric efficiency of the compressor is a function of the ratio of the inlet to outlet specific volumes and the clearance volume fraction, i.e.

$$e_{v,i} = 1 + c - c \cdot \frac{v_4}{v_5} \tag{3.9}$$

In the real situation the actual volumetric efficiency is less than the ideal volumetric efficiency because the effect of the pressure losses in the intake and discharge valves of the compressor, the re-expansion of the vapour in the clearance volume, and the heating of the vapour during the intake stroke,

$$e_{v,a} = r \cdot e_{v,i} \tag{3.10}$$

The mass flow rate of the compressor can be described as a function of the actual volumetric efficiency of the compressor, the specific volume at the compressor inlet, and the compressor volume displacement rate,

$$\dot{m}_r = e_{v,a} \cdot \frac{D}{v_4} \tag{3.11}$$

The isentropic efficiency of the compressor is defined by the

following equation,

$$e_i = \frac{h_s - h_4}{h_5 - h_4} \qquad (3.12)$$

The following specified data are required for the compressor model:

- the volume displacement rate of the compressor,
- the clearance volume fraction of the compressor,
- the isentropic efficiency of the compressor,
- the ratio of actual to ideal volume efficiency,
- the inlet refrigerant temperature and pressure, and
- the outlet refrigerant pressure.

The compressor model is used to calculate the following parameters:

- the refrigerant flow rate,
- the refrigerant outlet temperature, and
- the compressor thermodynamic power.

3.1.4 Expansion Valve

A conventional thermostatic expansion valve is used in the study. The valve controls the amount of superheat at the point between the two suction line liquid subcooling heat exchangers (the interchangers). The required input for the

superheat controlled expansion valve is:

- degrees of superheat.

3.1.5 Interchangers

There are two interchangers in the air-conditioning system model. At the second interchanger, the suction gas entering the heat exchanger is always dry. The heat exchanger effectiveness of the second interchanger is based on the heat capacity rate to the suction gas due to the fact that the heat capacity rate of the suction gas is less than the heat capacity rate of the liquid. The heat exchanger effectiveness of the second interchanger can be expressed as the following:

$$\varepsilon_{he2,d} = \frac{T_4 - T_3}{T_7 - T_3} \tag{3.13}$$

The gas entering the first interchanger may be dry or wet. If it is dry, the heat exchanger effectiveness of the first interchanger is:

$$\varepsilon_{he1,d} = \frac{T_3 - T_2}{T_8 - T_2} \tag{3.14}$$

If the suction gas entering the first interchanger is wet, the heat exchanger effectiveness for the first interchanger is based on the heat capacity rate to the liquid because the heat capacity of the liquid is less than that of the suction line gas. For wet refrigerant entering the heat transfer effectiveness of the first interchanger is:

$$\varepsilon_{hel,w} = \frac{T_8 - T_9}{T_8 - T_2} \tag{3.15}$$

The input values of the two suction line liquid subcooling heat exchangers model are:

- the heat exchanger effectiveness of the first interchanger at the dry condition,
- the heat exchanger effectiveness of the first interchanger at the wet condition, and
- the heat exchanger effectiveness of the second interchanger at the dry condition.

Point 3 is determined by the expansion valve. Point 7 is determined by the fact that the refrigerant leaving the receiver is saturated liquid. The interchanger model is used to determine the conditions of the following points 2, 4, 8, and 9, shown on Figure 3.1 and Figure 3.2.

3.2 Thermodynamic Cycle Analysis

The thermodynamic cycle analysis determines the refrigerant condition at all the key points. By using these key points refrigerant conditions, the heat transfer per unit mass for the evaporator is calculated as:

$$q_{ev} = h_2 - h_1 \tag{3.16}$$

the heat transfer per unit mass for the condenser is:

$$q_{cd} = h_5 - h_6 \tag{3.17}$$

the heat transfer per unit mass for the first interchanger is:

$$q_{he1} = h_3 - h_2 = h_8 - h_9 \tag{3.18}$$

the heat transfer per unit mass for the second interchanger is:

$$q_{he2} = h_4 - h_3 = h_7 - h_8 \tag{3.19}$$

and the compressor work per mass is:

$$w_{cp} = h_5 - h_4 \tag{3.20}$$

The heat capacities based on the refrigerant side analysis are:

for the evaporator,

$$Q_{ev} = \dot{m}_r \bullet q_{ev} \tag{3.21}$$

for the condenser,

$$Q_{cd} = \dot{m}_r \bullet q_{cd} \tag{3.22}$$

for the first interchanger,

$$Q_{he1} = \dot{m}_r \bullet q_{he1} \tag{3.23}$$

for the second interchanger,

$$Q_{he2} = \dot{m}_r \bullet q_{he2} \tag{3.24}$$

and for the compressor power,

$$W_{cp} = \dot{m}_r \bullet w_{cp} \tag{3.25}$$

3.3 Air-Conditioning System Performance

The following equations represent the air-conditioning

system performance.

The system net total cooling capacity is:

$$Q_{total,net} = Q_{ev} - W_{FM} \tag{3.26}$$

The net sensible cooling capacity is:

$$Q_{sen,net} = Q_{ev} \cdot SHF_{ev} - W_{FM} \tag{3.27}$$

The latent cooling capacity is:

$$Q_{lat} = Q_{total,net} - Q_{sen,net} \tag{3.28}$$

The system energy consumption is:

$$W_{ET} = W_{CM} + W_{FM} \tag{3.29}$$

W_{CM} is compressor motor power consumption, and W_{FM} is evaporator fan motor power consumption. W_{FM} is calculated according to fan law:

$$W_{FM} = W_{FM,0} \cdot \left(\frac{CFM}{CFM_0}\right)^3 \tag{3.30}$$

CFM is the actual air flow rate, CFM_0 is the reference air flow rate, and the $W_{FM,0}$ is the evaporator fan motor power consumption at CFM_0.

The compressor power consumption is:

$$W_{CM} = \frac{W_{cp}}{e_E} \tag{3.31}$$

where, e_E is compressor motor electrical efficiency.

The coefficient of performance of the air-conditioning system is:

$$COP = \frac{Q_{total}}{W_{ET}} \tag{3.32}$$

3.4 Solution Algorithm

A brief outline of computer program solution algorithm is as follows.

step 1 Initialize the parameters: geometric dimensions, source conditions T_{src} and RH_{src}, sink temperature, compressor volumetric displacement rate **CFH**, and source flow rate **CFM**.

step 2 Assume an evaporating temperature (T_e) and a condensing temperature (T_c).

step 3 Solve the refrigerant thermodynamic cycle for T_e and T_c to determine temperature, pressure, and enthalpy values at all key points.

step 4 Calculate the system refrigerant flow rate $\dot{m}_r$ from the compressor model.

step 5 Calculate the evaporator total cooling capacity based on refrigerant side.

step 6 Calculate the evaporator total cooling capacity, sensible cooling capacity, latent cooling capacity, sensible heat factor, and air leaving condition from the evaporator model.

step 7 Calculate the condenser heat transfer capacity from refrigerant side and then substitute this value into condenser model to calculate condensing temperature T_c.

step 8 Compare the evaporator total cooling capacity result from refrigerant side with the result from evaporator model. If the capacities are not within an acceptable tolerance, assume new value of T_c, and T_c and then go back to step 2 to start a new calculation. If the capacities are within an acceptable tolerance, go to next step to continue calculation.

step 9 Compare the calculated T_c with assumed T_c. If the condensing temperatures T_c are not within an acceptable tolerance, go back to step 2 by using T_c calculated in step 7 to start a new cycle of calculation. If the condensing temperatures T_c are within an acceptable tolerance, then go to next step.

step 10 Output the required parameters as $Q_{sen,net}$, Q_{lat}, leaving air temperature and relative humidity.

Computer program listing for the air conditioning system model and sample outputs are presented in the Appendix II, and III. The computer utilities used consisted of subroutines for refrigerant properties, heat transfer coefficients, and air properties. The refrigerant property subroutines are based on Kartsonnes and Erth [1971]. The heat transfer coefficient subroutines are by Oskarsson [1988]. The subroutines for air properties, based on ASHRAE [1989] data, were written by Professor Krakow and are unpublished. Listings of the code for these subroutines are in Oskarsson [1988].

3.5 Nomenclature

A	area
c	compressor clearance volume ratio
$c_{p,snk}$	specific heat of sink
C_{max}	maximum fluid heat capacity rate
C_{min}	minimum fluid heat capacity rate
C_{snk}	heat capacity rate of sink
CFH	compressor volumetric displacement rate
CFH_0	reference compressor volumetric displacement rate
CFM	evaporator air flow rate
CFM_0	reference evaporator air flow rate
COP	coefficient of performance
D	compressor volume displacement rate
e_E	compressor motor electrical efficiency
e_i	isentropic efficiency

$e_{v,a}$	actual volumetric efficiency
$e_{v,i}$	ideal volumetric efficiency
h	enthalpy at key point
h_s	enthalpy of refrigerant at compressor outlet for isentropic compression
$\dot{m}_r$	system refrigerant mass flow rate
$\dot{m}_{r,0}$	system refrigerant mass flow rate; reference value
$\dot{m}_{snk}$	sink mass flow rate
NTU	number of transfer units
q_{cd}	condenser heat transfer per unit mass of refrigerant
q_{ev}	evaporator heat transfer per unit mass of refrigerant
q_{hc1}	first interchanger heat transfer per unit mass of refrigerant
q_{hc2}	second interchanger heat transfer per unit mass of refrigerant
q_{SR}	heat transfer per unit mass of refrigerant in the two-phase and transition region
q_{WR}	heat transfer per unit mass of refrigerant in the superheated region
Q	heat transfer rate
Q_{cd}	condenser heat transfer rate
Q_{ev}	evaporator heat transfer rate
Q_{hc1}	first interchanger heat transfer rate
Q_{hc2}	second interchanger heat transfer rate

Q_{lat} latent cooling capacity

$Q_{scn,net}$ net sensible cooling capacity

$Q_{total,net}$ system net total cooling capacity

r ratio of actual to ideal volumetric efficiency

RH_{src} inlet air relative humidity

SHF_{ev} evaporator sensible heat factor

T refrigerant temperature at key point

T_c condensing temperature

T_e evaporating temperature

T_{src} inlet air temperature

$T_{snk,1}$ temperature of sink entering the condenser

$T_{snk,2}$ temperature of sink leaving the condenser

U overall heat transfer coefficient

v specific volume

W_{cp} compressor thermodynamic power

W_{CM} compressor power consumption

W_{FM} fan motor power consumption

$W_{FM,0}$ fan motor power consumption at CFM_0

W_{ET} total system energy consumption

ΔT temperature difference

ϵ coil heat exchanger effectiveness

ϵ_{cd} condenser heat exchanger effectiveness

ϵ_{c0} condenser heat exchanger effectiveness at $\dot{m}_{r,0}$

ϵ_{c1} condenser heat exchanger effectiveness coefficient

$\epsilon_{hc1,d}$ first interchanger heat exchanger effectiveness coefficient at dry condition

$\epsilon_{hc2,d}$ second interchanger heat exchanger effectiveness coefficient at dry condition

$\epsilon_{hc1,w}$ first interchanger heat exchanger effectiveness coefficient at wet condition

Subscripts

1 to 9 key points, see Figure 3.1 and 3.2

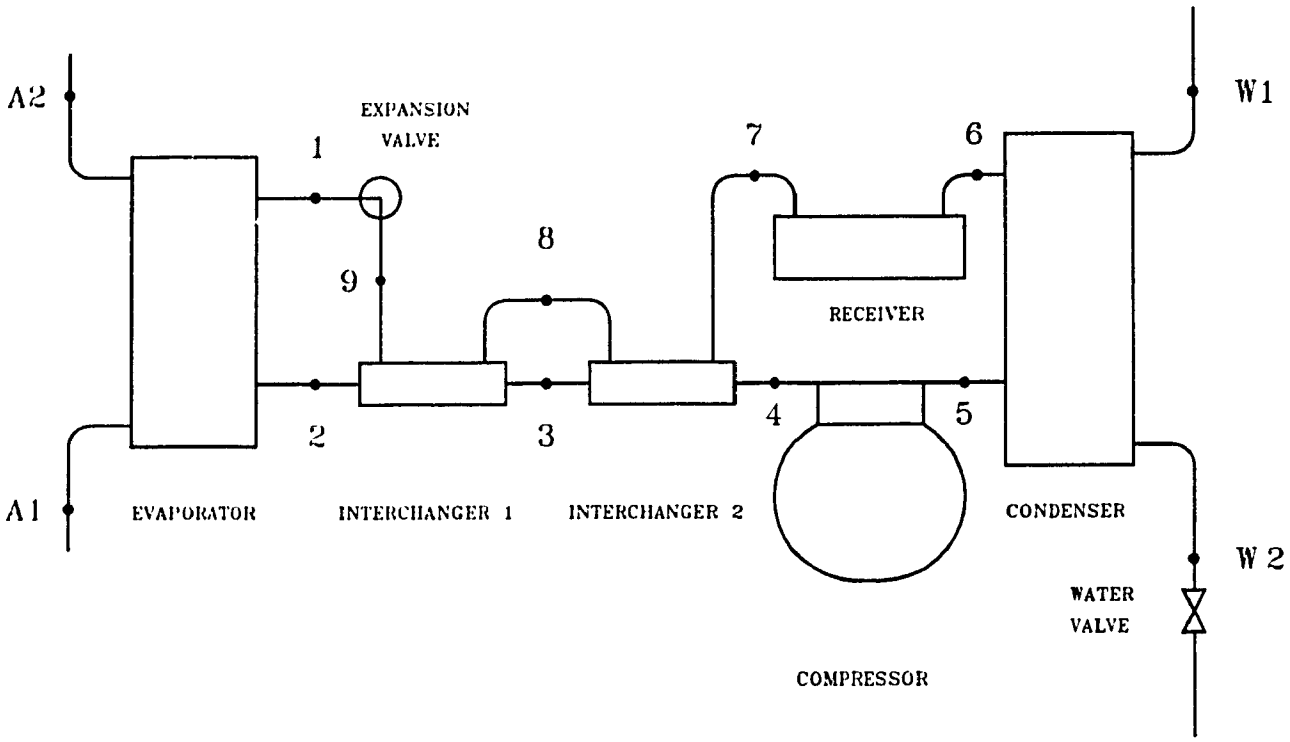

Figure 3.1. Air-conditioning system.

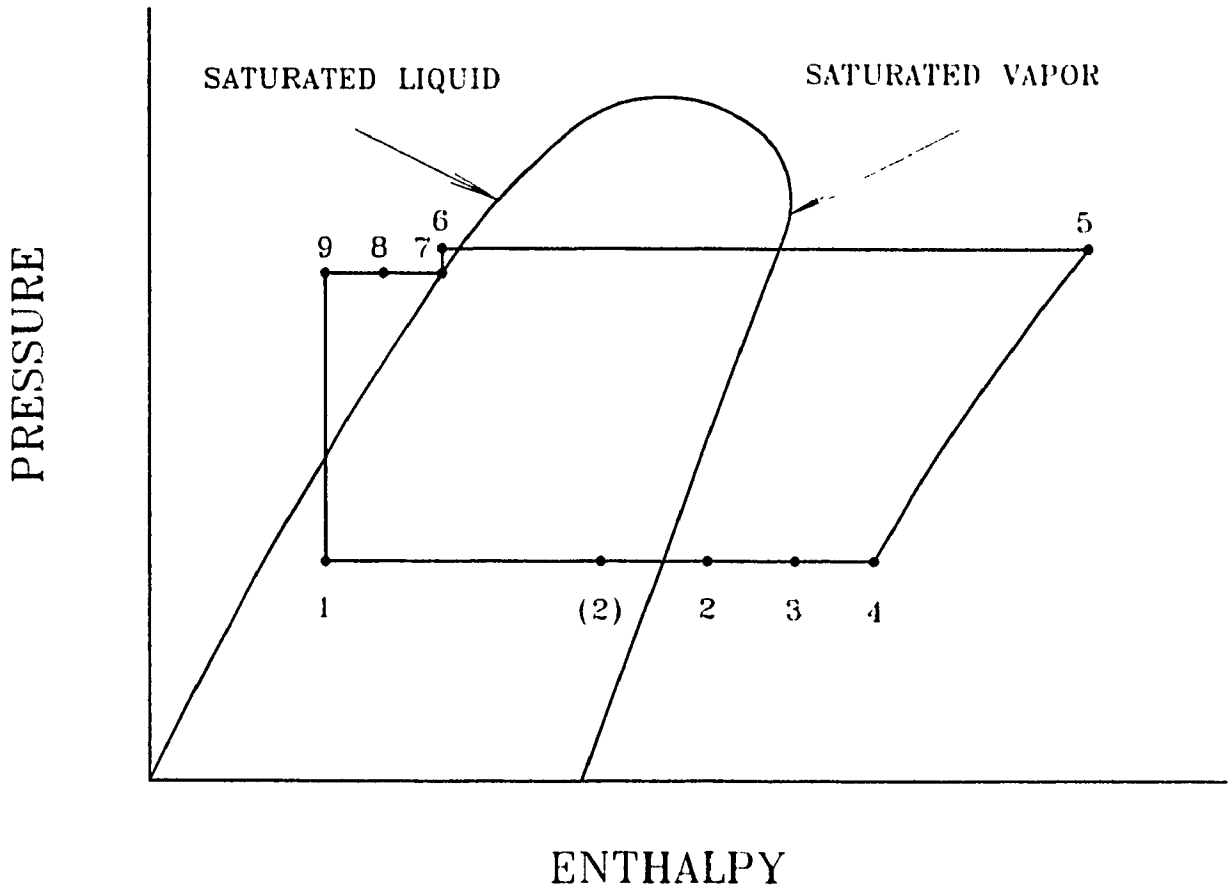

Figure 3.2. Pressure-enthalpy diagram of air-conditioning system.

CHAPTER 4

VALIDATION OF MODELS

4.1 Introduction

The evaporator model and the air-conditioning system model presented in chapter 3, have been validated during the research. The first step is to validate the evaporator model by confirming that the evaporator model was satisfactory after changes had been made from the Oskarsson et al. [1989] model. Two evaporators, an eight-row coil and a four-row coil, have been tested to validate the evaporator model. The air-conditioning system model was then validated. Only the four row evaporator has been used to compare system model predictions with the experimental results to validate the air-conditioning system model.

4.1.1 The Evaporators

The two evaporators which are used in the validation have different geometrical dimensions and different circuit arrangements. The first evaporator has eight rows in its depth, nine rows in its height, and 6 circuits as shown in Figure 4.1. The rows in depth (8) of the this evaporator do not equal the number of its circuits (6). The eight-row evaporator has the following dimensions:

- face area of the coil is 1.125 ft^2,
- width of the coil is 1.5 feet,
- height of the coil is 0.75 feet,
- fin density of the coil is 12 fins/inch,
- fin thickness is 0.006 inches,
- tube outer diameter is 0.378 inches, and
- tube inside diameter is 0.305 inches.

The second coil has four rows in depth, has 4 circuits and has 18 rows in its height. The rows in depth are equal to its circuits for the second evaporator as shown in Figure 4.2. The four row coil has the following dimensions:

- face area of the coil is 2.25 ft^2,
- width of the coil is 1.5 feet,
- height of the coil is 1.5 feet,
- fin density of the coil is 10 fins/inch,
- fin thickness is 0.006 inches,
- tube outer diameter is 0.378 inches, and
- tube inside diameter is 0.305 inches.

Refrigerant 12 was used in this research to validate both the eight-row and the four-row evaporator model.

4.1.2 The Experimental Air-Conditioning System

An air-conditioning system was constructed in this research to validate the air-conditioning system model. The system, which is shown in Figure 3.1 and 3.2, is a vapour compression air-conditioning system.

The total capacity and air flow rate (**CFM**) were calculated by an energy balance from the measurements taken from the refrigerant-side, the water-side, and the air-side. The sensible capacity, the latent capacity and the condensate were calculated from air temperature and relative humidity measurements. Condensate was collected and compared with the calculated amount of condensate. The average deviation between those two values is 9%.

During the experiment, the frequency of electricity supplied to the evaporator fan motor is varied to change the evaporator air flow rate and the frequency of the electricity supplied to the compressor motor is also varied to vary the compressor volumetric displacement rate. The experimental system has the following characteristics:

- The four row coil was used as the system evaporator
- The sink for condenser was water.
- The refrigerant flow rate varied from 350 lb_m/hr to 520 lb_m/hr.
- The air flow rate ranged from 630 CFM to 1114 CFM.

Refrigerant 12 was used in this research to validate the air-conditioning system model.

4.2 The Method of Validation

Validations for both the evaporator model and the air-

conditioning system model are accomplished as follows. Experiments are performed at the different steady-state experimental conditions to obtain the experimental results. A data collecting and data recording computer was used to scan measurement points once every 3 second. The averaged measured values were then recorded every 30 minutes. Experimental results were collected for operations at different steady-state conditions. Numerical evaporator and system models were used to obtain operation performance predictions of the evaporators or the air-conditioning system at those steady-state conditions. The model predictions were compared with the experimental results.

In this research, the comparisons were completed by plotting the experimental results and model predictions on the same graphs with the same scales on the both X and Y axes. Each point on the graph represented a steady-state point. The reading on the X axis represented the test result of that point, while the reading on the Y axis was the model prediction. On each graph, there is a straight line from the left bottom corner to the top right corner. This line is the basic zero deviation line. If the point was plotted on this line, zero deviation had been found for that operation point. The closer the point to this line is, the better agreement is between the experimental results with model prediction values.

4.3 Experiments

4.3.1 Experimental System

The air-conditioning system tested was similar to the one shown in Figure 3.1. The experimental system had an oil separator. The experiments were used to validate both evaporator and air-conditioning system models. The refrigerant side measured values were:

- pressures at 5 points, at compressor inlet, between compressor outlet and oil separator inlet, between oil separator outlet and condenser inlet, condenser outlet, and evaporator outlet, and
- temperatures at all key points, at inlet and outlet of all components.

The air side measured values were:

- 2 temperatures at inlet and outlet of evaporator,
- 2 relative humidities at inlet and outlet of evaporator, and
- velocity at the centre of evaporator face area.

The condenser cooling water measured values were:

- temperatures at inlet and outlet, and
- water flow rate.

Total condenser cooling water consumption was also measured in order to check the water flow rate.

The following values were measured to monitor compressor

motor and evaporator fan motor operation:

- power consumption, and
- frequency of the power input.

The condensate from the evaporator was collected and weighted.

4.3.2 Experimental Instrumentation

Type T thermocouples were used to measure temperatures at different key points on the system on both the refrigerant side and the water side.

Air side temperatures and relative humidities were measured by humidity and temperature probes. In these probes, temperature is measured with an electrical resistance type temperature sensor and relative humidity is measured by a capacitance type humidity sensor.

Pressures at different points on the refrigerant and the air side are measured by strain gauge type pressure transducers. The water flow rate was monitored by positive displacement volumetric type flow transmitter.

The air velocity was measured by a thermal anemometer velocity sensor. This velocity sensor was uncalibrated and used only for an indication of the order of magnitude of the air velocity. This value was generally lower than the calculated average air velocity. Pressure transducers and relative humidity probes were calibrated before and during the course of the experiments in order to limit the inaccuracies due to the experimental instruments. All the connecting wires

were shielded with metal to avoid possible noise influence.

A computer was used to process the sensor signals taken from the experimental system. The computer converts the signals into values of the temperature, the relative humidity, the flow rate etc., recorded and displayed the values on screen. Those experimental results were scanned every 3 seconds, and were averaged and recorded for every half an hour by the computer. Each test lasted for a period of approximately seven hours.

Results are plotted on figure 4.3 to figure 4.8. A value of 0.75 for the quality at the starting point of the transition region was utilized because it is the most accurate value for those two evaporators and the air-conditioning system under the performed experimental condition. It is found that there is no significant influence by varying Lewis number, LE, for both the eight row and the four row evaporator. The evaporator model used a value of 0.95 for the Lewis number.

4.4 Evaporator Model Validation

The evaporator experimental results for both wet and dry conditions are compared with its model predictions in Figures 4.3, 4.4, 4.5, 4.6, 4.7 and 4.8. Each point on these graphs represents a steady-state operating condition. The model was used to predict the conditions of the outlet air, the total, sensible and latent cooling capacity of the evaporator at that

particular point.

In order to validate the models, the model prediction must be calculated at the same conditions as the experimental ones. For evaporator model validation the following input data must be provided directly from the experimental results:

- geometric dimensions of the evaporator which was used in validation,
- evaporator air velocity (calculated),
- refrigerant flow rate (calculated),
- air temperature at evaporator inlet,
- air relative humidity at evaporator inlet,
- refrigerant temperature at evaporator inlet, and
- refrigerant quality at evaporator inlet.

Figure 4.1 indicates that the eight-row coil has 6 refrigerant circuits. The air flow direction is normal to the refrigerant flow direction.

During validation, two methods have been used to simulate this eight-row evaporator coil. The first method is to "lump" the coil together to predict the evaporator performance. The second method is to divide the evaporator into sub-coils according to the number of refrigerant circuits. Each circuit of the evaporator is considered as a sub-coil. A series of consecutive sub-coils are added together to formulate that evaporator. Results showed that the second method was superior to the eight-row coil evaporator because the deviation of

predictions were relatively smaller than using the first method. The comparisons of predicted and experimental results of the eight-row coil are plotted on Figures 4.3, 4.4, and 4.5.

Predicted and experimental results on total cooling capacity are compared in Figure 4.3 The ranges of total cooling capacity are between 17500 BTU/hr and 24500 BTU/hr based on the experimental results. The model predictions of total cooling capacity compare very well with the experimental results. The graph shows that the deviation range on the total cooling capacity is between -3% and +1% with most deviations between -2% to 0%. The graph shows that the experimental results of the total cooling capacity for the eight-row coil, in general, are slightly higher than those of the model predictions but the accuracy is still very satisfactory.

Figure 4.4 is the comparison of predicted and experimental results for the sensible cooling capacity. The range of sensible cooling capacity for the eight row coil is from 14000 BTU/hr to 22000 BTU/hr based on experimental results. The model predictions of sensible cooling capacity compare well with the experimental results. The figure shows that the range of deviations of the sensible cooling capacity, in general, is between -9% and +2% with most deviations within a range of -5% to +1%.

The range of latent cooling capacity is from 500 BTU/hr to 4800 BTU/hr based on experimental data as shown in figure

4.5. The range of the deviation for the latent cooling capacity is mainly between -20% and +30% with most deviations within a range of -10% to +15%. The range of deviations of the latent cooling capacity for the eight-row coil seems relatively large.

The number of rows of the 4 row coil equals the number of refrigerant circuits. Figure 4.2 shows that the air flow direction of this coil is normal to the direction of the refrigerant. There are two methods, the "lumped" method and the "sub-coil" method, used to formulate and validate the four row evaporator coil. Results show only minor disparities between the two methods. The "lumped" coil method was finally chosen since this method is relatively simple and the calculation speed by using this method is much faster than using "sub-coil" method. Figures 4.6, 4.7, and 4.8 show the experimental and model prediction results on the four-row coil.

The range of the total cooling capacity of this coil is between 19000 BTU/hr and 27500 BTU/hr based on experimental results. Figure 4.6, which compares the predicted and experimental total cooling capacity, shows that the range of deviations is about ±5% with the most deviations within -2% to +4%. The model predictions of the total cooling capacity compare very well with experimental results for this four-row coil.

The range of the sensible cooling capacity for the four

row coil is from 16500 BTU/hr to 24000 BTU/hr based on experimental results. Figure 4.7 shows that the range of deviations on predicted and experimental sensible cooling capacity are from -8% to +2%. Most of the model predictions of the sensible cooling capacity are lower than the experimental results but still within a satisfactory range.

The range of the latent cooling capacity for this evaporator is from 400 BTU/hr to 4600 BTU/hr. Figure 4.8 shows the range of deviations of the latent cooling capacity. The ranges are estimated from -10% to +25% with some points slightly larger. The model predictions, in general, are higher than experimental results. The range of deviations seem relatively large.

From Figures 4.3, 4.4, 4.5, 4.6, 4.7, and 4.8 the conclusions that can be made for the evaporator model, can be expressed as follows.

- The accuracy of the evaporator model in calculating total cooling capacity is quite satisfactory.
- The accuracy of the model in calculating sensible cooling capacity is quite satisfactory.
- There are large deviations between the model predictions and experiment results in latent cooling capacity.

There are many possible sources of errors or deviation in

the evaporator model validation. The possible causes of the deviation will be discussed later in this chapter with the air-conditioning model.

4.5 Air-Conditioning System Model Validation

The air-conditioning system with the 4 row coil as its evaporator, was tested for system model evaluation. The experimental results are compared with the air-conditioning system model prediction.

For the system model validation, the simulation used averaged input values, which are derived directly from experimental results. These averaged input data are:

- compressor clearance volume (decimal) fraction,
- isentropic compression efficiency,
- compressor motor electrical efficiency,
- condenser heat transfer effectiveness,
- degrees of subcooling at condenser outlet,
- degrees of superheat controlled by the expansion valve, and
- heat transfer effectiveness of interchangers.

Other input values of the air-conditioning system model at a particular steady-state operating point are determined from experimental results. For each operating point the following values were specified:

- air temperature at evaporator inlet,
- air relative humidity at evaporator inlet,

- evaporator air flow rate, CFM,
- compressor volumetric displacement rate, and
- condensing pressure.

The model is then used to calculate the system total cooling capacity, sensible cooling capacity, latent cooling capacity, and sensible heat factor. Validation was done using evaporator cooling capacity as the system total cooling capacity in order to eliminate error due to fan modelling.

The results of the model prediction and experimental results are plotted in Figure 4.9, 4.10, and 4.11. Each point on the graphs represents a steady-state operating condition. The X axis value of one point is its experimental result which is plotted against the model prediction on the Y axis value.

Figure 4.9 shows the comparison of the experimental and the predicted results of total cooling capacity. The range of the total cooling capacity is from 19000 BTU/hr to 28000 BTU/hr based on experimental results. The deviation of experimental and model prediction results are, in general, from -6% to +10% with some deviations larger than +15%. The results are satisfactory.

The model predicted and experimental results of sensible cooling capacity are compared on Figure 4.10. The range of the sensible cooling capacity is from 17000 BTU/hr to 24000 BTU/hr. Figure 4.10 shows that the deviations are about ±10% with most deviations within ±7% and some points are slightly larger than +10%. The results are still very satisfactory.

In Figure 4.11, the experimental and prediction results of latent cooling capacities are compared. The range of the latent cooling capacities is from 400 BTU/hr to 4500 BTU/hr based on experimental prediction. The figure shows that the deviations of the latent cooling capacities range from -1% to +20%. Almost all the deviations are within the range of +4% to +18%.

Based on Figure 4.9, 4.10, and 4.11 the conclusions that can be made for the air-conditioning system model maybe expressed as follows.

- The accuracy of the model in calculating total cooling capacity is quite satisfactory.
- The accuracy of the model in calculating sensible cooling capacity is satisfactory.
- The deviations between the predicted and experimental values of latent cooling capacity, in general, are high.

4.6 Discussion of the Deviations between the Predicted and Experimental Results

The causes of the deviations between model predictions and experimental results are very complex. Instrumentation inaccuracies (especially relative humidity readings), oscillations due to expansion valve hunting, and oil in the refrigerant, affect the experimental accuracies. The model simplifications, and the averaged model input values can be

thought of as the possible causes of the model inaccuracy.

4.6.1 Effect of Relative Humidity Reading

It was noticed during the study that a small error from the relative humidity sensor reading can cause a very large error between the calculated condensation values and the collected experimental condensation values. The accuracy of inlet and outlet air relative humidity sensors in the operating range were the possible main cause of the deviation of the latent cooling capacity between the model predictions and the experimental values. In this research, effort had been made to study the influence of the reading error of the relative humidity sensors. It was noticed that a -3% reading error of the relative humidity sensors on both inlet and outlet air of the air-conditioning system can cause as much as 40% error between the model predictions and the measured experimental values on the evaporator condensate. The average deviation between the calculated values and measured values of condensate is 9% in this research after the calibration.

4.6.2 Effect on the Time Averaged Values

The experimental system uses a thermostatic expansion valve to control the amount of superheat at the point between the two interchangers. During the operation, the expansion valve is opened wider or closed a little bit to adjust the superheat. The adjusting movement changes the system

pressures. As a result, the refrigerant side of the air-conditioning system oscillated during the adjusting movement. The oscillations may cause errors.

4.6.3 Effect from the Oil Mixed in the Refrigerant

There is oil mixed in the refrigerant of the experimental air-conditioning system even though the oil separator was used in the experimental system. The oil inside the refrigerant can cause the following problems:

- The oil inside the refrigerant changes the values of heat transfer resistance in heat exchangers, i.e., evaporator, condenser, and interchangers.
- The evaporator model and the air-conditioning system model were analyzed by assuming pure refrigerant properties. Since oil was mixed with the refrigerant, the refrigerant properties may have been slightly different from those of pure refrigerant.

The effect of the oil mixed in the refrigerant is very complex, it depends on both the type of refrigerant as well as the percentage content of oil mixed in the refrigerant. Further research is required to be performed on this subject.

4.6.4 The Model Uncertainty

The following are some possible causes of deviation in the evaporator model and the air-conditioning system model.

These causes may effect the calculated data deviation.

- The models were simplified by using numbers of input values which used averaged values derived from experiments. Because the experimental operation range is a broad one, these averaged values may cause slight deviation between the calculated results and real experimental values.
- The air-conditioning system model uses a simple compressor model and a simple condenser model. These simple models may cause deviation between the calculated results and experimental values.
- In the experimental air-conditioning system, an oil separator was used to separate oil, which was mixed with the refrigerant from the refrigerant itself. There was a pressure difference between the oil separator inlet and outlet. In the air-conditioning system model, this pressure difference was not accounted for.
- The "three region" evaporator model, which was used in both evaporator and air-conditioning system model, does not account for specific refrigerant circuiting. It may account for deviations between the calculated and real experimental evaporating temperature T_e.

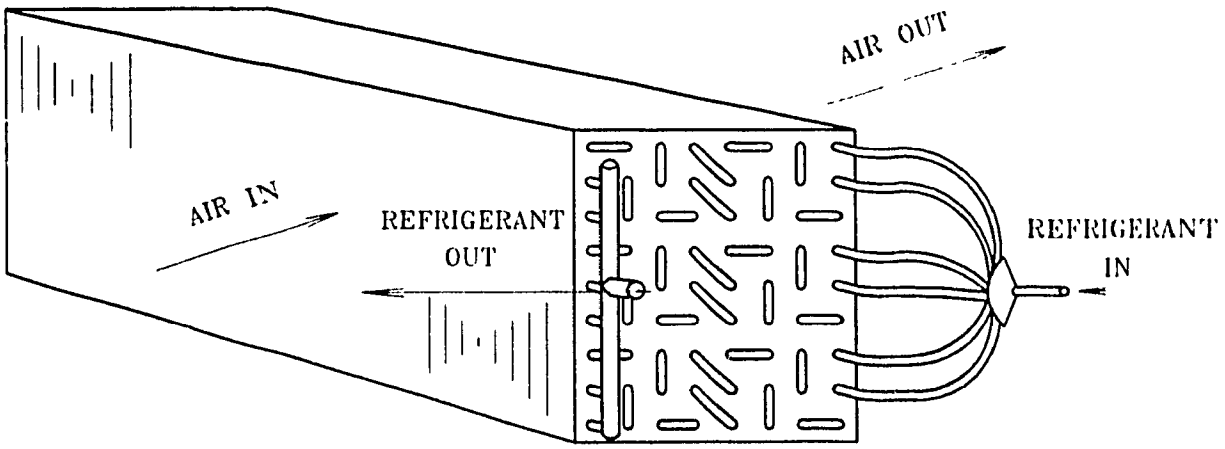

Figure 4.1. Eight-row evaporator.

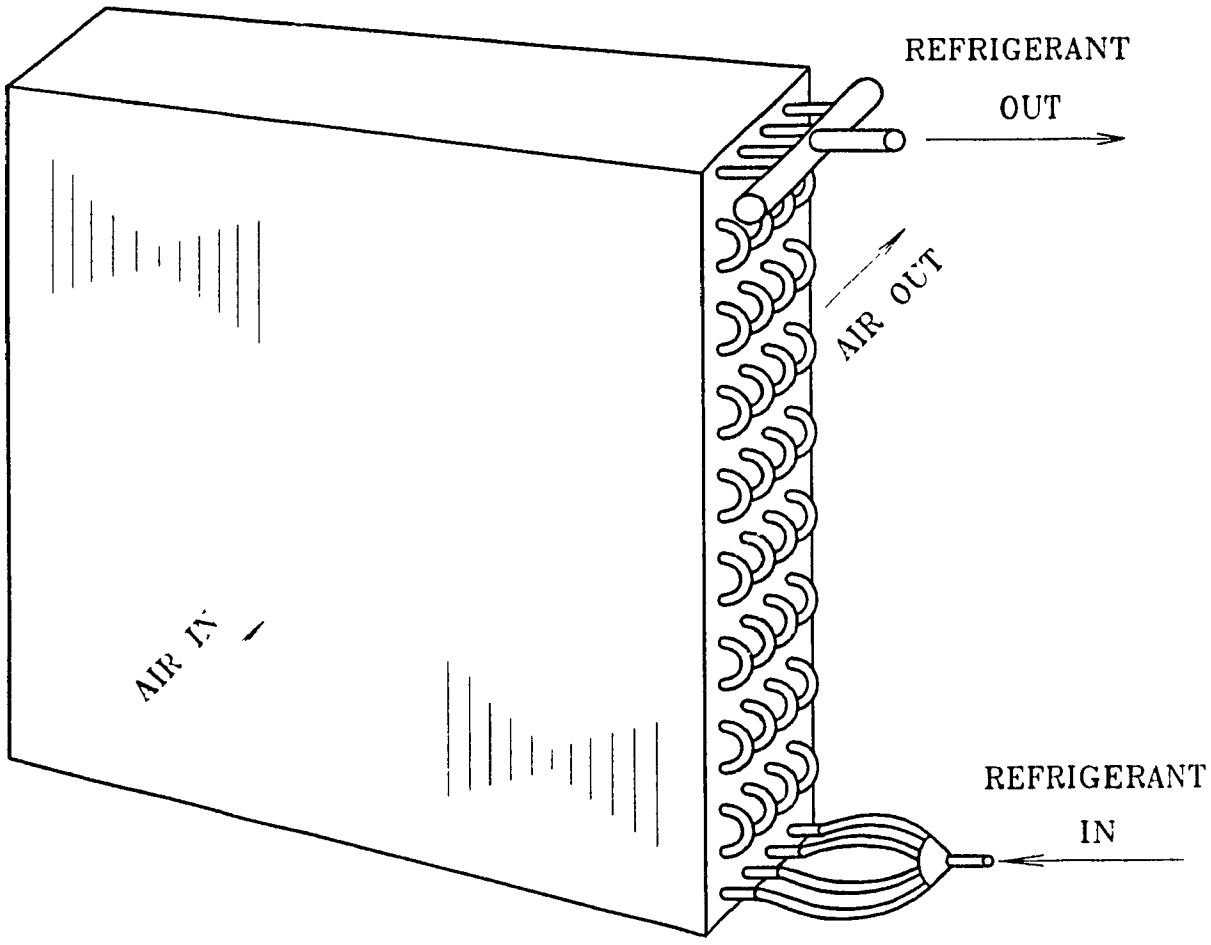

Figure 4.2. Four-row evaporator.

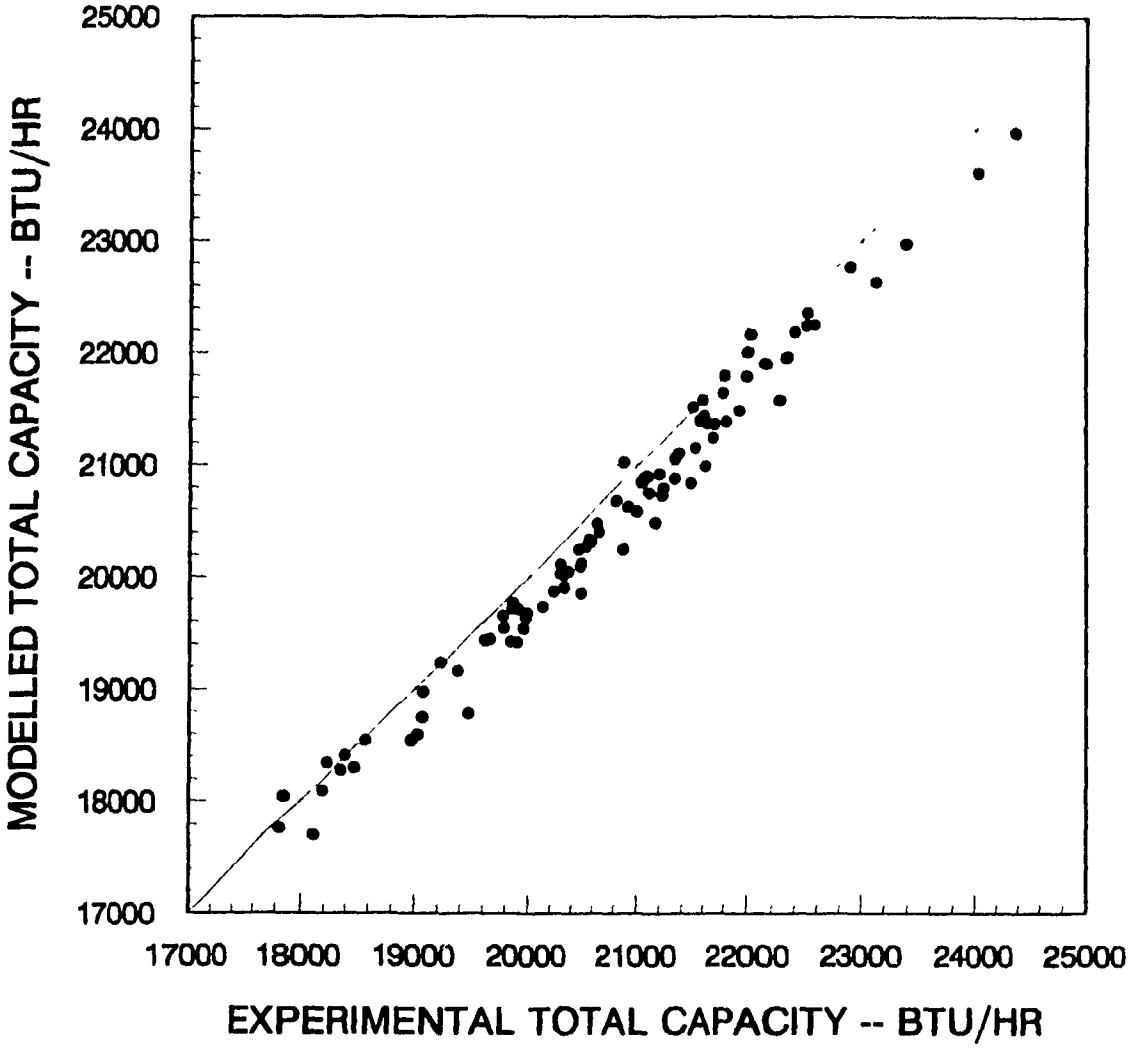

Figure 4.3. Total cooling capacity comparison of the eight-row evaporator.

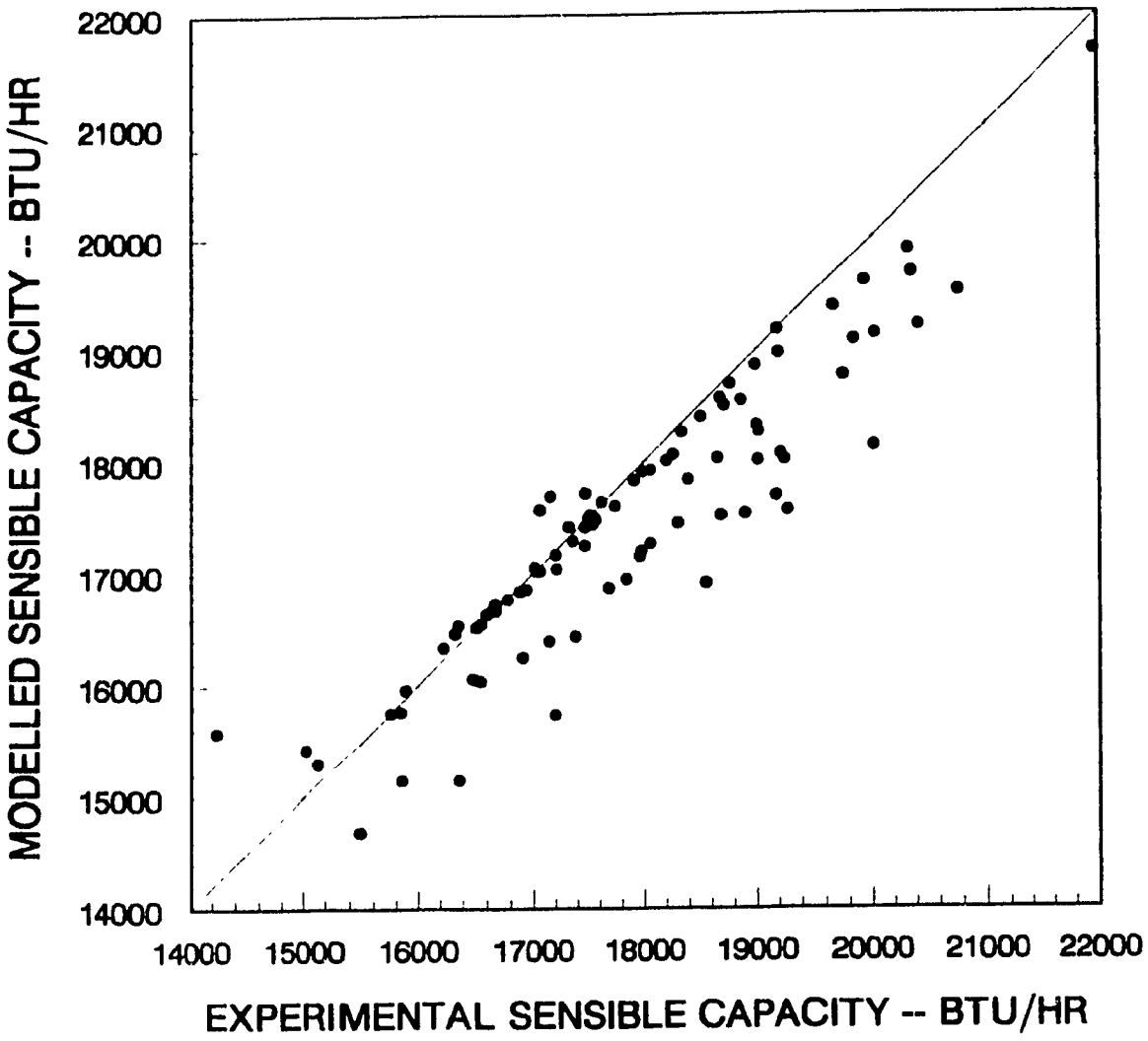

Figure 4.4. Sensible cooling capacity comparison of the eight-row evaporator.

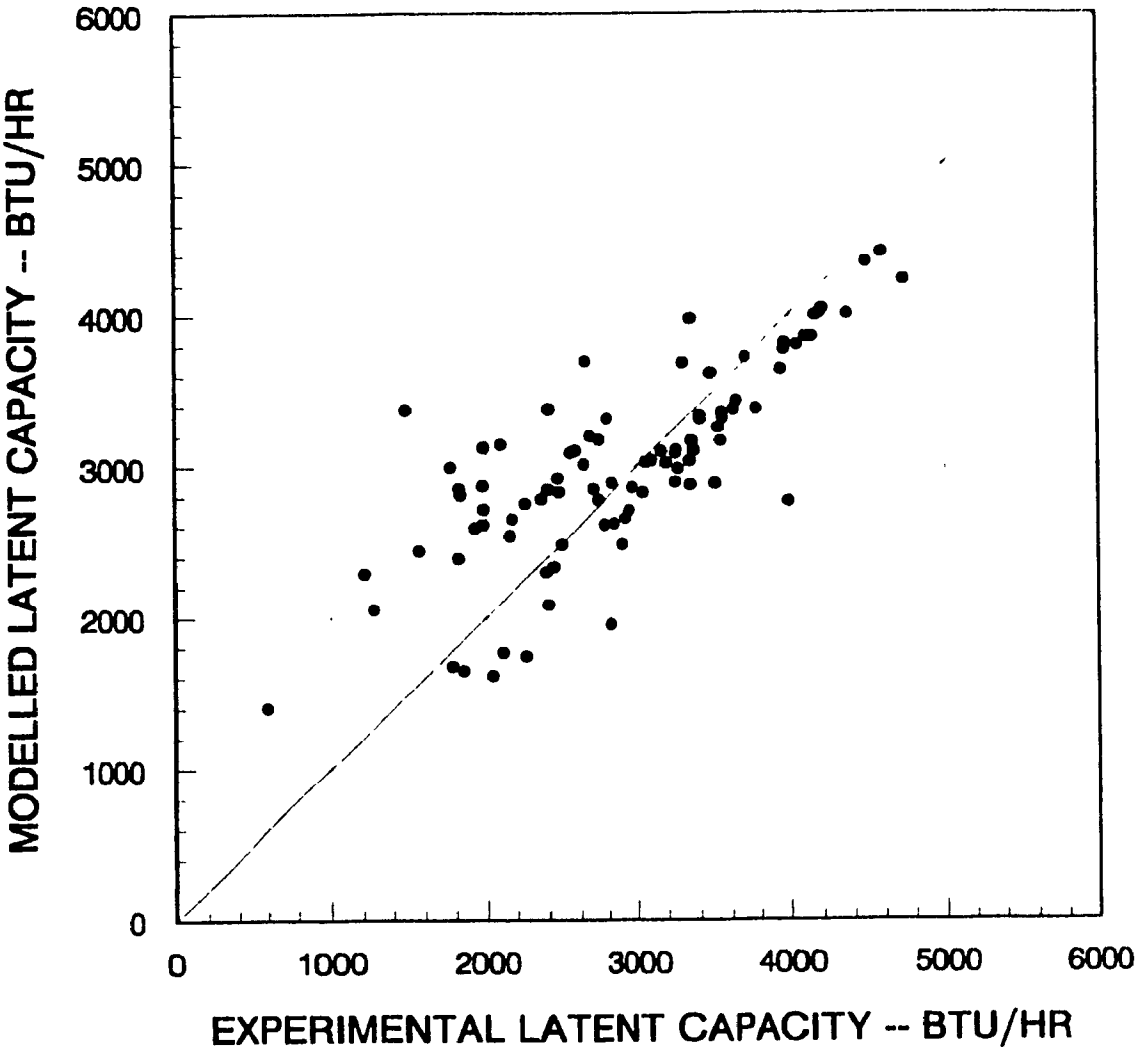

Figure 4.5. Latent cooling capacity comparison of the eight-row evaporator.

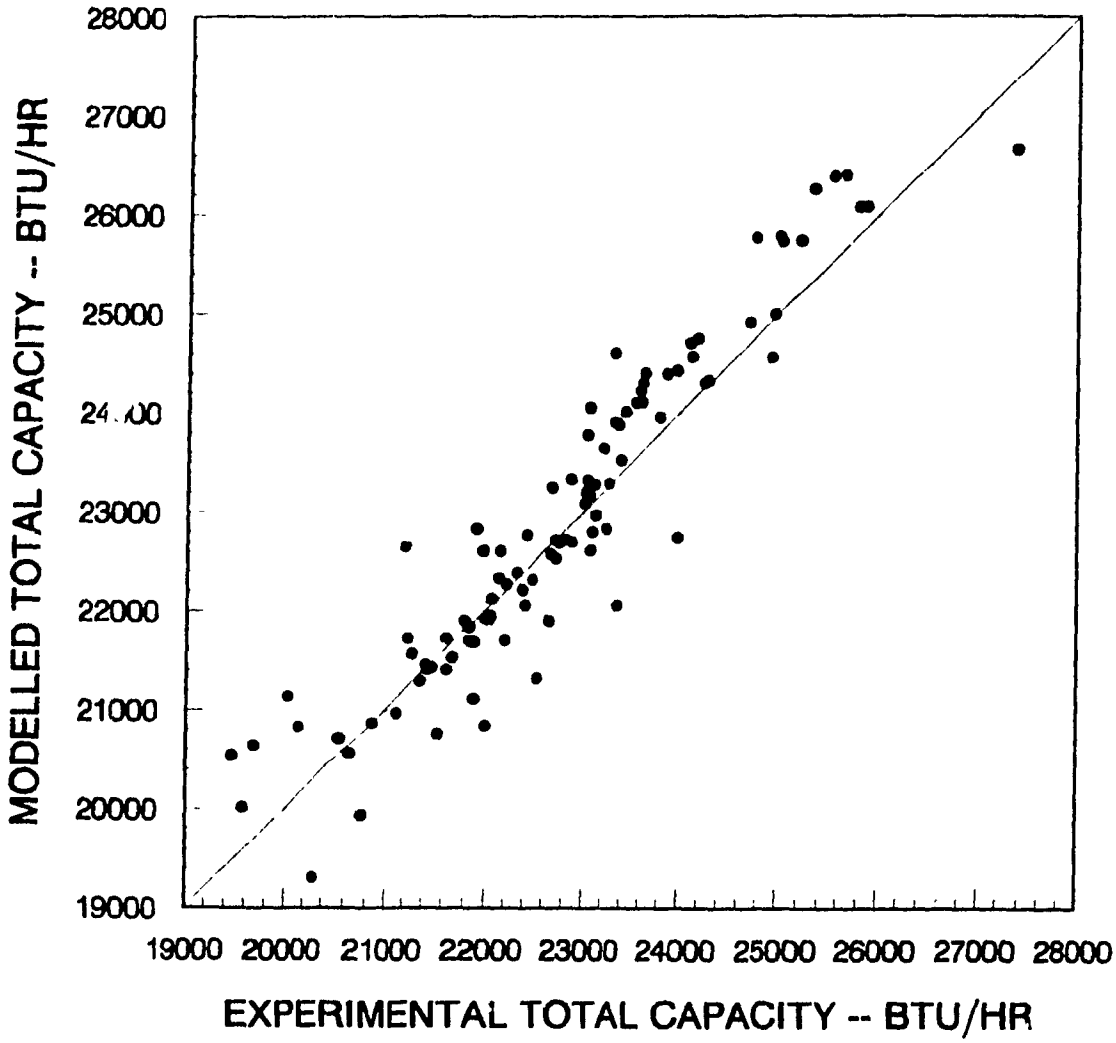

Figure 4.6. Total cooling capacity comparison of the four-row evaporator.

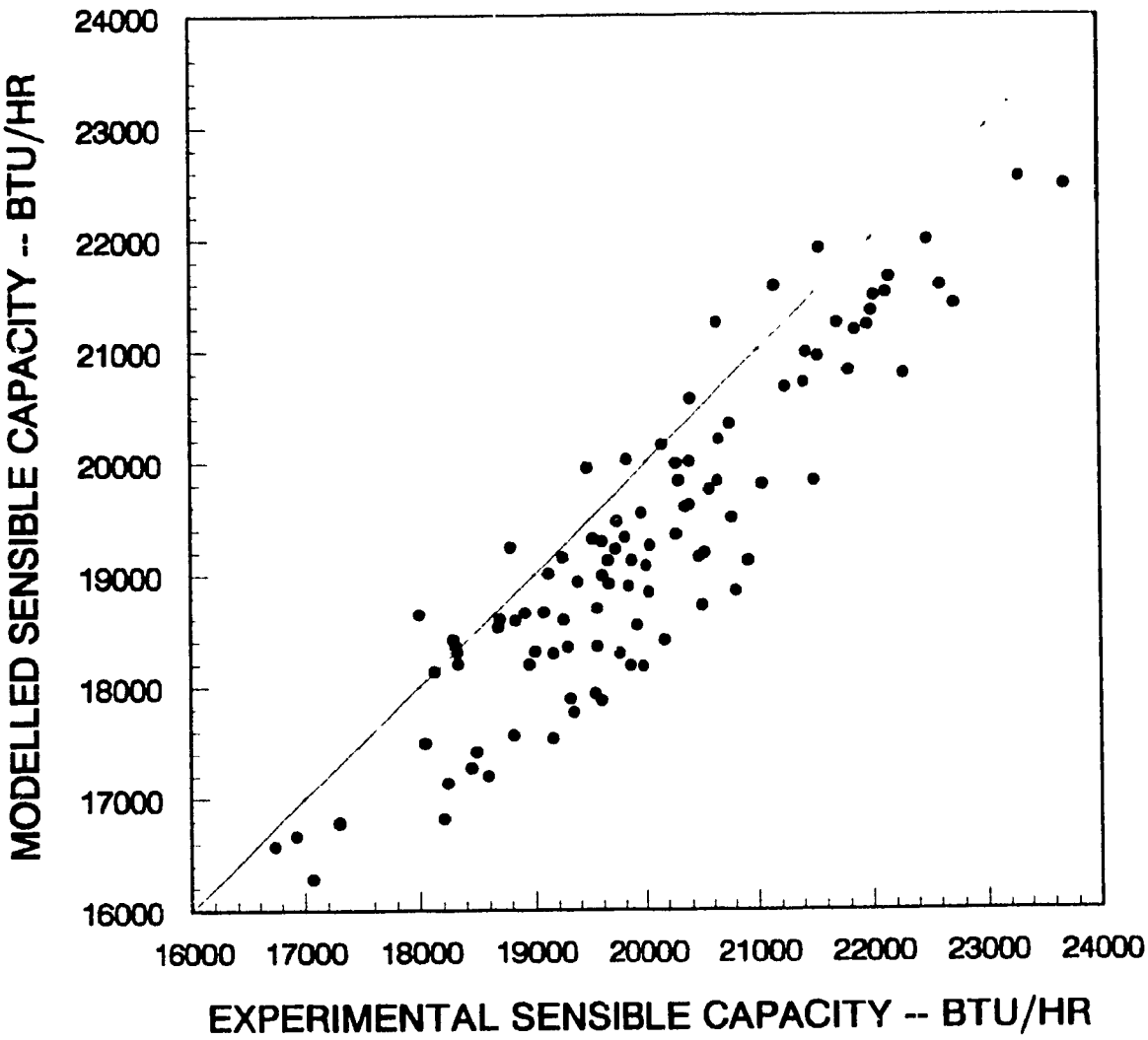

Figure 4.7. Sensible cooling capacity comparison of the four-row evaporator.

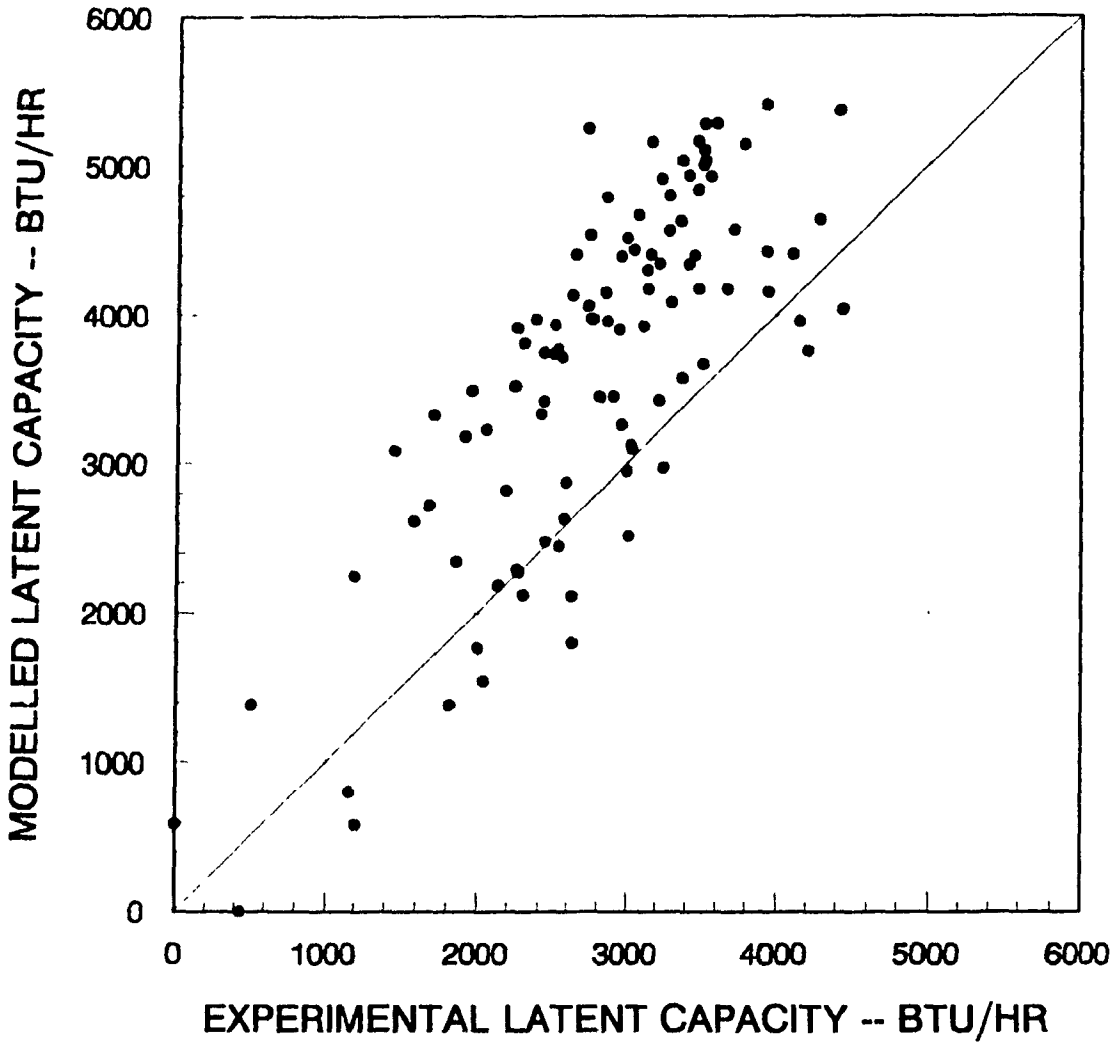

Figure 4.8. Latent cooling capacity comparison of the four-row evaporator.

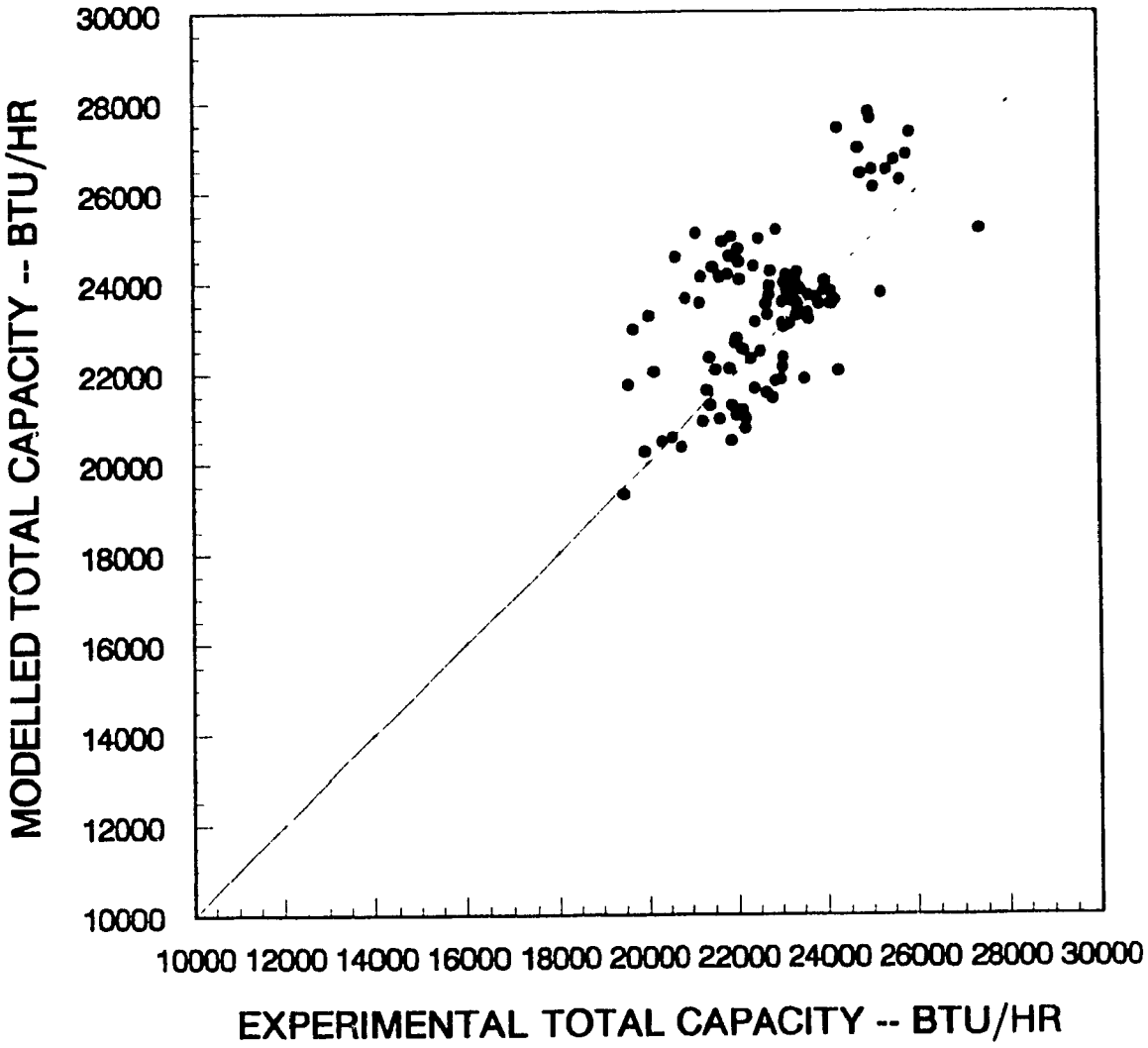

Figure 4.9. Total cooling capacity comparison of the air-conditioning system.

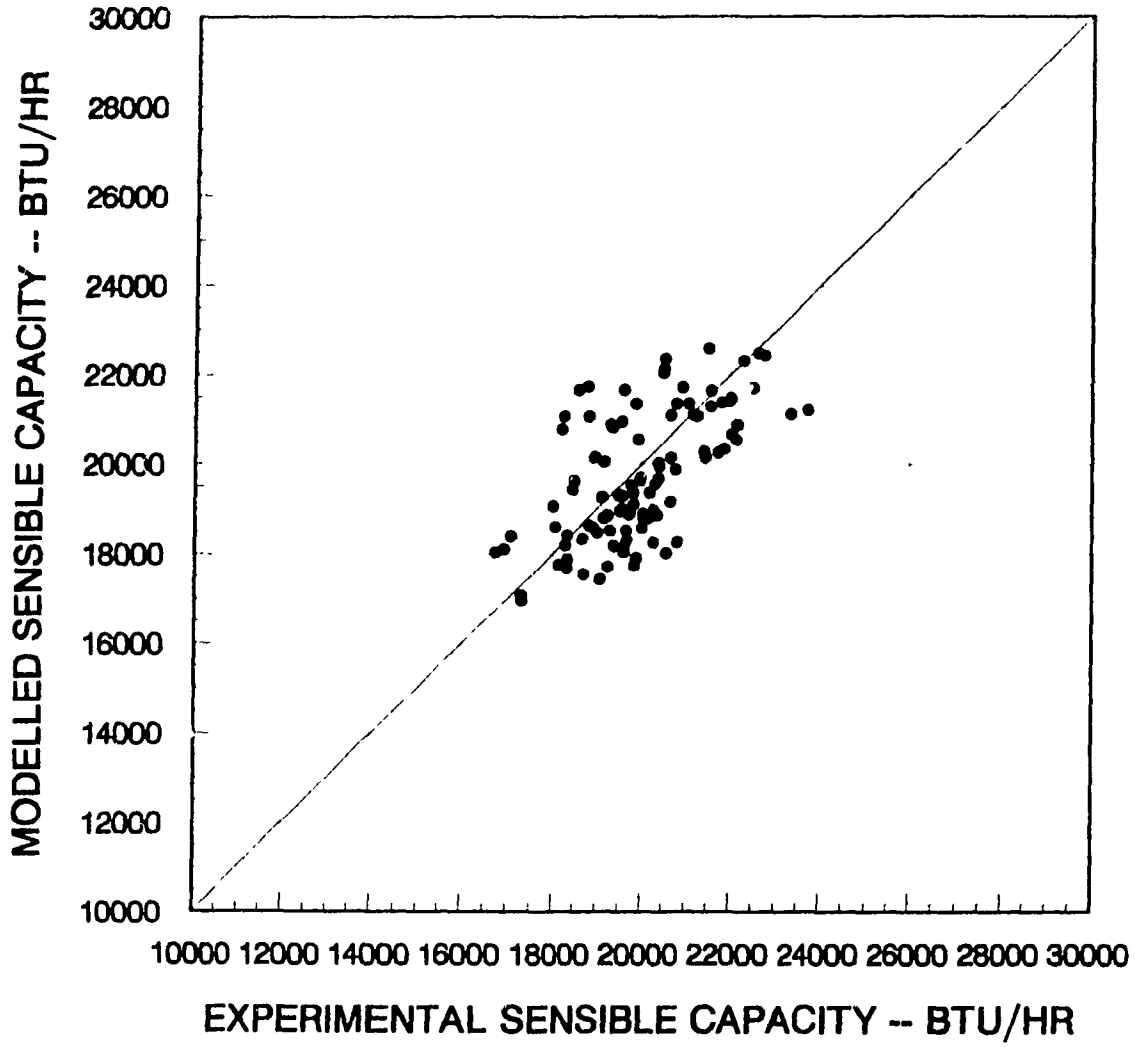

Figure 4.10. Sensible cooling capacity comparison of the air-conditioning system.

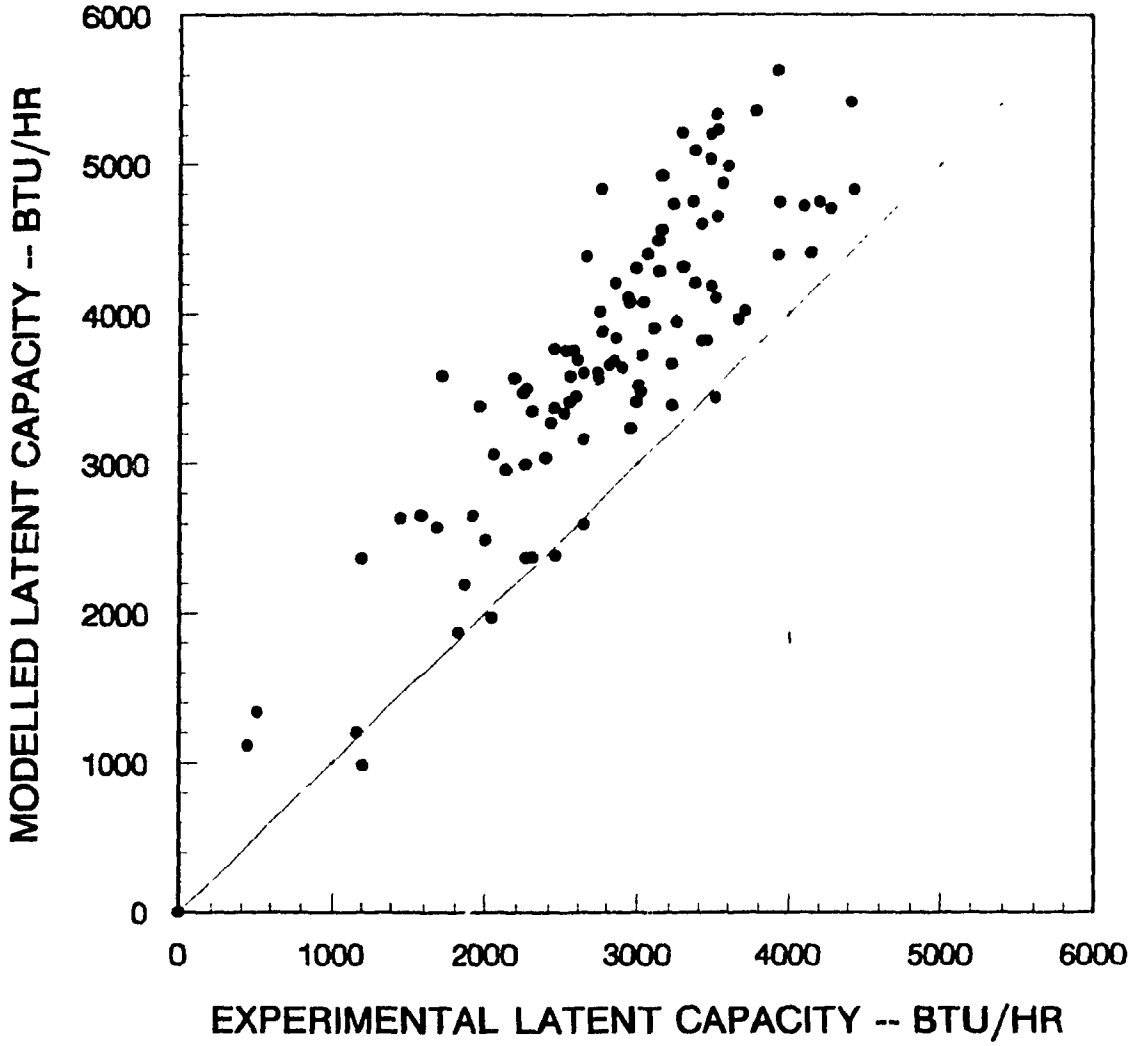

Figure 4.11. Latent cooling capacity comparison of the air-conditioning system.

CHAPTER 5

AIR-CONDITIONING SYSTEM PERFORMANCE PREDICTION BY USING AN AIR-CONDITIONING SYSTEM MODEL

5.1 Overview

Krakow et al. [1987] present a performance map of a heat pump to determine heat pump performance using a variable speed compressor. In the present research effort, similar maps which are suitable for an air-conditioning system are proposed. In the previous chapter, the evaporator model and the air-conditioning system model were validated. Based on the above validation, performance maps were created.

5.2 Map Construction Techniques

The steady-state operating performance of an air-conditioning system is dependent on numerous variables. Four variables: the evaporator air flow rate (**CFM**), the compressor volumetric displacement rate (**CFH**), the source air temperature (T_{SRC}), and the source air relative humidity (RH_{SRC}), have decisive influences on performance. The source air state is considered to be the state of the air entering the evaporator. These four items can be divided into two sets according to each physical characteristic. The first set, which includes air flow rate and compressor volumetric

displacement rate, relates to evaporator fan and compressor motor speeds. The second set, which includes source air temperature and source air relative humidity, relates to the source condition.

In this research, maps were created by keeping one set of variables constant and then changing the other set of variables to obtain a set of steady-state performance points. If the source air temperature and the source air relative humidity are maintained constant, changing the evaporator air flow rate and/or the compressor volumetric displacement rate, will lead to the changing of the system performance. Each particular pair of evaporator air flow rates and compressor volumetric displacement rates represents a steady-state operating point. By plotting all the points and connecting them, the first set of steady-state system performance maps at the constant values of T_{SRC} and RH_{SRC} were created. If the evaporator inlet air flow rate and the compressor volumetric displacement rate are maintained constant, changing the source air temperature and/or relative humidity create the second set of steady-state system performance maps.

In this research, the four row coil evaporator, which was validated in chapter 4, was used to create performance maps, to study and to predict the performance of the air-conditioning system. All the maps which are mentioned below are only suitable to predict the performance of this particular four row evaporator air-conditioning system.

However, the method of creating maps, which was introduced in this chapter, could be used to create maps to predict the performance for other air-conditioning systems.

In order to create the performance maps, some average values, which were derived from the experimental results, were utilized as the input values for the model. Two methods, the "lumped" method and the "sub-coil" method, were used to create maps. Results show that at the low latent capacity the "sub-coil" method gives better results. This method was finally chosen to create performance maps.

5.3 Performance Maps

Three performance maps have been created in this research are shown in Figures 5.1, 5.2, and 5.3. Figures 5.1 and 5.2 show net sensible cooling capacity versus latent cooling capacity with air flow rate and compressor volumetric displacement rate as parameters. Figure 5.3 shows the air-conditioning system net sensible cooling capacity versus latent cooling capacity with source temperature and source relative humidity as parameters.

The performance maps (Figures 5.1 and 5.2) were created by maintaining the air-conditioning system source air temperature and relative humidity constant. The values of the evaporator air flow rate and the compressor volumetric displacement rate were changed incrementally to obtain predictions of the system performance. The model predictions

were then plotted to create the maps.

For Figure 5.1, the values of the source air temperature equals 68°F and air relative humidity equals 0.45. For Figure 5.2, the source air temperature equals 76°F and relative humidity equals 0.55. In these two figures, the value of air flow rate was initially at 600 CFM and was incrementally changed four times in steps of 200 CFM to a final value of 1400 CFM. The value of the compressor volumetric displacement rate was initially at 430 CFH and was changed four times by increments of 85 CFH to a final value of 770 CFH. The total 25 steady-state operating points represent the range of the air-conditioning system performance at the given constant air inlet conditions.

In the performance map Figure 5.3, the evaporator air flow rate and compressor displacement rate were kept constant while changing the input values of the source air temperature and relative humidity. The model calculated results were then plotted to obtain the performance map. On this map the evaporator air flow rate has a constant value of 1000 cubic feet per minute and the compressor displacement rate equals 600 cubic feet per hour. The value of the source air temperature was initially at 64°F, and was changed four times by increments of 4°F to a final value of 80°F. The value of the source air relative humidity was initially at 0.40, and was changed four times by increments of 0.05 to a final value of 0.60. The total 25 points represent the air-conditioning

system performance at the given constant air flow rate and compressor displacement rate operating conditions.

5.4 Performance Prediction of Maps

The performance maps of Figures 5.1 and 5.2 were formed by maintaining the constant source air physical condition and changing the inlet air flow rate and compressor volumetric displacement rate.

Figure 5.1 indicates that decreasing the compressor displacement rate and/or increasing the evaporator air flow rate will decrease the system latent cooling capacity.

Figures 5.1, and 5.2 show the relationship between the net sensible cooling capacity and two variables: the evaporator inlet air flow rate and compressor volumetric displacement rate. The figures indicate that increasing air flow rate and/or compressor volumetric displacement rate, in general, will increase the system net sensible cooling capacity.

Figure 5.2, when compared with Figure 5.1, shows the effect of changing the source air temperature and relative humidity on the system performance.

Figure 5.3 was produced by maintaining the constant air flow rate and compressor volumetric displacement rate and varying the source air temperature and the source air relative humidity. Figure 5.3 shows variation of the net sensible and latent cooling capacities of the system when the source air

temperature and the source air relative humidity were varied.

5.5 Map Accuracy

There are two major sources of possible deviations on the above performance maps. First of all, since some average values were used as input values, the maps have slight deviations from real operation performance. Furthermore, the maps were created by using a pure refrigerant subroutine, but in the real operation some oil is absorbed by the refrigerant. As discussed in section 4.4.2, the predicted values are slightly higher than those of the real operation.

5.6 Performance Map Usage

The performance maps are very useful tools on both research and industrial operation. The graphs can be used to quickly and directly determine an air-conditioning system performance. The use of the maps can be considered as the following.

1. The subject of this thesis is to study the behaviour of an air-conditioning control system. The performance maps created in this chapter are being used to determine the ranges of cooling capacity and dehumidification capacity for which the air-conditioning system can possibly be controlled. Within those ranges of capacities the ranges of compressor motor speed and fan motor speed can be determined. Those ranges of speeds can easily be

transferred into ranges of electricity frequency thus determining the limits of frequency of electricity supply to compressor and fan motors.

2. The maps could be used to predict the performance of a new air-conditioning system over a whole operating range before actually building one. Researchers and engineers can use the air-conditioning system model discussed in this paper and change some parameters of a particular air-conditioning system to get the predictions of the system. The predictions can then be used to create maps according to the above discussed steps. If the performance on the maps does not meet the required performance, they can simply adjust the input parameters by changing some components of the air-conditioning system to meet the requirement.

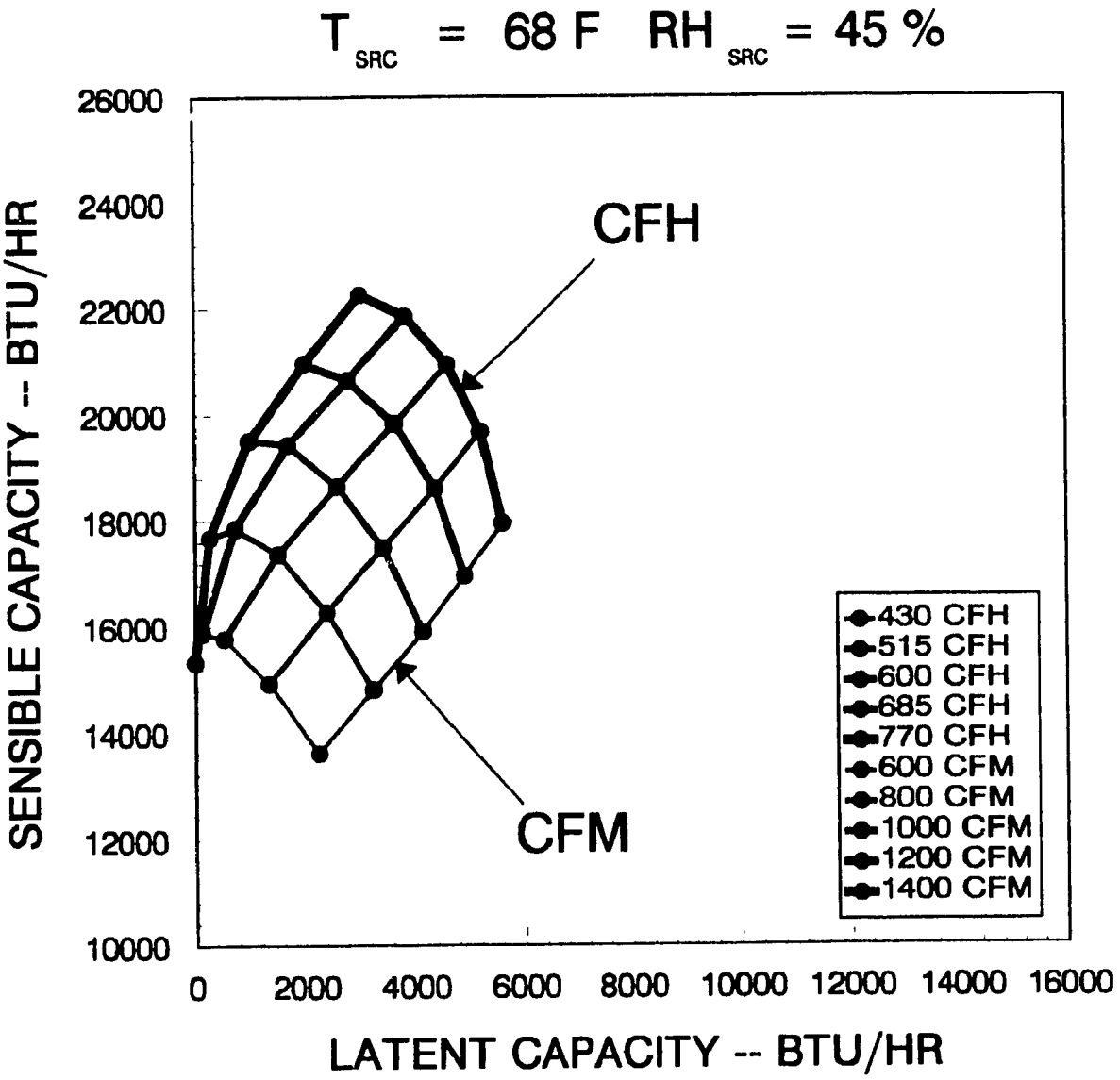

Figure 5.1. Experimental system capacities with a source temperature of 68°F and relative humidity of 45%.

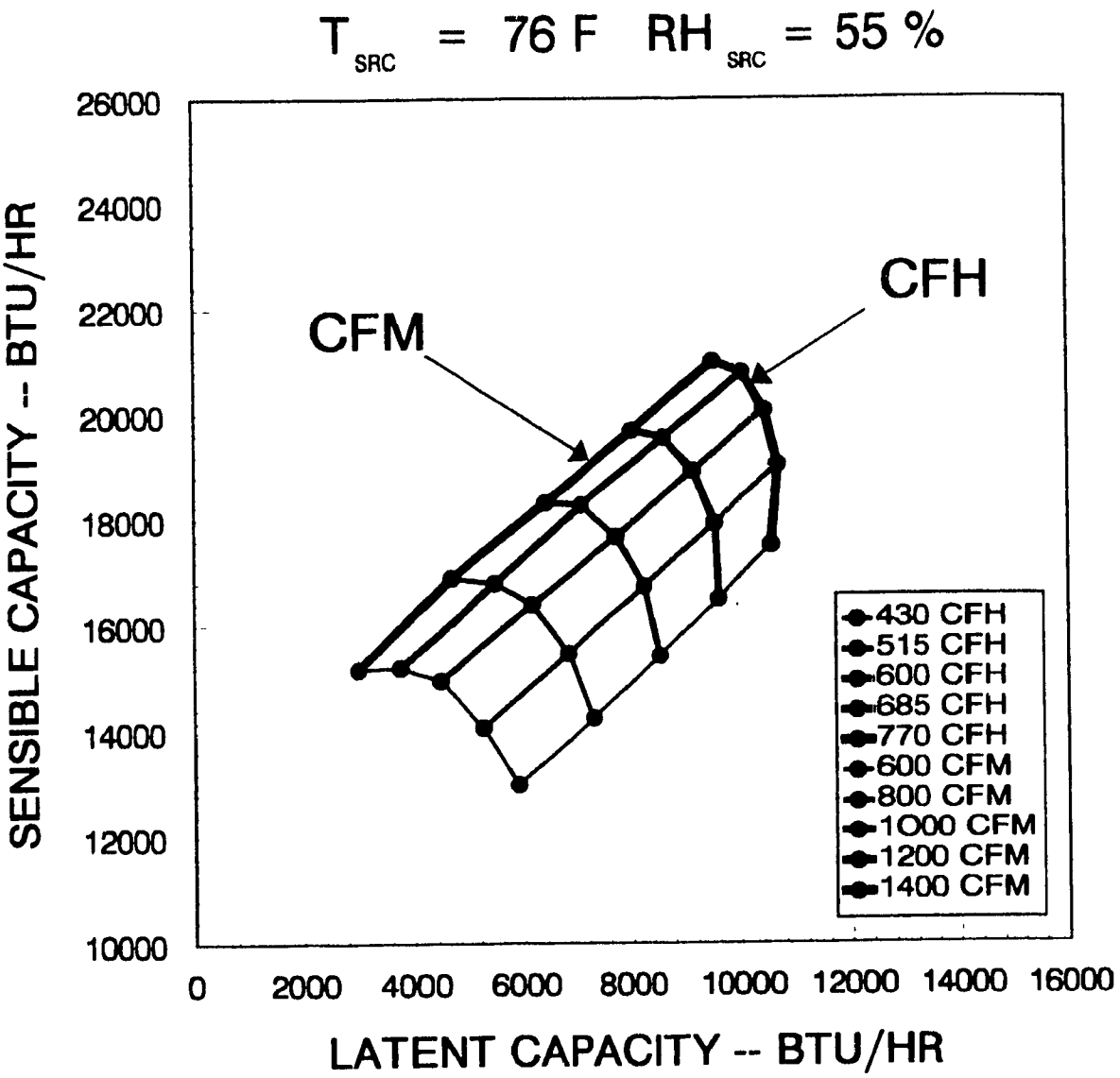

Figure 5.2. Experimental system capacities with a source temperature of 76°F and relative humidity of 55%.

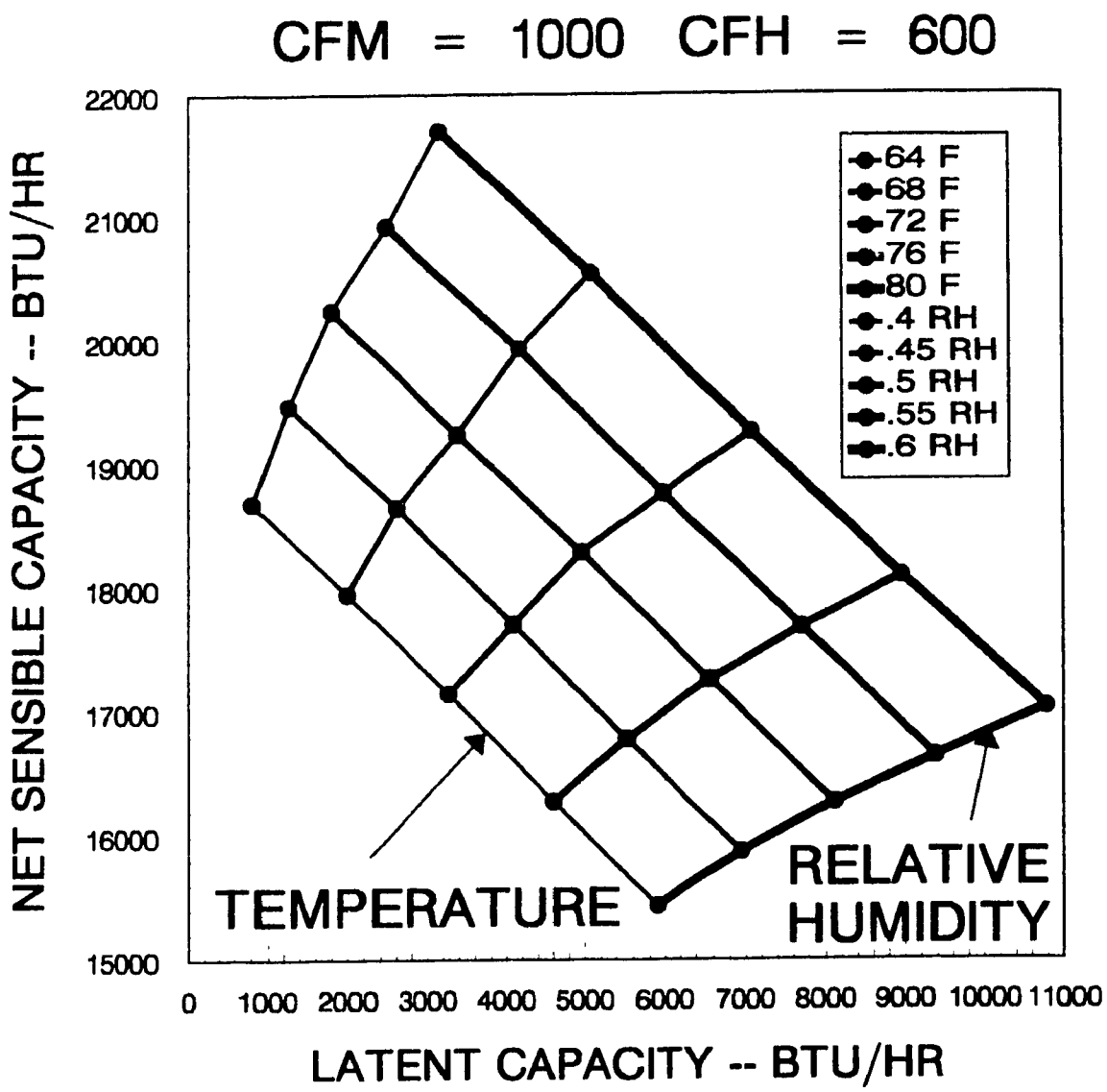

Figure 5.3. Experimental system capacities with a compressor volumetric displacement rate of 600 CFH and a evaporator air flow rate of 1000 CFM.

CHAPTER 6

PROPORTIONAL-INTEGRAL-DERIVATIVE CONTROL OF AIR-CONDITIONING SYSTEM

6.1 Introduction

The basic parameters to be controlled in an air-conditioning system are the space air temperature and the space air relative humidity. In the current research, the controlling action is implemented by varying the compressor volumetric displacement and the evaporator air flow rates by varying the compressor and fan motor speeds respectively. In the automatic control loop of the air-conditioning system, a sensor measures the controlled variable, temperature or relative humidity, and then transfers a signal to a controller. The controller compares that signal value with a set point value and then supplies a control signal to an inverter. The electric power wiring to a motor passes through the inverter. The inverter modulates the frequency of the electric power supply according to the control signal. The speed of the motor is proportional to the frequency of the electrical power supply. The inverter therefore reacts to that control signal to vary the speed of the compressor or fan motor for corrective action. The set-point is the desired value which the controller tries to maintain.

There are many ways to control the air-conditioning system, such as on-off control and proportional-integral-derivative control. In this research the control method used is the proportional-integral-derivative (PID) control. The literature survey shows that the previous studies used a PID control method in air-conditioning applications only to control space temperature. The very important parameter, space relative humidity, is not purposefully controlled with the controlling space temperature action. In this study, two PID controllers are used to simultaneously control both space temperature and relative humidity. This is the main difference between this study and the previous ones.

6.1.1 The sensor

A humidity and temperature probe is used in this research to sense the experimental space conditions. As described in chapter 4, in the controlling loop the space air temperature was measured by an electrical resistance type sensor and the space air relative humidity was monitored by an capacitance type sensor in the probe.

6.1.2 The controller

A microcomputer was used as the controller in this project. The controller was programmed to perform three tasks.

The first task was set to scan instantaneous values of space air temperature every 120 seconds, to process that

scanned space temperature by comparing that present value with set point value and then to send the controlling command to the inverter to control space air temperature.

The second task was set to scan instantaneous values of space relative humidity every 10 seconds, to process that scanned value and then to send a controlling command, which was determined by comparing the present value with the set point value, to the inverter to control space relative humidity.

The third task was to record the values of the space air temperature, the space air relative humidity, air velocity at the evaporator inlet, and compressor and fan motor power inputs for data analysis of the air-conditioning system.

6.1.3 The Inverters

There were two alternating current (AC) variable frequency type controllers, called inverters, used in this research. The first was used to control the speed of the evaporator fan motor and the second one was used to control the speeds of the compressor motor. The frequency outputs from these inverters, in the controlling range, have proportional response to the controlling signals which were sent by the microcomputer.

6.2 Proportional-Integral-Derivative (PID) Control Theory

As it has been mentioned before, two controllers are used

in this research. The controllers operate in the proportional-integral-derivative pattern. The control algorithm of this pattern according to ASHRAE [1991], can be described as:

$$OUT(t) = k_p \bullet e(t) + k_i \bullet \int e(t)\,dt + k_d \bullet de(t) \qquad (6.1)$$

where:

$$e(t) = SP - PV \qquad (6.2)$$

When k_i and k_d are both equal to zero the controller operates as a proportional-only control mode. In the proportional-only control operation the controller outputs a controlling signal proportional to the control variable. Such systems tend to oscillate from one extreme of the controlled variable to the other.

Proportional-only control can be improved by adding an integral mode to the controller to allow it to become proportional-integral (PI) control. The integral term, which is proportional to the history of the error, sums the error (from the starting time to present time) and then adds an integral term to the proportional control output. The integral term forces the system error to be centred around the set-point. In some of the applications the third term (derivative term) is added to let the controller have a faster response and greater stability. A control signal, which is provided by the derivative term, is proportional to the rate at which the

error is changing. The derivative term speeds up or slows down the response of the system to the disturbances. Sometimes the derivative term is not used because this term has a sensitive response to noisy signals and is difficult to tune.

6.3 The Experimental System Description

The experimental system includes software and hardware. The system controlling algorithm, the relationship between power frequency and air flow rate, and the relationship between power frequency and compressor displacement rate are the system software. The air-conditioning system is the experimental system hardware.

6.3.1 Experimental System Controlling Algorithm

The input and output of the experimental PID control loop are scaled into percentage in order to operate the control loop by using control algorithms without a time input. The controller scans the system input and output at a specified rate. Equation (6.1) is then be written as the following:

$$OUT = K_p \bullet EP + K_1 \bullet \Sigma EP + K_d \bullet (EP - EP_{pre}) \qquad (6.3)$$

where EP is the error which is scaled as a percentage, i.e.

$$EP = \frac{SP - PV}{I_{max} - I_{min}} \bullet 100\% \qquad (6.4)$$

I_{max} is maximum possible value of PV and has the same units as

the set point signal value, and I_{min} is minimum possible value of PV and has same units as I_{max} has. The values of K_i and K_d are dependent on the scanning rate of the controller.

The outputs are sent to the inverters to control power frequency. The inverters react the command to vary power frequency proportional with the percentage output value,

$$HZ \propto OUT \tag{6.5}$$

The motor rotation speed is directly proportional to the power input frequency. It can be expressed as:

$$RPM \propto HZ \tag{6.6}$$

The air flow rate (**CFM**) of the evaporator is then proportionally controlled by the controlling output value since **CFM** is proportional to fan speed in the operation range. The relationship of air flow rate to the controller output value is:

$$CFM \propto RPM_{fan} \propto HZ_{fan} \propto OUT_{fan} \tag{6.7}$$

The compressor volumetric displacement rate (**CFH**) of the system is proportionally controlled by the compressor rotation speed. The relationship between compressor volumetric displacement rate and controller output value can then be written as:

$$CFH \propto RPM_{cpr} \propto HZ_{cpr} \propto OUT_{cpr} \qquad (6.8)$$

6.3.2 Relationship Between Power Frequency and Air Flow Rate

A PID controller is used in this study to control the space air relative humidity. The PID controller uses the space air relative humidity (which is the inlet air relative humidity of the evaporator coil) as the PID controller input signal. The PID controller processes that signal by using equation 6.3 and 6.4 and then sends the output signal to an inverter. This inverter varies the frequency of the electricity thereby varying the evaporator fan motor speed, thus controlling the air flow rate of the air-conditioning space.

The air flow rate increases during the experiments if the space relative humidity is lower than the set-point value and decreases if the space relative humidity is higher than the set-point **SP**. The changing of the air flow rate is done by changing the frequency of the power input of evaporator fan motor. The lower fan motor Hz causes lower air flow rate of the system and the higher fan otor Hz causes higher air flow rate of the system in the most operating range.

In the following, 60 Hz was chosen as the basic frequency because the electricity available locally has a frequency of 60 Hz. The relationship between the air flow rate at 60 Hz frequency and a specific frequency can be determined by using the following relation. First the fan motor rotational speed

at a specific frequency is determined by:

$$RPM_{a,spHZ} = RPM_{a,60HZ} \bullet \frac{HZ_{a,specify}}{60} \qquad (6.9)$$

The air flow rate (CFM) versus motor speed (RPM) can then be determined according to the fan law i.e.

$$\begin{aligned} CFM_{spHZ} &= CFM_{60HZ} \bullet \frac{RPM_{a,spHZ}}{RPM_{a,60HZ}} \\ &= CFM_{60HZ} \bullet \frac{HZ_{a,specify}}{60} \end{aligned} \qquad (6.10)$$

6.3.3 Relationship Between Power Frequency and Compressor Volumetric Displacement Rate

A PID control system is used in this study to control the space air temperature. The PID controller uses the space air temperature, which is the input air temperature of the evaporator coil, as the PID controller inlet signal. The PID controller processes the signal from the sensor and then sends a control signal according to equation 6.3 and 6.4 to an inverter. The inverter varies the frequency of the electricity, thereby varying the compressor motor speed, in order to control the compressor volumetric displacement rate.

Changing the frequency of the power input to the compressor motor changes the compressor volumetric displacement rate which directly effects the system refrigerant flow rate.

60 Hz was used as the basic power frequency for the same reason as for the fan motor power. The relationship between the compressor volumetric displacement rate at the frequency of 60 Hz and at the specific frequency can be calculated by using the following relation. The compressor motor rotation speed at a specific frequency is determined by:

$$RPM_{r,spHZ} = RPM_{r,60HZ} \bullet \frac{HZ_{r,specify}}{60} \qquad (6.11)$$

The relationship of the compressor volumetric displacement rates between that compressor working at 60 Hz frequency and working at a specific frequency can then be described as:

$$CFH_{spHZ} = CFH_{60HZ} \bullet \frac{HZ_{r,specify}}{60} \qquad (6.12)$$

6.3.4 The Experimental System

The air-conditioning system, which is described in section 3.1, was used in this research. The system, which used 4 row-coil as its evaporator was located in an experimental space. The air leaving the air-conditioning system went directly into the experimental space and mixes with the space air. During the experiments, heating loads and/or humidity loads were added into the space to simulate a real air-conditioning operation. The space air then entered the air-conditioning system and was cooled and dehumidified by the evaporator.

The air-conditioning system set points were determined by system equilibrium at the following conditions:

- the space set point temperature was 68°F,
- the space set point relative humidity was 45 percent,
- fan motor power frequency at set point was 60 Hz,
- compressor motor power frequency was also 60 Hz,
- 3000 Watts heater power was put into the space,
- 1000 Watts humidifier power was put into the space,
- air flow rate at set point was 1000 CFM (cubic feet per minute),
- compressor volumetric displacement rate at set point was 640 CFH (cubic feet per hour), and
- the total cooling capacity at set point was 20600 BTU/hr.

These values represent average values encountered during the experiment.

The air-conditioning system cooling capacity range and dehumidification range are represented by the performance maps discussed in chapter 5. The following ranges of the experimental conditions were used:

- the minimum fan motor power frequency was 30 Hz,

- the maximum fan motor power frequency was 88 Hz,
- the minimum compressor motor power frequency was 40 Hz,
- the maximum compressor motor power frequency was 72 Hz,
- the range of heater power input to the space was from 0 to 3850 Watts, and
- the range of humidifier power input to the space was from 0 to 2000 Watts.

At 60 Hz, the evaporator fan air flow rate was determined by experimentation to be 1000 CFM. At 60 Hz, the compressor volumetric displacement rate was determined from the compressor manufacture specifications to be 640 CFH. By using equations 6.9 to 6.12 the experimental system air flow rate range was determined from 500 CFM to 1467 CFM, and range of refrigerant flow rate was from 427 CFH to 768 CFH. From performance maps, the total cooling capacity range, at those operation ranges, were from 14000 BTU/hr when the compressor motor works at 40 Hz and evaporator fan motor works at 30 Hz to 26000 BTU/hr when compressor motor worked at 72 Hz and evaporator fan motor works at 88 Hz.

6.4 Conditioned Space

The air-conditioning system, which was used to study PID control, was located in the conditioned space. The volume of

the space was 2700 cubic feet. The mass of air in the space at set point was approximately 200 lb_m.

6.5 Tuning PID Controllers

A trial-and-error method was used in this study to tune the two PID controllers.

6.5.1 Trial-and-Error Method

In this research, the tuning process was divided into the following three steps.

The first step is to tune the space relative humidity PID controller. During the tuning, compressor speed was held at a constant value. First the scan rate was set at 10 seconds. The controller was then tuned as a proportional-only controller. The K_p was determined such that the controlling signal did not oscillate between 0% and 100% rapidly. The controller was then set as a proportional-integral controller. The K_i was determined such that the control signal stabilized at the set point value. The last part was to set the controller as a PID controller. The derivative gain K_d was determined.

The second step was to tune the space temperature PID controller. During the tuning, the fan speed was held at a constant value. The scan rate of this controller was selected to be 120 seconds, which is much larger then the scan rate of the space relative humidity PID controller. The controller was then tuned as a proportional-only controller in order to

select the proportional gain K_p. The K_p was determined such that the control signal did not oscillate between 0% and 100% rapidly. The controller was then set as proportional-integral controller. The integral gain K_i was determined such that the control signal was stabilized at its set point value. The derivative gain K_d for this controller was also tuned during the research. It was found that the derivative term did not improve control. Therefore, the value of K_d was selected to be 0.

The last step was to combine the above two PID controllers into one in order to simultaneously control the space temperature and relative humidity.

6.5.2 K_p, K_i, and K_d for Relative Humidity Control

By using the trial-and-error method the PID control coefficients have been selected as the following:

$$K_p = 10.0$$

$$K_i = 1.0$$

$$K_d = 0.1$$

The following values of the control parameters were used.

I_{max} = 0.75 relative humidity

I_{min} = 0.25 relative humidity

SP = 0.45 relative humidity

Scr_{RH} = 10 seconds

6.5.3 K_p, K_i, and K_d for Temperature Control

By using the trial-and-error method, proportional, integral, and derivative gains have been decided as the following:

$$K_p = -10.0$$

$$K_i = -0.1$$

$$K_d = 0.0$$

The following values for the control parameters were used.

I_{max}	=	100	°F
I_{min}	=	50	°F
SP	=	68	°F
Scr_{temp}	=	120	seconds

6.5.4 Discussion the Tuning Results

The selection of positive or negative values of the PID control coefficients are determined by the system operation characteristics.

In the experiment, two different scan rates were chosen to control space temperature and space relative humidity. A much longer (120 seconds) scan rate was selected to scan values of space temperature compared with the much shorter (10 seconds) scan rate to scan values of space relative humidity. The different values of scan rate were used because space relative humidity responded faster than space air temperature to changes in the system. The different scan rates were also

selected to avoid adverse interaction between the two control systems.

6.6 Experimental Results

The air-conditioning system has been tested after the two sets of K_p, K_i, and K_d have been chosen. During the experiments both space temperature and space relative humidity were controlled simultaneously. The experimental results have been recorded and plotted.

6.6.1 Experimental Description

Figure 6.1, 6.2, and 6.3 give a typical control result. This test was done in typical summer day. The experiment began at 9:00 am (Eastern Daylight Saving time) and ended at 1:00 pm the next day. The experiment lasted for 28 hours. Ambient conditions during experiment were as follows:

- relative humidity was 0.60,
- the highest dry bulb temperature was 84°F, and
- the lowest dry bulb temperature was 68°F.

The experimental conditions were:

- the set-point of experimental space temperature was 68°F,
- the set-point of space relative humidity was 0.45,
- maximum heater power was 3850 Watts, and
- maximum humidifier power input was 1000 Watts.

The following were the initial test conditions:

- space relative humidity was 0.48,
- space dry bulb temperature was 72°F,
- heater power input was 2000 Watts, and
- humidifier power input was 1000 Watts.

During this experiment the heating power was varied from 2000 watts to 3850 watts, and humidifier power also was varied from 0 watts to 1000 watts as shown in Figures 6.1 and 6.3. The experimental results have been recorded by the computer and have been plotted in Figures 6.1, 6.2, and 6.3. Figure 6.1 combines four graphs. It shows the relationship among the humidifier power input, fan power consumption, the air velocity at evaporator coil, and the space relative humidity. Three graphs plotted in Figure 6.2, present the relationships among space heating power input, compressor power consumption and space temperature during experiment. Figure 6.3 shows the total system power inputs during the experimental period. The graph includes the humidifier power input, the heating power input and the total power input. The graphs show that the system has been very well controlled for both space air temperature and air relative humidity.

6.6.2 Discussion of the Experimental Results

The total load input to the conditioned space can be divided into two parts, the applied loads and ambient loads. The applied loads include heater power input and humidifier

power input. The ambient loads include conductive heat transfer, solar radiation, and infiltration. The amount of applied loads can be controlled by adding or reducing the heater and/or humidifier power input. The amount of ambient loads can not be controlled and were determinable during the experiment. It is estimated that the ambient loads comprised from 0 to 50 percent of the total system load. The 0% occurred during the night and 50% occurred during the day.

It has been clearly indicated in Figure 6.1 that the space relative humidity remained at the set-point value of o.45 all the time during the test except at the beginning of the experiment and from the hours 6:45 to 14:20. The deviation from this time period can be explained by the fact that humidifier power input has been cut down to zero between hour 6:45 and hour 23:45 in the conditioned space so that no more moisture had been evaporated into space by humidifier. The space relative humidity is gradually back to set point. This action can be considered due to infiltration. From the hours 6:45 to 14:20, the fan power and air velocity were at their maximum. It is noticed from Figure 6.1 that the fan power graph is very well associated with the humidifier power input. Increasing the humidifier power will lead to decreasing the fan power consumption until the system reaches a new balance. This controlling pattern is expected. It can also be noticed that the evaporator face air velocity and fan power have the same pattern of graphs associated with the humidifier power.

Figure 6.2. shows that the space temperature is maintained at the set-point value during the experiment. Except at the beginning of experiment, the highest deviation is less then 0.5°F. Graphs show that compressor power consumption is positively associated with heating and total power input. It is noticed from the graphs that the compressor power consumption is decreased, from hour 10:00 to 16:00, without applied loads input decreasing. This phenomenon is due to the fact that the total space loads decreased during the night. Hour 10:00 equals 7:00 pm and hour 16:00 equals 1:00 am. During this time period, the ambient temperature gradually dropped to 68°F which equals the conditioned space temperature. Since the temperature differences gradually reduced to zero, the conductive heat transfer from the walls and windows gradually decreased to zero. Also, there is no solar radiation during the night. The main latent load in the evening was due to infiltration which was relatively small. As the results show, the system compressor power consumption is decreased significantly during this period. The compressor power consumption increased from hour 24 to 28 which is from 9:00 am to 1:00 pm. At this time the ambient loads increased though windows, walls, and door. As the result, the compressor power consumption increased during this time period because the total loads in the conditioned space were increased.

Figure 6.1 and 6.2 present a very clear indication that the space relative humidity and the space temperature are very

well controlled in the conditioned space by using the above two PID controllers. Based on the test results, the conclusion can be made that both the space temperature and the space relative humidity have been simultaneously maintained at the set points value during the experiment. The controlling strategy, by controlling compressor speed in order to control the space temperature and controlling fan motor speed to control space relative humidity, was successful.

6.7 Automatic Control Strategy

The control system used in this research is to control fan motor speed to control space relative humidity, and to control compressor motor speed to control space temperature. During the course of the current research, efforts were made to control compressor motor speed to control space relative humidity, and to control fan motor speed to control space temperature. It was not possible to determine PID coefficients for this alternate control strategy. In order to determine the reason, four more system performance maps, Figure 6.4 to 6.7, were made. In these maps source temperature (T_{SRC}) and source relative humidity (RH_{SRC}) are held constant while evaporator air flow rate (**CFM**) and compressor volumetric displacement rate (**CFH**) are varied.

- Figure 6.4 is net sensible cooling capacity versus **CFM** for different **CFH**s.
- Figure 6.5 is net sensible cooling capacity versus

CFH for different **CFM**s.

- Figure 6.6 is latent cooling capacity versus **CFH** for different **CFM**s.
- Figure 6.7 is latent cooling capacity versus **CFM** for different **CFH**s.

These figures can be divided into two set, and analyzed by comparing system performance characteristics of each set.

Figure 6.4 and 6.5 are the first set showing the net sensible cooling capacity characteristics. Figure 6.4 shows increasing **CFM** may result in increased or decreased net sensible cooling capacity depending on the operating condition. This occurs because the gain in evaporator heat transfer due to increased **CFM** is negated by the increased fan motor power consumption. The fan motor power consumption is proportional to the cube of **CFM** according to Equation 3.30. At low **CFH** and high **CFM**, increasing the **CFM** results in decreased net sensible cooling capacity therefore the control is not applicable for this region. For other operating conditions, increasing the **CFM** results in increased net sensible cooling capacity therefore control is applicable for these region. Figure 6.5 shows increasing the **CFH** always results in increased net sensible cooling capacity therefore control is applicable for all operating condition.

Figure 6.6 and 6.7 are the second set showing the latent cooling capacity characteristics. Figure 6.6 shows increasing the **CFH** results in increased latent cooling capacity for all

operating condition. Therefore, control is always applicable. Figure 6.7 shows increasing the CFM results in decreased latent cooling capacity for all operating condition. Therefore, control is always applicable.

6.8 Speed Limitations

A semi-hermetic compressor was used in the experimentation. The compressor motor speed was 1750 rpm with a power supply frequency of 60 Hz. It was observed during the experiment that at low compressor speeds with a power supply frequency less than 40 Hz, there was a possibility of excess vibration. It was also observed that at low fan speeds and high compressor speeds there was a possibility of coil frosting.

6.9 Nomenclature

CFH	compressor volumetric displacement rate
CFH_{spHz}	compressor volumetric displacement rate at specific compressor motor frequency
CFH_{60Hz}	compressor volumetric displacement rate at 60 Hz compressor motor frequency.
CFM	evaporator air flow rate
CFM_{spHz}	evaporator air flow rate at specific fan motor frequency
CFM_{60Hz}	evaporator air flow rate at 60 Hz fan motor frequency

EP	deviation in percentage
EP_{pre}	previous deviation in percentage
e(t)	the present deviation from set point at time t
$HZ_{a,specify}$	specific fan motor power frequency
$HZ_{r,specify}$	specific compressor motor power frequency
I_{max}	maximum value of PV which has the same units as the set point signal value
I_{min}	minimum value of PV which has same units as I_{max} has
k_d	derivative gain constant
k_i	integral gain constant
k_p	proportional gain constant
OUT	controller output
OUT_{cpr}	compressor motor controller output
OUT_{fan}	fan motor controller output
PV	present value at time t. Here the present values are the actual value of the space temperature or the space relative humidity
RH_{SRC}	source relative humidity
$RPM_{a,spHz}$	fan motor rotational speed at a specific frequency
$RPM_{a,60Hz}$	fan motor rotational speed at 60 Hz frequency
$RPM_{r,spHz}$	compressor motor rotational speed at a specific frequency
$RPM_{r,60Hz}$	compressor motor rotational speed at 60 Hz frequency
Scr_{RH}	scan rate to control space relative humidity
Scr_{temp}	scan rate to control space temperature
SP	set point value. Here the set points are the

	desired values of the space temperature or the space relative humidity
t	time
T_{SRC}	source temperature

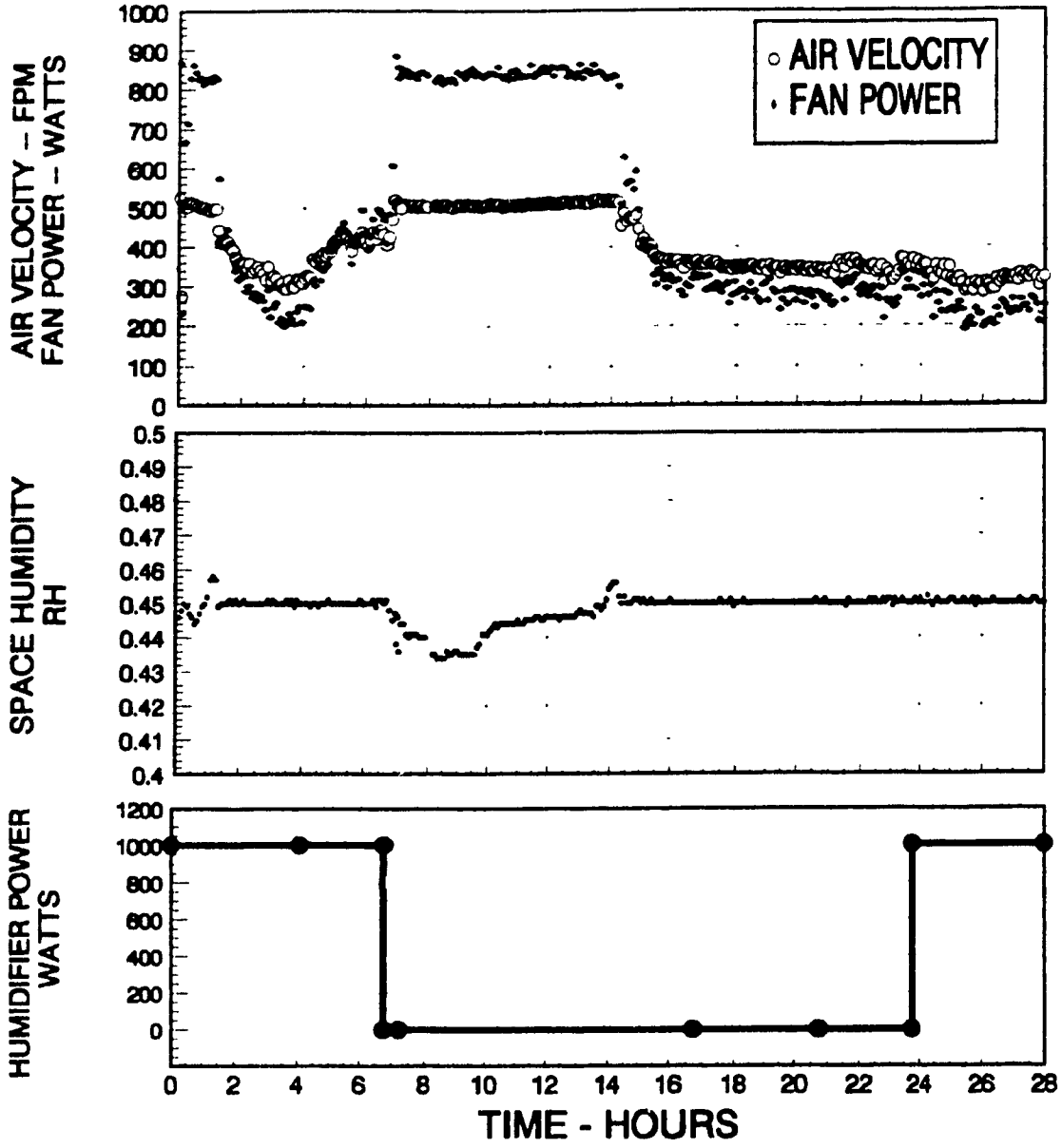

Figure 6.1. Experimental results--space relative humidity, humidifier power, space air velocity and fan power versus time.

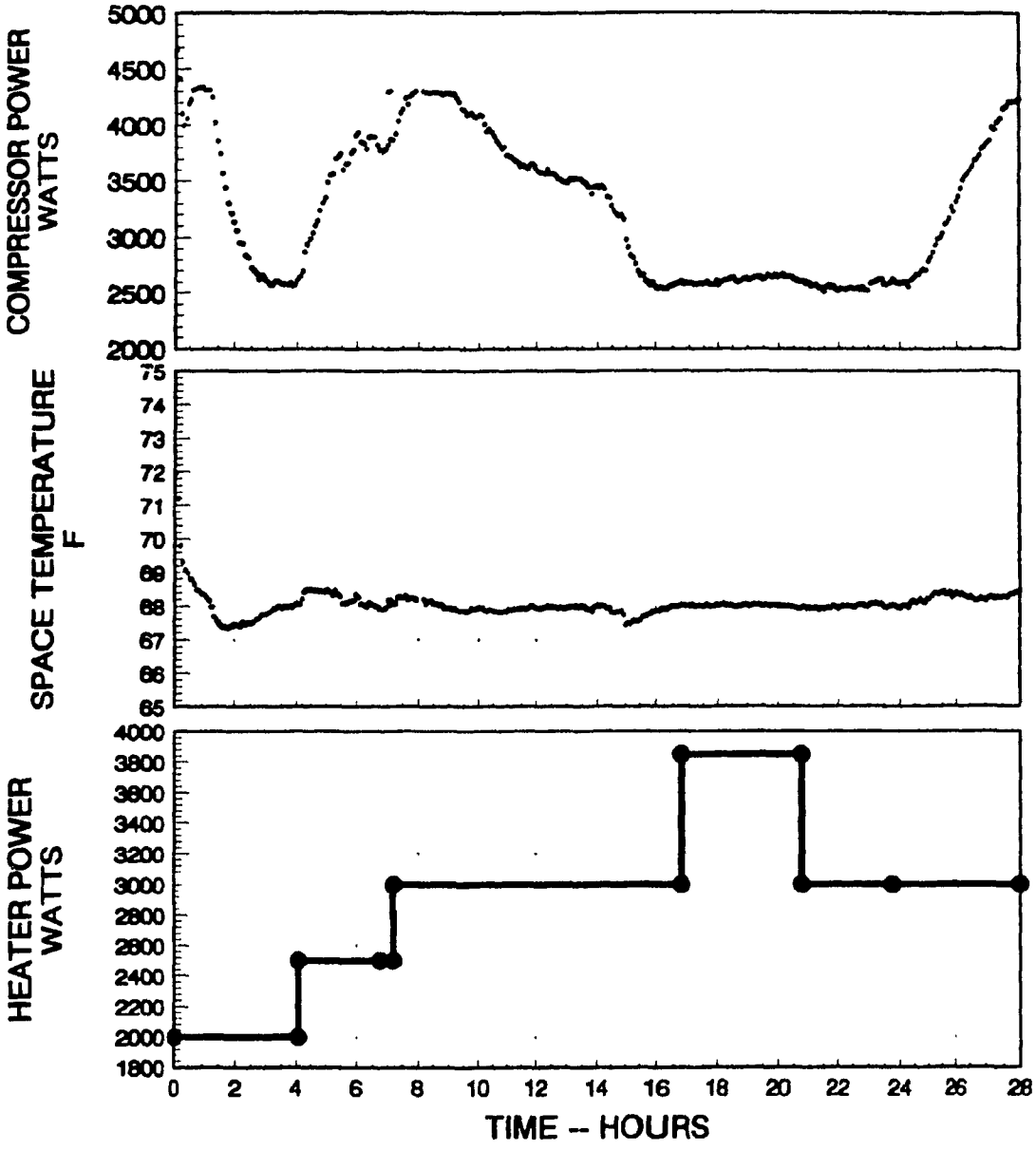

Figure 6.2. Experimental results--space temperature, compressor power and heater power versus time.

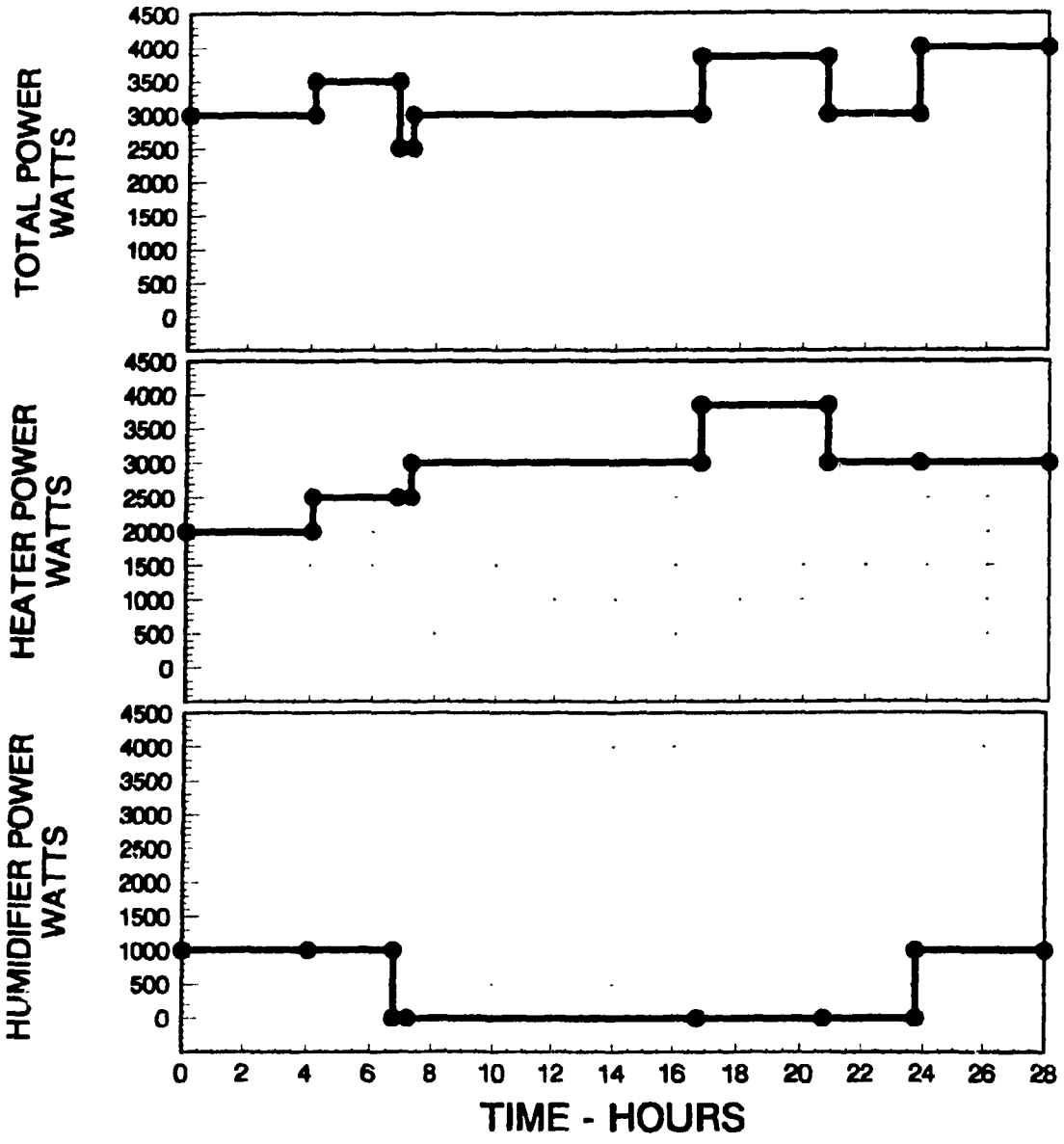

Figure 6.3. Space power input, heater, humidifier, and total power versus time.

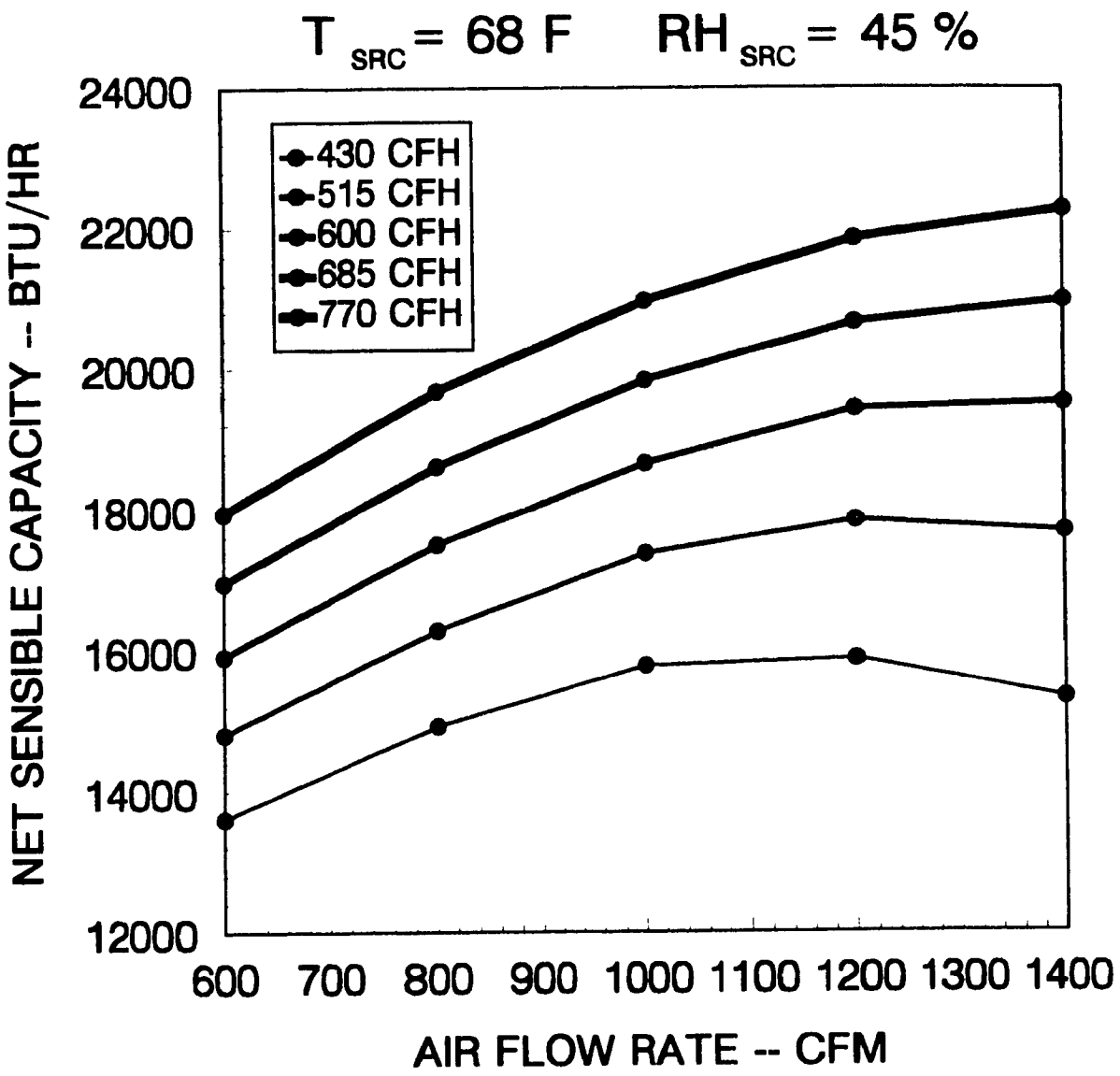

Figure 6.4. System net sensible capacity versus evaporator air flow rate.

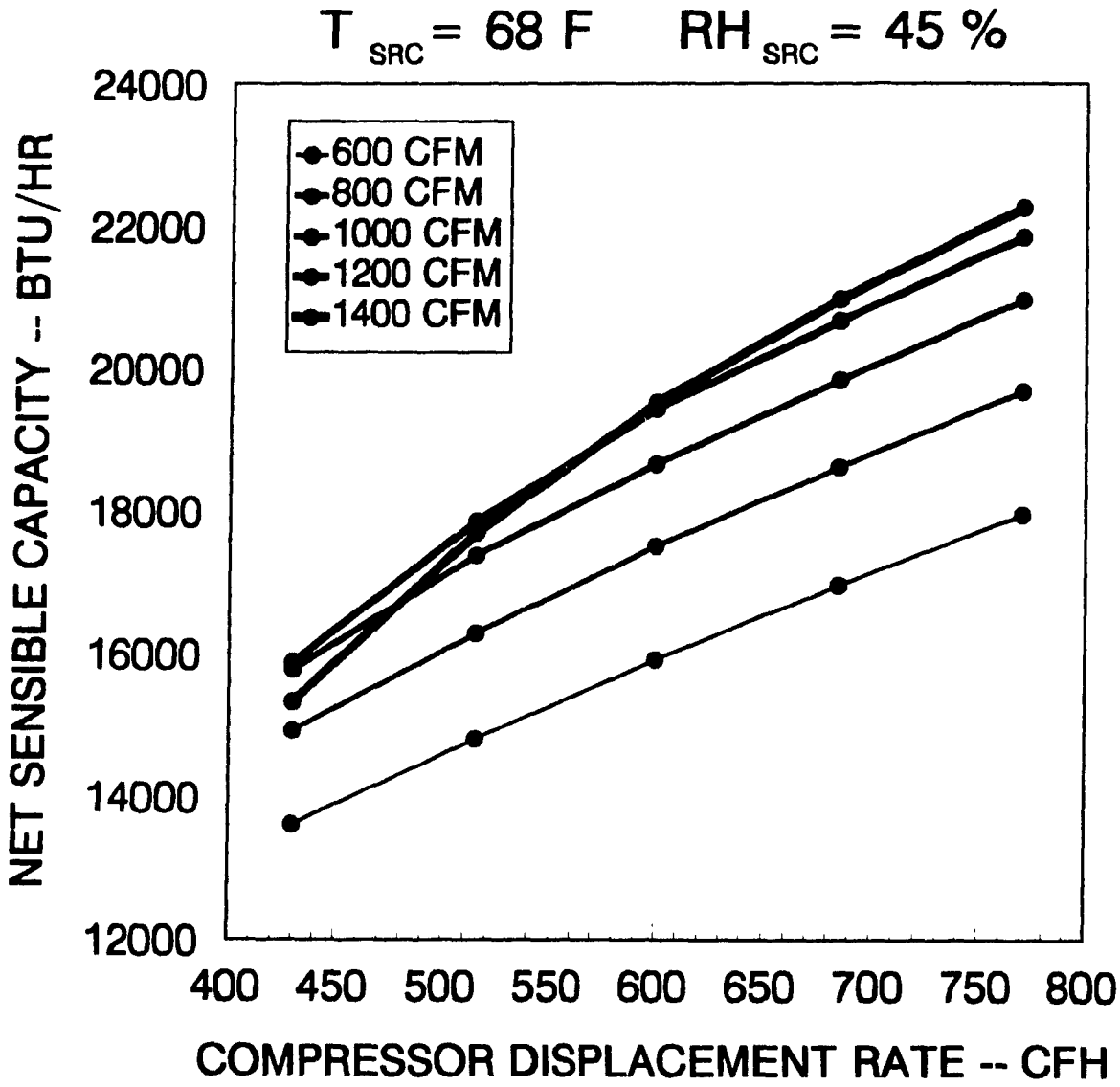

Figure 6.5. System net sensible capacity versus compressor volumetric displacement rate.

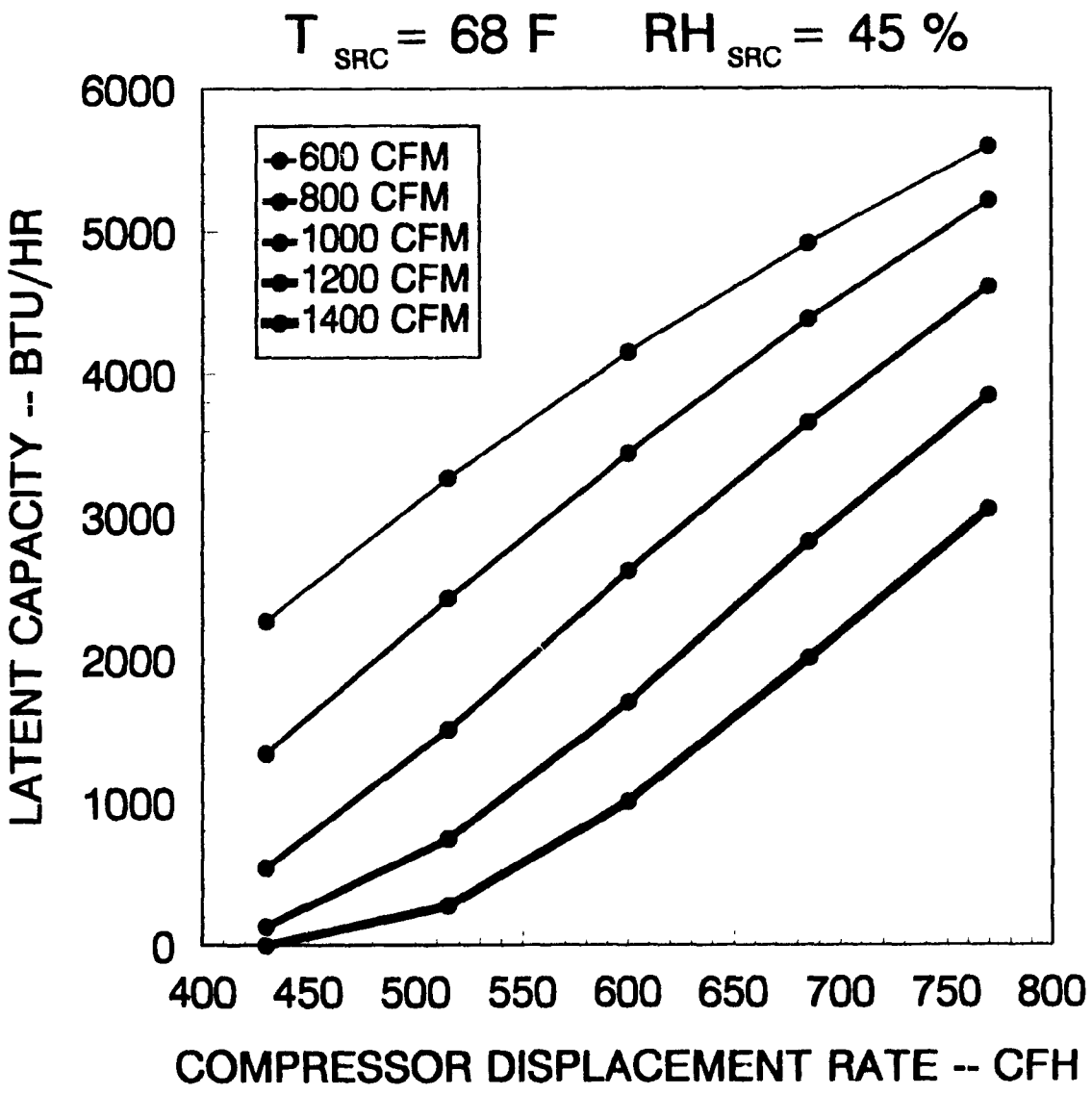

Figure 6.6. System latent capacity versus compressor volumetric displacement rate.

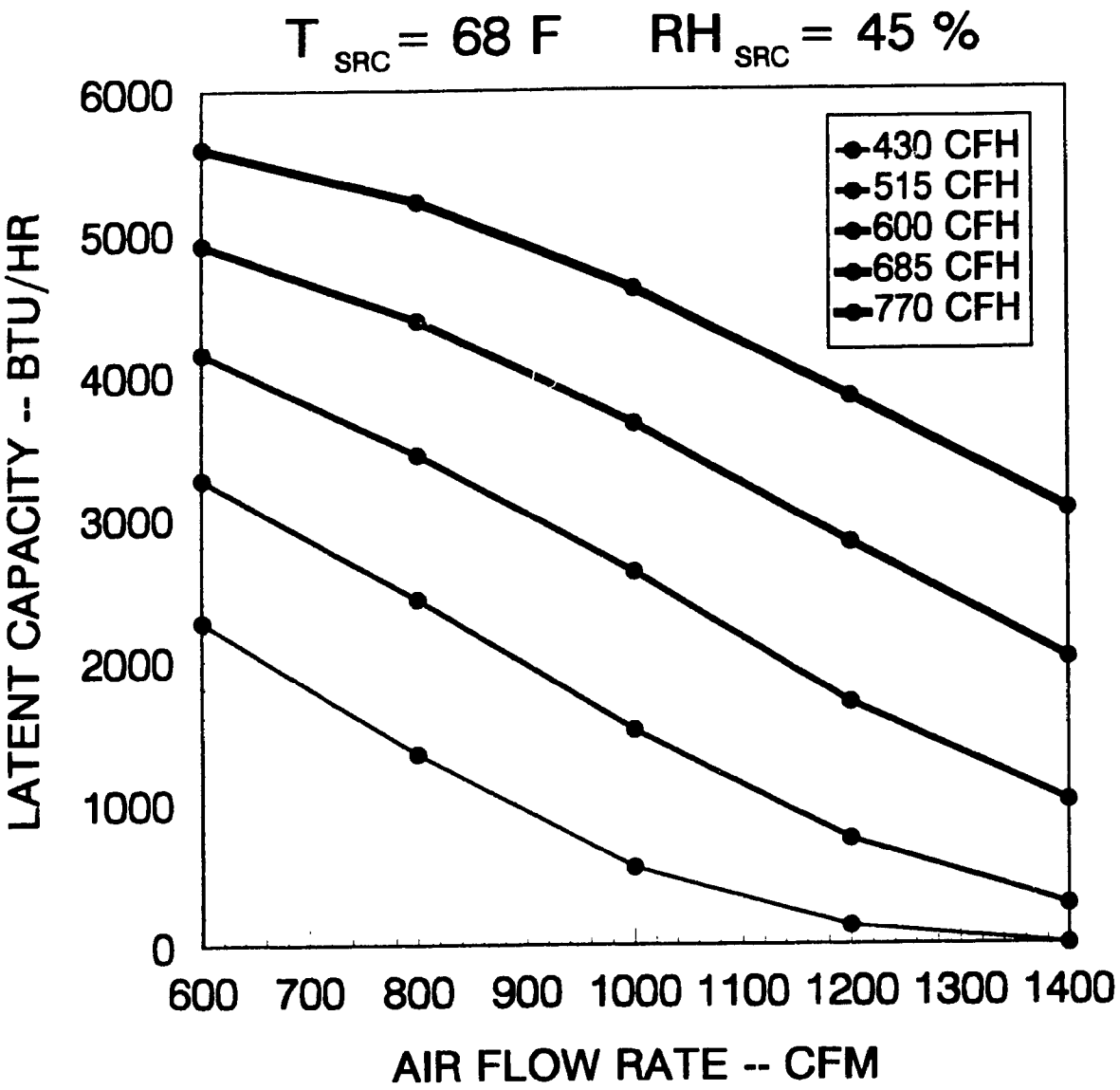

Figure 6.7. System latent capacity versus evaporator air flow rate.

CHAPTER 7

CONCLUSIONS

A proportional-integral-derivative controlling system to simultaneously ccntrol space air temperature and space relative humidity has been studied in this thesis. This control system used two PID control loops. One was utilized to control the evaporator motor speed, thereby varying the evaporator air flow rate, in order to control space relative humidity. Another one controlled compressor motor speed, thereby varying the compressor volumetric displacement rate, in order to control space air temperature. Experiments were done to study the control system.

An air-conditioning system model, which is derived from Krakow and Lin [1986] heat pump model, has been developed in this thesis. The system model employed the three-region evaporator model by Oskarsson et. al. [1989]. The model has been validated experimentally and been used to create performance maps.

Based on the experimental results for both the PID control system and the air-conditioning system model the following conclusions can be made.

1 The studied proportional-integral-derivative controlling system successfully controlled the space temperature and

relative humidity. The differential of space temperature during experiment is within ±0.5°F. The differential of relative humidity is ±0.01. Thus space air temperature and relative humidities may accurately be controlled by using the PID control method.

2 The present control strategy, by simultaneously controlling fan motor speed in order to control the conditioned space relative humidity and controlling compressor speed in order to control the space temperature, was successful. The alternate control strategy, controlling compressor motor speed to control space relative humidity and controlling fan motor speed to control space temperature, does not appear practically feasible.

3 The air-conditioning system model is satisfactory to simulate an air-conditioning system performance. The model shows ranges of sensible and latent cooling capacities for which an air-conditioning system is suitable. The performance maps, which were created by model, provided direct and convenient tools to study system behaviour, to determine and to optimize air-conditioning system performance.

Energy consumption was not studied in this research. Future studies comparing energy consumption of air-conditioning systems, for specific applications, using PID control with on-off control are needed.

REFERENCES

ASHRAE, 1989, ASHRAE Handbook 1989 Fundamentals, American Society of Heating, Refrigeration, and Air Conditioning Engineers, Inc.

ASHRAE, 1991, ASHRAE Handbook 1991 Heating, Ventilating and Air-Conditioning Applications, American Society of Heating, Refrigeration, and Air Conditioning Engineers, Inc.

Bekker, J.E., Meckl, P.H., Hittle, D.C., 1991, "A Tuning Method For First-Order Processes With PI Controllers", Vol. 97, Part 2.

Brothers, P.W., Warren, M.L., 1986, "Fan Energy Use in Variable Air Volume Systems", ASHRAE Transactions, Vol. 92, Part 2B.

Cecchini, C., Marchal, D., 1991, "A Simulation Model of Refrigerating And Air-Conditioning Equipment Based on Experimental Data", ASHRAE Transactions, Vol. 97, Part 2.

Fertik, H.A., Ross, C.W., 1967, "Direct Digital Control Algorithm With Anti-Windup Feature", ISA Transactions, Vol. 6.

Goff, K.W., 1966, "Estimating Characteristics and Effects of Noisy Signals", ISA Journal, November.

Goff, K.W., 1966, "A Systematic Approach to DDC Design", ISA Journal, December.

Hamilton, J.F., Miller, J.L., 1990. "A simulation Program For Modelling An Air-Conditioning System", ASHRAE Transactions, Vol. 96, Part 1.

Howell, R.H., Ganesh, R., Sauer, H.J., 1987, "Comparison of Two Control Strategies To Simulate Part-Load Performance of A Simple Air-Conditioning System", ASHRAE Transactions, Vol. 93, Part 2.

Kartsonnes, G.T., Erth, R.A., 1971, "Computer Calculations of the Thermodynamic Properties of Refrigerants 12, 22, and 502" ASHRAE Transactions, Vol.77, Part 2.

Kays, W.M., London, A.L., 1964, Compact Heat Exchangers, McGraw-Hill Book Company.

Krakow, K.I., Lin, S., 1987. "A Numerical Model of Heat Pumps Having Various Means of Refrigerant Flow Control and Capacity Control", ASHRAE Transactions, Vol. 93, Part 2.

May, W.B., Borresen, B.A., Hurley, C.W., 1982, "Direct Digital Control of a Pneumatically Actuated Air-Handling Unit", ASHRAE Transactions, Vol.88, Part 2.

Nesler, C.G., Stoecker, W.F., 1984, "Selecting the Proportional and Integral Constants in the Direct Digital Control of Discharge Air Temperature", ASHRAE Transactions, Vol. 90, Part 2B.

Oskarsson, S.P., 1988. "Evaporator Modelling Under Conditions of Dry, Wet, and Frosted Finned Surfaces", Master Thesis, Concordia University, Montreal, Canada.

Oskarsson, S.P., Krakow, K.I., Lin, S., 1990. "Evaporator Models For Operation With Dry, Wet, and Frosted Finned Surfaces Part I: Heat Transfer and Fluid Flow Theory", ASHRAE Transactions, Vol. 96, Part 1.

Oskarsson, S.P., Krakow, K.I., Lin, S., 1990. "Evaporator Models For Operation With Dry, Wet, and Frosted Finned Surfaces Part II: Evaporator Models and Verification", ASHRAE Transactions, Vol. 96, Part 1.

Shavit, G., Brandt, S.G., 1982, "The Dynamic Performance of a Discharge Air-Temperature System With a P-I Controller", ASHRAE Transactions, Vol. 88, Part 2.

Shaw, A., Luxton, R.E., 1988, "A Comprehensive Method of Improving Part-Load Air-Conditioning Performance", ASHRAE Transactions. Vol. 94, Part 1.

Spitler, J.D., Pedersen, C.O., Hittle, D.C., Johnson, D.L., 1986, "Fan Electricity Consumption for Variable Air Volume", ASHRAE Transactions. Vol. 92, part 2B.

Stoecker, W.F., Daber, R.P., 1978, "Conserving Energy in Dual-Duct Systems by Reducing the Throttling Ranges of Air-Temperature Controllers", ASHRAE Transactions. Vol. 84, Part 1.

Stoecker, W.F., Rosario, L.A., Heidenreich, M.E., Rhelan, T.R., 1978, "Stability of an Air-Temperature Control Loop", ASHRAE Transactions. Vol. 84, Part 1.

Stoecker, W.F., Stoecker, P.A. 1989, Microcomputer control of Thermal and Mechanical Systems, Van Nostrand Reinhold Book Company.

Wallenborg, A.O., 1991, "A new Self-Tuning Controller For HVAC Systems", ASHRAE Transactions, Vol. 97, Part 1.

Ziegler, J.G., Nichols, N.B., 1942. "Optimum Settings for Automatic Controllers", ASME Transactions, Vol. 64.

BIBLIOGRAPHY

Atkinson, G.V., 1986, "VAV System Volume Control Using Electronic Strategies", ASHRAE Transactions, Vol. 92, Part 2B.

Chapman, W.F., 1984, "Back to Basics in HVAC Control", ASHRAE Transactions, Vol. 90, Part 2B.

Coggan, D.A., 1986, "Control Fundamentals Apply more than ever to DDC", ASHRAE Transactions, Vol. 92, Part 1B.

Dabiri, A.E., 1982, "A Steady State Computer Simulation Model for Air-to-Air Heat Pumps", ASHRAE Transactions, Vol. 88, Part 2.

Johnson, G.A., 1984, "Retrofit of a Constant Volume Air System for Variable Speed Fan Control", ASHRAE Transactions, Vol. 90, Part 2B.

Krakow, K.I., Lin, S., 1990, "Secondary Heat Transfer in Heat Pumps", ASHRAE Transactions, Vol. 96, Part 1.

Krakow, K.I., Lin, S., Matsuki, K., 1987, "A Study of Primary Effects of Various Means Of Refrigerant Flow Control and

Capacity Control on the Seasonal Performance of a Heat Pump", ASHRAE Transactions, Vol. 93, Part 2.

Krakow, K.I., Lin, S., Oskarsson, S.P., 1990, "A Method Determining The Effects of Coil Geometry and Fan Type on Evaporator Frosting", ASHRAE Transactions, Vol. 96, Part 1.

Mcquiston, F.C., 1981, "Finned Tube Heat Exchangers: State of the Art for the Air Side", ASHRAE Transactions, Vol. 87, Part 1.

McQuiston, F.C., Parker, J.D., 1988, Heating, Ventilation, and Air-Conditioning Analysis and Design, John Wiley & Sons, Inc.

Turaga, M., Lin, S., Fazio, P.P., 1988, "Correlations for Heat Transfer and Pressure Drop Factors for Direct Expansion Air Cooling And Dehumidifying Coils", ASHRAE Transactions, Vol. 94, Part 2.

Virk, G.S., Loveday, D.L., 1991, "A Comparison of Predictive, PID, and On/off Techniques for Energy Management and Control", ASHRAE Transactions, Vol. 97, Part 2.

Walker, C.A., 1984, "Application of Direct Digital Control to a Variable Air Volume System", ASHRAE Transactions, Vol. 90, Part 2B.

Warwick, K., 1990, Control Systems An Introduction, Prentice Hall Book Company.

Wichman, P.E., 1984, "Improved Local Loop Control Systems", ASHRAE Transactions, Vol. 90, Part 2B.

Williams, V.A., 1984, "Energy Conservation by Direct Digital Control", ASHRAE Transactions, Vol. 90, Part 2B.

APPENDIX I

TABLE OF CONVERSION FACTORS

Length

1 ft = 0.30480 m	1 m = 3.2808 ft
1 in = 2.5400 cm	1 cm = 0.39370 in

Area

1 ft^2 = 0.092903 m^2	1 m^2 = 10.76392 ft^2

Volume

1 ft^3 = 28.317 litre	1 litre = 0.035315 ft^3

Mass

1 lb_m = 0.4535924 kg	1 kg = 2.204622 lb_m

Energy

1 BTU = 1.0551 kJ	1 kJ = 0.948 BTU

Power

1 BTU/hr = 0.29307 W	1 W = 3.412 BTU/hr

Pressure

1 PSI = 6.89476 kPa	1 kPa = 0.14504 PSI

Temperature

T(°F) = 1.8 × T(°C) + 32	T(°C) =(T(°F)-32)÷1.8

Temperature Difference

T(°F) = 1.8 × T(°C)	T(°C) = 5/9 × T(°F)

Specific Heat

1 BTU/(lb_m•°F) = 4.1868 kJ/(kg•K)

1 kJ/(kg•K) = 0.2388 BTU/(lb_m•°F)

APPENDIX II

COMPUTER PROGRAM LISTINGS

```
      PROGRAM ACSYSE2
      DIMENSION CFMX(5),CFHX(5),TSRCX(5),RHSRCX(5)
      COMMON/XOUT/QTOTX(5,5),SHFX(5,5),QSENX(5,5),QLATX(5,5),
     #COPX(5,5),I,J
      COMMON/AA/TC,TE,VFACE
      COMMON/AB/HTEI1D,HTEI2D,HTEI1W,KCYC
      COMMON/AC/CHTCAP,CHTE0,CHTE1,DTSC,TSNK,QCOND,ICD
      COMMON/AE/EHOV1,CCOV1,EDTSH3,EX3,ROWDT,CIRC,IMIX
      COMMON/AR/DCFH,CL,REFLO,EFFI0,DEFFI,QCO0,DQCO,EE0,
     #DEE,FLOF,VERMD,IVE
      COMMON/GEOM/DO,Y,DI,KFIN,FPI,HT,ROWD,HC,DC,LENGTH,
     #FINS,S,DPTH,CKTS,ROWH,WDTH,FACOIL,HCONT,HFOULI,
     #NCKTS,IGEOM
      COMMON/CONST/XSET,CPAD,HFGW
      COMMON/TD/DTSH
      COMMON/TRC/CFHZ,CFMZ,K
      COMMON/PWR/EPOWER,CFPWR,EFPWR0,CFM0
      REAL MFA,MFR,KFIN,LENGTH
      CHARACTER*20 FNAME,FNAME2,FNAME3,FNAME4
C
C     DESCRIPTION OF PROGRAM
C
C     INPUT
C     ICALC      IF ICALC=1 CFM AND CFH CHANGED;
C                IF ICALC=2 TSRC AND RHSRC CHANGED;
C                IF ICALC=3 CFM AND RHSRC CHANGED;
C                IF ICALC=4 CFM AND TSRC CHANGED;
C                IF ICALC=5 CFH AND RHSRC CHANGED;
C                IF ICALC=6 CFH AND TSRC CHANGED
C     TSRC0      INITIAL SOURCE TEMP
C     DTSRC      SOURCE TEMP VARIATION
C     NTSRC      SOURCE TEMP NUMBER
C     RHSRC0     INITIAL SOURCE RH
C     DRHSRC     SOURCE RH VARIATION
C     NRHSRC     SOURCE RH NUMBER
C     TSNK       SINK TEMP
C
C     COMPRESSORS
C     NREF       REFRIGERANT NUMBER  12 22 502
C     DCFH0      INITIAL DISPLACEMENT   CU.FT/HR
C     DDCFH      DISPLACEMENT VARIATION   CU.FT/HR
C     CL         CLEARANCE VOLUME DECIMAL FRACTION
C     REFLO      REFERENCE MASS FLOW RATE
C     EFFI0      ISENTROPIC EFFICIENCY AT REFLO
C     DEFFI      D(EFFI)/D(MASS FLOW RATIO)
C     QCO0      HEAT TRANSFER COEFFICIENT (CRANKCASE) AT REFLO
```

```
C     DQCO      D(QCO)/D(MASS FLOW RATIO)
C     EE0       COMPRESSOR MOTOR ELECTRICAL EFFICIENCY AT
C               REFLOW
C     DEE       D(EE)/D(MASS FLOW RATIO)
C     VERMD     VOLUME EFFICIENCY RATIO; BASED ON
C               MANUFACTURES'
C               DATA
C     IVE       IF IVE=1 USE VERMD;
C               IF IVE=2 USE VER
C
C     CONDENSER
C     DTSC      DEGREES F SUBCOOLING
C     CHTE0     COND HT TRANS EFFECTIVENESS COEF
C     CHTE1     COND HT TRANS EFFECTIVENESS COEF
C               CHTE=CHTE0+CHTE1*PPHR
C     CHTCAP    COND HT CAPACITY  BTU/(HR DEG F)
C     ITC0      INITIAL APPROX OF TC
C               IF ITC0=0 THEN TC=TSNK+20
C               IF ITC0 > 0 THEN TC=ITC0
C     ICD       IF ICD=0 AIR COOLED
C               IF ICD=1 WATER VALVE CONTROL
C     PCD       PC FOR WATER VALVE CONTROL
C
C     EVAPORATOR INPUT
C     CFM0      INITIAL AIR FLOW RATE     CFM
C     DCFM      AIR FLOW RATE VARIATION   CFM
C     ITE0      INITIAL APPROX OF TE
C               IF ITE=0 THEN TE=TSRC1-30
C
C     INTERCHANGERS 1 2  SUCTION/LIQUID
C     HTEI1D    HT TRANS EFFECTIVENESS - ENTERING SUCTION
C               SIDE DRY
C     HTEI2D    HT TRANS EFFECTIVENESS - ENTERING SUCTION
C               SIDE DRY
C     HTEI1W    HT TRANS EFFECTIVENESS - ENTERING SUCTION
C               SIDE WET
C
C     THROTTLING DEVICE
C    DTSH     DEGREES F SUPERHEAT FOR THERMO EXPANSION VALVE
C
C     DATA FOR AIR CONDITIONING SYSTEM PERFORMANCE
C     EFANW     EVAPORATOR FAN WATTS
C     CFANW     CONDENSER FAN WATTS
C
C     QUANTITIES CALCULATED BY SYSTEM
C     QEVAP QCOND POWER QHI QRV   BTUH
C     PPHR      LBM/HR
C
      WRITE(5,10)
   10 FORMAT(4X,'INPUT FILE NAME    ?  '$)
      READ(5,15) FNAME
   15 FORMAT(A20)
```

```
      OPEN(UNIT=1,FILE=FNAME,STATUS='OLD')
      WRITE(5,20)
   20 FORMAT(4X,'OUTPUT FILE 2 NAME ?  '$)
      READ(5,15) FNAME2
      OPEN(UNIT=2,FILE=FNAME2,STATUS='NEW')
      WRITE(5,25)
   25 FORMAT(4X,'OUTPUT FILE 3 NAME ?  '$)
      READ(5,15) FNAME3
      OPEN(UNIT=3,FILE=FNAME3,STATUS='NEW')
      WRITE(5,30)
   30 FORMAT(4X,'OUTPUT FILE 4 NAME ?  '$)
      READ(5,15) FNAME4
      OPEN(UNIT=4,FILE=FNAME4,STATUS='NEW')
C
      WRITE(2,35)
   35 FORMAT(/,2X,'PROGRAM VERSION: ACSYSE2-1993 MAY 07')
C
      WRITE(2,40) FNAME
   40 FORMAT(/,4X,'INPUT FILE NAME:     ',A20)
      WRITE(2,45) FNAME2
   45 FORMAT(/,4X,'OUTPUT FILE 2 NAME:  ',A20)
      WRITE(2,50) FNAME3
   50 FORMAT(/,4X,'OUTPUT FILE 3 NAME:  ',A20)
      WRITE(2,55) FNAME4
   55 FORMAT(/,4X,'OUTPUT FILE 4 NAME:  ',A20)
      READ(1,*) ICALC
      WRITE(2,60) ICALC
   60 FORMAT(11X,'ICALC',/,5X,I10)
      WRITE(3,65) ICALC
   65 FORMAT(' \ ICALC ',I5)
C
      READ(1,*) TSRC0,DTSRC,RHSRC0,DRHSRC,TSNK,NEVP,NCPR,
     #NTSRC,NRHSRC
      WRITE(2,70) TSRC0,DTSRC,RHSRC0,DRHSRC,TSNK,NEVP,NCPR,
     #NTSRC,NRHSRC
   70 FORMAT(/,10X,'TSRC  DTSRC  RHSRC DRHSRC   TSNK   NEVP',
     #'   NCPR  NTSRC NRHSRC',/,7X,2F7.1,2F7.3,F7.1,4I7)
C
C     COMPRESSOR
      READ(1,*)   DCFH0,DDCFH,CL,REFLO,VERMD,IVE
      WRITE(2,75) DCFH0,DDCFH,CL,REFLO,VERMD,IVE
   75 FORMAT(/,4X,'COMPRESSOR',//,9X,'DCFH0     DDCFH',
     #'         CL     REFLO     VERMD',
     #'        IVE',/,4X,2F10.1,F10.3,F10.1,F10.4,I10)
C
      READ(1,*) EFFI0,DEFFI,QCO0,DQCO,EE0,DEE
      WRITE(2,80) EFFI0,DEFFI,QCO0,DQCO,EE0,DEE
   80 FORMAT(/,9X,'EFFI0      DEFFI      QCO0       DQCO',
     #'        EE0       DEE',/,4X,6F10.4)
C
C     CONDENSER
      READ(1,*)   DTSC,CHTE0,CHTE1,CHTCAP,ITC0,ICD,PCD
```

```
      WRITE(2,85) DTSC,CHTE0,CHTE1,CHTCAP,ITC0,ICD,PCD
   85 FORMAT(/,4X,'CONDENSER',//,10X,'DTSC     CHTE0',
     #'     CHTE1    CHTCAP      ITC0        ICD',
     #'       PCD',/,4X,F10.2,2F10.6,F10.1,2I10,F10.0)
C
C     EVAPORATOR
C
      READ(1,*) NREF,XSET,CPAD,HFGW,IMIX,ITE0
      WRITE(2,90) NREF,XSET,CPAD,HFGW,IMIX,ITE0
   90 FORMAT(/,4X,'EVAPORATOR',//,11X,'NREF      XSET',
     #'      CPAD      HFGW      IMIX      ITE0',
     #/5X,I10,2F10.3,F10.2,2I10)
C
C-----------------------------
C  COIL GEOMETRY IS SPECIFIED
C-----------------------------
C
      READ(1,*) WDTH,HT,DPTH,CKTS,ROWH,ROWD
      WRITE(2,95) WDTH,HT,DPTH,CKTS,ROWH,ROWD
   95 FORMAT(/,11X,'WDTH        HT      DPTH      CKTS',
     #6X,'ROWH      ROWD',/,5X,3F10.4,3F10.2)
C
      READ(1,*) DO,DI,Y,KFIN,FPI
      WRITE(2,100) DO,DI,Y,KFIN,FPI
  100 FORMAT(/,13X,'DO         DI          Y      KFIN',
     *7X,'FPI',/,5X,3F10.5,2F10.2)
C
      READ(1,*) HCONT,HFOULI
      WRITE(2,105) HCONT,HFOULI
  105 FORMAT(/,10X,'HCONT    HFOULI',/,5X,2F10.0)
C
C-------------------------------------------------------
C INCOMING AIR AND REFRIGERANT PROPERTIES ARE SPECIFIED.
C-------------------------------------------------------
C
      READ(1,*) CFM0,DCFM
      WRITE(2,110) CFM0,DCFM
  110 FORMAT(/,11X,'CFM0      DCFM',/5X,2F10.1)
C
C     INTERCHANGER - SUCTION-LIQUID HEAT EXCHANGER
      READ(1,*)   HTEI1D,HTEI2D,HTEI1W
      WRITE(2,115) HTEI1D,HTEI2D,HTEI1W
  115 FORMAT(/,4X,'HEAT EXCHANGER',//,8X,'HTEI1D',
     #'    HTEI2D    HTEI1W',/,4X,4F10.3)
C
C     THROTTLING DEVICE
      READ(1,*) DTSH
      WRITE(2,120) DTSH
  120 FORMAT(/,4X,'THROTTLING DEVICE',//,10X,'DTSH',/,
     #4X,F10.3)
C
      READ(1,*) CFANW,EFANW0
```

```
      WRITE(2,125) CFANW,EFANW0
  125 FORMAT(/,4X,'DATA FOR SYSTEM PERFORMANCE',
     #' COEFFICIENT',//,9X,'CFANW    EFANW0',/,4X,2F10.0/)
      CFPWR=CFANW*3.413
      EFPWR0=EFANW0*3.413
C
      WRITE(2,290)
C
C-------------------------------------------------------
C VARIABLES USED IN PROPERTY SUBROUTINES ARE INITIALIZED
C BY CALLING THE FOLLOWING DATA SUBROUTINES.
C-------------------------------------------------------
C
      CALL DATA(NREF)
      CALL DATAV(NREF)
      CALL DATAK(NREF)
      CALL DATASH(NREF)
      IGEOM=1
      KCYC=0
      FLOF=0
      TSRC=TSRC0
      RHSRC=RHSRC0
C     DATA = REFRIGERANT PROPERTIES PARAMETERS
C
      ITR=100
      IF(ITE0.EQ.0) THEN
          TE=TSRC-30
      ELSE
          TE=ITE0
      END IF
      IF((ITC0.EQ.0) .AND. (ICD.EQ.0)) THEN
          TC=TSNK+20
          IF(DTSC.LT.0) TC=TSNK+25-DTSC
      ELSE
          TC=ITC0
      END IF
C
      IF(ICD.EQ.1) THEN
         TC=TSAT(0,PCD)
      END IF
      IF(I.GE.2) THEN
          DTSR=TSRC-TE
          TE=TSRC-DTSR
      END IF
C
      WRITE(4,130)
  130 FORMAT('\ VFACE  PPHR   EH    CC   X1    TE  TA1',
     #'  RH1    SHF DTSH3    X3   CFM  CFH')
      NCOL=13
      NROW=NCPR*NEVP
      WRITE(4,135) NROW,NCOL
  135 FORMAT(2X,2I4)
```

```
C
      IF (ICALC.EQ.1) THEN
          TSRC=TSRC0
          RHSRC=RHSRC0
          DO 155 I=1,NCPR
          DO 155 J=1,NEVP
          DCFH=DCFH0+(I-1)*DDCFH
          CFHX(I)=DCFH
          CFHZ=DCFH
          CFM=CFM0+(J-1)*DCFM
          CFMX(J)=CFM
          VFACE=CFM/(WDTH*HT)
          CFMZ=CFM
          CALL SYSTEM(TSRC,RHSRC,CFM,0)
          CALL SYSTEM(TSRC,RHSRC,CFM,1)
          WRITE(2,290)
  155     CONTINUE
C
          WRITE(3,140)
  140     FORMAT('\       QTOTX       SHFX      QSENX'
     #     QLATX       CFHX       CFMX       COPX')
          DO 145 I=1,NCPR
          DO 145 J=1,NEVP
  145     WRITE(3,150) QTOTX(I,J),SHFX(I,J),QSENX(I,J),
     #    QLATX(I,J),CFHX(I),CFMX(J),COPX(I,J)
          DO 160 J=1,NEVP
          DO 160 I=1,NCPR
  160     WRITE(3,150) QTOTX(I,J),SHFX(I,J),QSENX(I,J),
     #    QLATX(I,J),CFHX(I),CFMX(J),COPX(I,J)
  150     FORMAT(2X,F10.0,F10.3,4F10.1,F10.4)
C
      ELSEIF (ICALC.EQ.2) THEN
          DCFH=DCFH0
          CFHZ=DCFH
          CFM=CFM0
          CFMZ=CFM
          VFACE=CFM/(WDTH*HT)
          DO 180 I=1,NTSRC
          DO 180 J=1,NRHSRC
          TSRC=TSRC0+(I-1)*DTSRC
          TSRCX(I)=TSRC
          RHSRC=RHSRC0+(J-1)*DRHSRC
          RHSRCX(J)=RHSRC
          CALL SYSTEM(TSRC,RHSRC,CFM,0)
          CALL SYSTEM(TSRC,RHSRC,CFM,1)
          WRITE(2,290)
  180     CONTINUE
C
          WRITE(3,165)
  165     FORMAT('\       QTOTX       SHFX      QSENX'
     #    ,'      QLATX      TSRCX     RHSRCX       COPX')
          DO 170 I=1,NTSRC
```

```
            DO 170 J=1,NRHSRC
  170       WRITE(3,175) QTOTX(I,J),SHFX(I,J),QSENX(I,J),
     #      QLATX(I,J),TSRCX(I),RHSRCX(J),COPX(I,J)
            DO 185 J=1,NRHSRC
            DO 185 I=1,NTSRC
  185       WRITE(3,175) QTOTX(I,J),SHFX(I,J),QSENX(I,J),
     #      QLATX(I,J),TSRCX(I),RHSRCX(J),COPX(I,J)
  175       FORMAT(2X,F10.0,F10.3,2F10.1,2F10.3,F10.4)
C
        ELSEIF (ICALC.EQ.3) THEN
            TSRC=TSRC0
            DCFH=DCFH0
            CFHZ=DCFH
            DO 205 I=1,NEVP
            DO 205 J=1,NRHSRC
            CFM=CFM0+(I-1)*DCFM
            CFMX(I)=CFM
            VFACE=CFM/(WDTH*HT)
            CFMZ=CFM
            RHSRC=RHSRC0+(J-1)*DRHSRC
            RHSRCX(J)=RHSRC
            CALL SYSTEM(TSRC,RHSRC,CFM,0)
            CALL SYSTEM(TSRC,RHSRC,CFM,1)
            WRITE(2,290)
  205       CONTINUE
C
            WRITE(3,190)
  190       FORMAT('\       QTOTX       SHFX      QSENX'
     #      ,'      QLATX       CFMX     RHSRCX        COPX')
            DO 195 I=1,NEVP
            DO 195 J=1,NRHSRC
  195       WRITE(3,200) QTOTX(I,J),SHFX(I,J),QSENX(I,J),
     #      QLATX(I,J),CFMX(I),RHSRCX(J),COPX(I,J)
            DO 210 J=1,NRHSRC
            DO 210 I=1,NEVP
  210       WRITE(3,200) QTOTX(I,J),SHFX(I,J),QSENX(I,J),
     #      QLATX(I,J),CFMX(I),RHSRCX(J),COPX(I,J)
  200       FORMAT(2X,F10.0,F10.3,3F10.1,F10.3,F10.4)
C
        ELSEIF (ICALC.EQ.4) THEN
            DCFH=DCFH0
            CFHZ=DCFH
            RHSRC=RHSRC0
            DO 230 I=1,NTSRC
            DO 230 J=1,NEVP
            TSRC=TSRC0+(I-1)*DTSRC
            TSRCX(I)=TSRC
            CFM=CFM0+(J-1)*DCFM
            CFMX(J)=CFM
            VFACE=CFM/(WDTH*HT)
            CFMZ=CFM
            CALL SYSTEM(TSRC,RHSRC,CFM,0)
```

```
            CALL SYSTEM(TSRC,RHSRC,CFM,1)
            WRITE(2,290)
  230       CONTINUE
C
            WRITE(3,215)
  215       FORMAT('\       QTOTX       SHFX      QSENX'
     #      ,'      QLATX      TSRCX       CFMX       COPX')
            DO 220 I=1,NTSRC
            DO 220 J=1,NEVP
  220       WRITE(3,225) QTOTX(I,J),SHFX(I,J),QSENX(I,J),
     #      QLATX(I,J),TSRCX(I),CFMX(J),COPX(I,J)
            DO 235 J=1,NEVP
            DO 235 I=1,NTSRC
  235       WRITE(3,225) QTOTX(I,J),SHFX(I,J),QSENX(I,J),
     #      QLATX(I,J),TSRCX(I),CFMX(J),COPX(I,J)
  225       FORMAT(2X,F10.0,F10.3,2F10.1,F10.3,F10.1,F10.4)
C
       ELSEIF (ICALC.EQ.5) THEN
            TSRC=TSRC0
            CFM=CFM0
            CFMZ=CFM
            VFACE=CFM/(WDTH*HT)
            DO 255 I=1,NCPR
            DO 255 J=1,NRHSRC
            DCFH=DCFH0+(I-1)*DDCFH
            CFHX(I)=DCFH
            CFHZ=DCFH
            RHSRC=RHSRC0+(J-1)*DRHSRC
            RHSRCX(J)=RHSRC
            CALL SYSTEM(TSRC,RHSRC,CFM,0)
            CALL SYSTEM(TSRC,RHSRC,CFM,1)
            WRITE(2,290)
  255       CONTINUE
C
            WRITE(3,240)
  240       FORMAT('\       QTOTX       SHFX      QSENX'
     #      ,'      QLATX       CFHX     RHSRCX       COPX')
            DO 245 I=1,NCPR
            DO 245 J=1,NRHSRC
  245       WRITE(3,250) QTOTX(I,J),SHFX(I,J),QSENX(I,J),
     #      QLATX(I,J),CFHX(I),RHSRCX(J),COPX(I,J)
            DO 260 J=1,NRHSRC
            DO 260 I=1,NCPR
  260       WRITE(3,250) QTOTX(I,J),SHFX(I,J),QSENX(I,J),
     #      QLATX(I,J),CFHX(I),RHSRCX(J),COPX(I,J)
  250       FORMAT(2X,F10.0,F10.3,3F10.1,F10.3,F10.4)
       ELSE
C
            CFM=CFM0
            CFMZ=CFM
            VFACE=CFM/(WDTH*HT)
            RHSRC=RHSRC0
```

```
            DO 280 I=1,NCPR
            DO 280 J=1,NTSRC
            DCFH=DCFH0+(I-1)*DDCFH
            CFHX(I)=DCFH
            CFHZ=DCFH
            TSRC=TSRC0+(J-1)*DTSRC
            TSRCX(J)=TSRC
            CALL SYSTEM(TSRC,RHSRC,CFM,0)
            CALL SYSTEM(TSRC,RHSRC,CFM,1)
            WRITE(2,290)
  280       CONTINUE
C
            WRITE(3,265)
  265       FORMAT('\       QTOTX       SHFX      QSENX'
     #      ,'      QLATX       CFHX      TSRCX       COPX')
            DO 270 I=1,NCPR
            DO 270 J=1,NTSRC
  270       WRITE(3,275) QTOTX(I,J),SHFX(I,J),QSENX(I,J),
     #      QLATX(I,J),CFHX(I),TSRCX(J),COPX(I,J)
            DO 285 J=1,NTSRC
            DO 285 I=1,NCPR
  285       WRITE(3,275) QTOTX(I,J),SHFX(I,J),QSENX(I,J),
     #      QLATX(I,J),CFHX(I),TSRCX(J),COPX(I,J)
  275       FORMAT(2X,F10.0,F10.3,3F10.1,F10.3,F10.4)
          ENDIF
C
  290   FORMAT(1H1)
          STOP
          END
C
          SUBROUTINE SYSTEM(TSRC,RHSRC,CFM,KPRNT)
          DIMENSION Z(9)
          COMMON/XOUT/QTOTX(5,5),SHFX(5,5),QSENX(5,5),
         #QLATX(5,5),COPX(5,5),I,J
          COMMON/AA/TC,TE,VFACE
          COMMON/AB/HTEI1D,HTEI2D,HTEI1W,KCYC
          COMMON/AC/CHTCAP,CHTE0,CHTE1,DTSC,TSNK,QCOND,ICD
          COMMON/AE/EH0V1,CCOV1,EDTSH3,EX3,ROWDT,CIRC,IMIX
          COMMON/AR/DCFH,CL,REFLO,EFFI0,DEFFI,QCO0,DQCO,
         #EE0,DEE,FLOF,VERMD,IVE
          COMMON/CONST/XSET,CPAD,HFGW
          COMMON/GEOM/DO,Y,DI,FKIN,FPI,HT,ROWD,HC,DC,
         #LENGTH,FINS,S,DPTH,CKTS,ROWH,WDTH,FACOIL,HCONT,
         #HFOULI,NCKTS,IGEOM
          COMMON/PWR/EPOWER,CFPWR,EFPWR0,CFM0
          COMMON/SC/DHCD,PWR,DHEV,DHI1SS,DHI1LS,DHI2SS,
         #DHI2LS,VCI,VCC,VCO,PE,PC,T3,T8,T11,PPHR,EE,VER,X1,
         #DTSH3,X3,EPWR
          COMMON/TD/DTSH
          COMMON/TRC/CFHZ,CFMZ,K
C
          TA1=TSRC
```

```
      RH1=RHSRC
      XCHTE=0
      IF(KPRNT.EQ.1) GOTO 55
      WRITE(5,70) CFM,DCFH,TSRC,RHSRC,TE
      WRITE(5,75)
    5 ITR=200
      DTMX=2
      DQMN=1000000
      THI=1000
      TLO=-1000
      KSRCE=0
   10 K=0
   15 K=K+1
C
      DTSRCE=TSRC-TE
      IF(DTSRCE.GT.2) GOTO 25
      KSRCE=KSRCE+1
      IF(KSRCE.EQ.8) THEN
          WRITE(2,20) TSRC
          RETURN
      END IF
   20 FORMAT(/,2X,'ERROR - DTSRCE < 2 - TSRC = ',F10.2)
      TE=TSRC-5
      TC=TC-4
      GOTO 10
C
   25 CONTINUE
C
C     CALCULATE QEVP
C
   30 CALL CYCLE(TE,DTSH,TC,DTSC,0)
C
C     DETERMINATION OF MASS FLOWRATE BY COMPRESSOR MODEL
      VECI=1+CL-CL*VCI/VCO
      IF(IVE.EQ.1) THEN
          VE=VERMD*VECI
      ELSE
          VE=VER*VECI
      ENDIF
      CFH=DCFH*VE
      PPHR=CFH/VCI
      FLOF=PPHR/REFLO-1.0
C
      TCP=TC
      QCOND=PPHR*DHCD
      CHTE=CHTE0+CHTE1*PPHR
      IF(CHTE.GT.1) CHTE=1
C
      IF(ICD.EQ.0) THEN
          TC=TSNK+QCOND/(CHTE*CHTCAP)
      ELSE
          CHTCAP=QCOND/(TC-TSNK)/CHTE
```

```
      ENDIF
      THOT=TSNK+CHTE*(TC-TSNK)
C
      CALL EVAP(TA1,RH1,VFACE,TE,X1,PPHR,PPHDA,QEVAP,
     #SHF,TA2,ADP,HA1,HA2,AH,RH2,ADRH,SVA1,SVA2,
     #ADS,WA1,WA2,ASH)
      IGEOM=0
C
      QEVP=PPHR*DHEV
      TCLD=TA2
      WRITE(5,80) K,QEVP,QEVAP,PPHR,TLO,TE,THI,TC,
     #EDTSH3,EX3,DQMN
      IF(K.LT.2) GOTO 15
C
      IF(QEVP.GT.QEVAP) THI=TE
      IF(QEVP.LT.QEVAP) TLO=TE
      IF((TLO.LT.-999).OR.(THI.GT.999)) GOTO 35
C
      DELQ=ABS(QEVP-QEVAP)
      IF(DELQ.LT.DQMN) THEN
          DQMN=DELQ
          TEMN=TE
      ENDIF
      DEL=DELQ/(QEVP+QEVAP)
      IF(DEL.LT.0.002) GOTO 45
      IF(K.GT.17) GOTO 50
      IF(K.EQ.17) THEN
          TE=TEMN
          GOTO 15
      ENDIF
C
      TE2=TE
      QE2=QEVP
      QT2=QEVAP
      DTE21=TE2-TE1
      SQE=(QE2-QE1)/DTE21
      SQT=(QT2-QT1)/DTE21
      QE0=QE2-SQE*TE2
      QT0=QT2-SQT*TE2
      TE=(QT0-QE0)/(SQE-SQT)
      DELTE=TE-TE2
      IF(K.GT.8) DTMX=.2
      IF(ABS(DELTE).GT.DTMX) TE=TE2+SIGN(DTMX,DELTE)
      TE1=TE2
      QE1=QE2
      QT1=QT2
      GOTO 15
   35 TE1=TE
      QE1=QEVP
      QT1=QEVAP
      IF(QEVP.GT.QEVAP) GOTO 40
      TE=TE+4
```

```
      GOTO 15
   40 TE=TE-4
      GOTO 15
C
   45 DELTC=ABS(TC-TCP)
      IF (ICD.EQ.0) THEN
        IF(DELTC.GT.0.2) GOTO 15
        IF(K.LE.3) GOTO 15
      END IF
C
   50 QCOND=PPHR*DHCD
      RETURN
C
C     PRINTOUT
   55 QEVP=PPHR*DHEV
C       TCLD=TSRC-QEVP/HCSRC
      TCLD=TA2
      XEHTE=(TSRC-TCLD)/(TSRC-TE)
      QCOND=PPHR*DHCD
      QCD=CHTE*CHTCAP*(TC-TSNK)
      XCHTE=(THOT-TSNK)/(TC-TSNK)
      THOT=TSNK+QCOND/CHTCAP
      POWER=PWR*PPHR
      CMPWR=EPWR*PPHR
      EFPWR=EFPWR0*(CFM/CFM0)**3
      EPOWER=CMPWR+CFPWR+EFPWR
      QI1SS=PPHR*DHI1SS
      QI1LS=PPHR*DHI1LS
      QI2SS=PPHR*DHI2SS
      QI2LS=PPHR*DHI2LS
      COPC=QEVP/EPOWER
      XEAS=(HA1-HA2)/(HA1-AH)
      XCC=(ADP-TE)/(HA1-AH)
      QSEN=QEVAP*SHF
      QLAT=QEVAP-QSEN
      QSEN=QSEN-EFPWR
C
      IF(IVE.EQ.1) THEN
          VERX=VERMD
      ELSE
          VERX=VER
      ENDIF
C
      WRITE(2,85) CFM,DCFH,TSRC,RHSRC,VFACE,K
      WRITE(2,90) QEVP,QCOND,POWER,QI1SS,QI1LS,QI2SS,QI2LS
      WRITE(2,95) PPHR,DCFH,CFH,EPOWER,CMPWR,EFPWR,CFPWR
C
C     VERIFICATION OF SOLUTION
      WRITE(2,100) XCHTE,VERX,XEAS,XCC,COPC,EHOV1,CCOV1
      WRITE(2,105) QEVAP,QSEN,QLAT,SHF,QCD,CHTCAP
      WRITE(2,110) EDTSH3,EX3,PPHDA
      WRITE(2,115) T11,T8,TCLD,TSRC,TSNK,THOT,TE,T3
```

```
      WRITE(2,120) TA1,RH1,WA1,HA1,SVA1
      WRITE(2,125) TA2,RH2,WA2,HA2,SVA2
      WRITE(2,130) ADP,ADRH,ASH,AH,ADS
C
C     OUTPUT FROM CYCLE
      CALL CYCLE(TE,DTSH,TC,DTSC,1)
C
      IF(IVE.EQ.2) THEN
          VECCT=1+CL-CL*VCC/VCO
          CFHCC=PPHR*VCC
          VECC=CFHCC/DCFH
          VERCC=VECC/VECCT
          WRITE(2,60) CFHCC,VECC,VECCT,VERCC,FLOF
   60     FORMAT(/,9X,'CFHCC      VECC     VECCT     VERCC',
     #    '       FLOF',/,4X,F10.1,4F10.3)
      ENDIF
C
      QTOTX(I,J)=QEVAP
      SHFX(I,J)=SHF
      QSENX(I,J)=QSEN
      QLATX(I,J)=QLAT
      COPX(I,J)=COPC
C
      WRITE(4,65) VFACE,PPHR,EHOV1,CCOV1,X1,TE,TA1,RH1
     #,SHF,DTSH3,X3,CFMZ,CFHZ
   65 FORMAT(2X,F5.1,F6.1,F5.3,F6.3,F5.3,F6.2,F5.1
     #,F5.2,F7.4,F6.1,F6.3,F6.0,F5.0)
      RETURN
C
   70 FORMAT(/,2X,'SYSTEM CALLED:        CFM       DCFH',
     #'       TSRC     RHSRC         TE',
     #/,16X,3F10.1,F10.3,F10.1,/)
   75 FORMAT(/,3X,'K      QEVP     QEVAP  PPHR      TLO',
     #5X,'TE      THI    TC EDTSH    EX3       DQMN')
   80 FORMAT(1X,I3,2F9.0,F6.0,F8.1,F7.2,F8.1,F5.1,F6.1
     #,F6.3,F10.0)
   85 FORMAT(//,11X,'CFM       DCFH       TSRC     RHSRC',
     #5X,'VFACE          K',/,4X,3F10.1,F10.2,F10.1,I10)
   90 FORMAT(/,4X,'       QEVP     QCOND     POWER',
     #5X,'QI1SS     QI1LS     QI2SS     QI2LS',/,4X,7F10.0)
   95 FORMAT(/,10X,'PPHR       DCFH     CFH CI     EPOWER',
     #'     CMPWR',5X,'EFPWR      CFPWR',/,4X,7F10.1)
  100 FORMAT(/,9X,'XCHTE       VERX       XEAS        XCC',
     #'       COPC',5X,'EHOV1      CCOV1',
     #/,4X,F10.4,F10.3,2F10.5,F10.4,2F10.5)
  105 FORMAT(/,9X,'QEVAP       QSEN       QLAT        SHF',
     #,        QCD',4X,'CHTCAP',/,4X,3F10.0,F10.4,2F10.0)
  110 FORMAT(/,8X,'EDTSH3        EX3      PPHDA',
     #/,4X,F10.1,F10.3,F10.1)
  115 FORMAT(/,10X,'T11          T8',16X,'TCLD       TSRC',
     #/,4X,2F10.1,10X,2F10.1,//,10X,'TSNK      THOT',
     #18X,'TE         T3',/,4X,2F10.1,10X,2F10.1)
```

```
  120 FORMAT(/,11X,'TA1        RH1        WA1        HA1',
     #'       SVA1',/,4X,F10.2,F10.3,F10.6,2F10.4)
  125 FORMAT(/,11X,'TA2        RH2        WA2        HA2',
     #'       SVA2',/,4X,F10.2,F10.3,F10.6,2F10.4)
  130 FORMAT(/,11X,'ADP       ADRH        ASH         AH',
     #'        ADS',/,4X,F10.2,F10.3,F10.6,2F10.4)
      END
C
      SUBROUTINE CYCLE(TE,DTSH,TC,DTSC,IPRNT)
C     AIR CONDITIONING SYSTEM CYCLE ANALYSIS - THERMODYNAMIC
      COMMON/AB/HTEI1D,HTEI2D,HTEI1W,KCYC
      COMMON/AR/DCFH,CL,REFLO,EFFI0,DEFFI,QCO0,DQCO,EE0,
     #DEE,FLOF,VERMD,IVE
      COMMON/SC/DHCD,PWR,DHEV,DHI1SS,DHI1LS,DHI2SS,DHI2LS,VCI,
     #VCC,VCO,PE,PC,T3,T8,T11,PPHR,EE,VER,X1,DTSH3,X3,EPWR
      DIMENSION X(14),TS(14),P(14),H(14),T(14),V(14)
C
C      1   EXPANSION VALVE / EVAP
C      2   SAT VAP AT TE
C      3   EVAP/ I1
C      4   I1 / I2 - DTSH CONTROLLED BY EXPANSION VALVE
C      5   I2 / COMPRESSOR INLET
C      6   COMPRESSOR CRANKCASE
C      7   COMPR OUTLET - ISENTROPIC
C      8   COMPR / COND
C      9   SAT VAP AT TC
C     10   SAT LIQ AT TC
C     11   CONDENSER / RECEIVER
C     12   RECEIVER  / I2
C     13   I2 / I1
C     14   I1 / EXPANSION VALVE
C
C    |                /                                  /
C    |           11 (10)                              (9)   7    8
C  P |              /                                  /
C  R |             /                                  /
C  E |   14  13 12                                   /
C  S |          /                                    /
C  S |         /                                    /
C  U |        /                                    /
C  R |       /                                    /
C  E |      /                                    /
C    |     /                                    /
C    |    /                                    /
C    |   /                                    /
C    |  /                                    /
C    |   1                          (3)   (2)  3   4   5   6
C    |                                    /
C    |_____________________________________________________________
C                                                          ENTHALPY
C
```

```
C     PT 4 = SPECIFIED SUPERHEATED - EXP VALVE
C
C     <<--14--|          |------13-------|          |--12---<<
C             |          |               |          |
C     >>---3--[    I1    ]-------4-------[    I2    ]---5--->>
C
C      HTE=DT(ACTUAL)/DT(IDEAL)
C
C      HTEI?D=DT(VAPOUR)/DT(IDEAL)
C      IF CONDITION ENTERING HT. EX. (PT 4) IS DRY
C      DH FOR VAPOUR IS CRITICAL (MINIMUM)
C      CALC SUCTION SIDE CONDITIONS FIRST
C      CALC LIQUID SIDE CONDITIONS SECOND
C
C      HTEI?W=DT(LIQUID)/DT(IDEAL)
C      IF CONDITION ENTERING HT. EX. (PT 4) IS WET
C      DH FOR LIQUID IS CRITICAL (MINIMUM)
C      CALC LIQUID SIDE CONDITIONS FIRST
C      CALC SUCTION SIDE CONDITIONS SECOND
C
       IF(IPRNT.EQ.1) GOTO 70
C
C      PT 2  P X  KNOWN   T H REQ'D
       T(2)=TE
       X(2)=1
       CALL SATPRP(2,TE,PE,VFE,V(2),HFE,HFGE,H(2),SFE,SGE)
       VGE=V(2)
       HGE=H(2)
C
C      PTS 9 10   P X KNOWN  T H REQ'D
C      SAT COND AT PC
       T(9)=TC
       T(10)=TC
       X(9)=1
       X(10)=0
       CALL SATPRP(9,TC,PC,V(10),V(9),H(10),HFGC,H(9),
      #SF,SG)
C
       DO 5 I=1,6
       TS(I)=TE
     5 P(I)=PE
       DO 10 I=7,11
       TS(I)=TC
    10 P(I)=PC
C
C      PTS 11  P T X  KNOWN  H REQ'D
       T(11)=TC-DTSC
       X(11)=0
       CALL SATPRP(11,T(11),PSAT,V(11),VG,H(11),HFG,
      #HG,SF,SG)
C
C      PT 4  P T X KNOWN   H S REQ'D
```

```
      T(4)=TS(4)+DTSH
      X(4)=1
      CALL VAPOR(4,T(4),P(4),V(4),H(4),SV)
C
C     PT 12
      H(12)=H(11)
C     APPROX
      T(12)=T(11)
      TS(12)=T(12)
      X(12)=0
      CALL SATPRP(12,T(12),P(12),V(12),VG,HF,HFG,HG,SF,SG)
C
      P(13)=P(12)
      P(14)=P(12)
      TS(13)=T(12)
      TS(14)=T(12)
C
C     INTERCHANGER 2
C     PT 5
   15 DTI=T(12)-T(4)
      DTSS=HTEI2D*DTI
      T(5)=T(4)+DTSS
      X(5)=1
      CALL VAPOR(5,T(5),P(5),V(5),H(5),SCI)
      HEDH=H(5)-H(4)
      VCI=V(5)
C
C     INTERCHANGER 2
C     PT 13
      H(13)=H(12)-HEDH
      X(13)=0
      CALL TLIQ(13,H(13),T(12),T(13),V(13))
C
C     INTERCHANGER 1
C     PT 3
C     ASSUME PT 3 DRY
   20 T(3)=(HTEI1D*T(13)-T(4))/(HTEI1D-1)
      IF(T(3).LT.TS(3)) GOTO 25
      X(3)=1
      CALL VAPOR(3,T(3),P(3),V(3),H(3),SV)
      HEDH=H(4)-H(3)
C
C     INTERCHANGER 1
C     PT 14
      H(14)=H(13)-HEDH
      X(14)=0
      CALL TLIQ(14,H(14),T(13),T(14),V(14))
      GOTO 30
C
C     ASSUME PT 3 WET
   25 T(3)=TS(3)
      DTI=T(13)-T(3)
```

```
      DTLS=HTEI1W*DTI
      T(14)=T(13)-DTLS
      CALL SATPRP(14,T(14),PSAT,V(14),VG14,H(14),
     #HFG,HG,SF,SG)
      HEDH=H(13)-H(14)
C
C     PT 3
      H(3)=H(4)-HEDH
      CALL SATPRP(3,TS(3),PSAT,VF,VG,HF,HFG,HG,SF,SG)
      X(3)=(H(3)-HF)/HFG
      V(3)=VF+X(3)*(VG-VF)
C
C     PTS 7 AND 8
C
C     PT 7   P X S  KNOWN  T,H REQ'D
C     SCI=S(5)=S(7)
   30 IF(SCI.GT.SG7) GOTO 35
      X(7)=(SCI-SF7)/(SG7-SF7)
      T(7)=TS(7)
      H(7)=HF7+X(7)*HFG7
      GOTO 50
   35 X(7)=1
      K7=0
   40 IF(T(7).LT.TS(7)) T(7)=TS(7)
      CALL VAPOR(7,T(7),P(7),V(7),H(7),SV)
      K7=K7+1
      DEL=ABS(SV-SCI)
      IF(DEL.LT.0.000002) GOTO 50
      IF(K7.GT.16) GOTO 50
      IF(K7.GE.2) GOTO 45
      T1=T(7)
      S1=SV
      IF(SV.GT.SCI) T(7)=T(7)-4
      IF(SV.LT.SCI) T(7)=T(7)+4
      GOTO 40
   45 T2=T(7)
      S2=SV
      T(7)=T2+(SCI-S2)*(T2-T1)/(S2-S1)
      T1=T2
      S1=S2
      GOTO 40
C
C     PT 8  P X H  KNOWN   T VCO REQ'D
C
   50 EFFI=EFFI0+DEFFI*FLOF
      IF(EFFI.GT.1) EFFI=1
      QCO=QCO0+DQCO*FLOF
      IF(QCO.GT.1) QCO=1
      EE=EE0+DEE*FLOF
      IF(EE.GT.1) EE=1
C
      H(8)=H(5)+(H(7)-H(5))/EFFI
```

```
      IF(H(8).GT.HG7) GOTO 55
      X(8)=(H(8)-HF7)/HFG7
      VCO=VF7+X(8)*(VG7-VF7)
      T(8)=TS(8)
      GOTO 60
   55 X(8)=1
CCC      IF(KCYC.EQ.0) T(8)=T(5)+(T(7)-T(5))/EFFI
      CALL TVAP(8,P(8),H(8),T(7),T(8),V(8),SV)
      VCO=V(8)
   60 CONTINUE
C
C     PT 1  P H KNOWN   T X REQ'D
   65 T(1)=TE
      H(1)=H(14)
      X(1)=(H(1)-HFE)/HFGE
      V(1)=VFE+X(1)*(V(2)-VFE)
C
C     PT 6
      H(6)=H(5)+QCO*(H(8)-H(5))
      CALL TVAP(6,P(6),H(6),T(5),T(6),V(6),SV)
      VCC=V(6)
      X(6)=X(5)
C
C     CALCULATION OF VER
      VER=V(5)*(1+CL-CL*V(6)/V(8))/(V(6)*(1+CL-CL*V(5)/V(8)))
C
C     CALC CAPACITIES
      DHCD=H(8)-H(11)
      PWR=H(8)-H(5)
      EPWR=PWR/EE
      DHEV=H(3)-H(1)
      DHI1SS=H(4)-H(3)
      DHI1LS=H(13)-H(14)
      DHI2SS=H(5)-H(4)
      DHI2LS=H(12)-H(13)
      T3=T(3)
      T8=T(8)
      T11=T(11)
      X1=X(1)
      X3=X(3)
      DTSH3=T(3)-TS(3)
C
      KCYC=1
      IF(IPRNT.EQ.0) RETURN
C
C     PRINTOUT
   70 XHTEI2=0
      DT=T(12)-T(4)
      IF(ABS(DT).GT.0.0001) XHTEI2=(T(5)-T(4))/DT
      XHTEI1=0
      DT=T(13)-T(3)
      IF((ABS(DT).GT.0.0001).AND.(T(3).GT.TS(3)))
```

```
     #XHTEI1=(T(4)-T(3))/DT
      IF((ABS(DT).GT.0.0001).AND.(X(3).LT.0.9999))
     #XHTEI1=(T(13)-T(14))/DT
C
      WRITE(2,95) XHTEI1,XHTEI2
C
      XQCO=(H(6)-H(5))/(H(8)-H(5))
      WRITE(2,100) EFFI,QCO,EE,XQCO
C
      WRITE(2,105)
      DO 75 I=1,14
      IF((I.EQ.2).OR.(I.EQ.7).OR.(I.EQ.9).OR.(I.EQ.10)) GOTO
75
      TTS=T(I)-TS(I)
      WRITE(2,110) I,P(I),T(I),TS(I),H(I),X(I),V(I),TTS
   75 CONTINUE
      WRITE(2,105)
      DO 85 I=2,10
      IF((I.EQ.2).OR.(I.EQ.7).OR.(I.EQ.9).OR.(I.EQ.10)) GOTO
80
      GOTO 85
   80 TTS=T(I)-TS(I)
      WRITE(2,110) I,P(I),T(I),TS(I),H(I),X(I),V(I),TTS
   85 CONTINUE
C
      RETURN
C
   90 WRITE(2,115)
      STOP
C
   95 FORMAT(/,8X,'XHTEI1     XHTEI2',/,4X,2F10.3)
  100 FORMAT(/,10X,'EFFI       QCO         EE       XQCO',
     #/,4X,4F10.3)
  105 FORMAT(/,7X,'PT',9X,'P',9X,'T',8X,'TS',9X,'H',
     #9X,'X',9X,'V',4X,'T - TS')
  110 FORMAT(4X,I5,3F10.1,2F10.3,F10.4,F10.1)
  115 FORMAT(//,4X,'PT 3  DRY / PT 10 WET - STOP',/,1H1)
      END
C
C-------------------------------------------------------
C               S U B R O U T I N E   E V A P
C-------------------------------------------------------
      SUBROUTINE EVAP(TA1,RH1,VFACE,TR1,QUAL1,PPHR,MFA
     #,QEVAP,SHF,TA2MIX,ADPMIX,HA1,HA2MIX,AHMIX,RH2MIX
     #,ADRHMIX,SVA1,SVA2,ADSMIX,WA1,WA2MIX,ASHMIX)
      DIMENSION Z(9)
      COMMON/GEOM/DO,Y,DI,KFIN,FPI,HT,ROWD,HC,DC
     #,LENGTH,FINS,S,DPTH,CKTS,ROWH,WDTH,FACOIL
     #,HCONT,HFOULI,NCKTS,IGEOM
      COMMON/CONST/XSET,CPAD,HFGW
      COMMON/AE/EHOV1,CCOV1,EDTSH3,EX3,ROWDT,CIRC,IMIX
      COMMON/TRC/CFHZ,CFMZ,K
```

```
      REAL NF,MFA,MFR,KFIN,LENGTH,LEN2PH,LSUP,MFA2PH
      REAL MFASUP,MF2ASP,KA,NTU,MLHS,MRHS,NFSUP,LENSUP
      REAL MFA2PI,NFI,LE,MFA2
C
      IF(IGEOM.EQ.1) THEN
          CIRC=CKTS
          ROWDT=ROWD
          IF(IMIX.EQ.1) THEN
              DPTH=DPTH/ROWD
              ROWD=ROWD/CKTS
              CKTS=1
              NCKTS=CIRC
          ELSE
              NCKTS=1
          ENDIF
          FACOIL=WDTH*HT
          HC=HT/ROWH
          DC=DPTH/ROWD
          RPC=ROWD*ROWH/CKTS
          LENGTH=WDTH*RPC
          FINS=FPI*LENGTH*12
          S=1.0/(FPI*12)
      ENDIF
      TMEAN=0
      WMEAN=0
      MFR=PPHR/CIRC
      CALL SATPRP(1,TR1,PR1,VF,VG,HF,HFG,HG,SF,SG)
      HR1=HF+QUAL1*HFG
C
      DO 75 KMIX=1,NCKTS
      IF(KMIX.EQ.1) THEN
          HRLVG=0
          TA10=TA1
          RH10=RH1
          Z(1)=TA1
          Z(3)=RH1
          CALL PSYC(Z,3)
          WA10=Z(4)
          HA10=Z(5)
          MFA=VFACE*FACOIL*60/Z(9)
          QESEN=0
          QEVAP=0
          QAIR=0
      ENDIF
C
C     EVALUATE INLET AIR PROPERTIES.
C-------------------------------------
      Z(1)=TA1
      Z(3)=RH1
      CALL PSYC(Z,3)
      WA1=Z(4)
      HA1=Z(5)
```

```
      DPT1=Z(6)
      DENSA1=1.0/Z(9)
      SVA1=Z(9)
C
C     VARIABLES ARE INITIALIZED.
C---------------------------------
      X2EST=0
      DTSH=0
      IWRN=0
      KK3=0
      I2=0
      IH=0
      C=0
      J1=0
      K1=0
      LK=0
      JFLAG=0
      KFLAG=0
      TCOND1=0
      TCOND2=0
      RESI2P=0
      COND=0
      LL=0
      KK=0
      XX=0
      QR1HD=0
      QR2HD=0
      TWS1HD=0
      TWS2HD=0
      DPQ1HD=0
      DPQ2HD=0
      REY1HD=0
      REY2HD=0
      TCO1HD=0
      TCO2HD=0
      TCDL1=0
      TCDL2=0
      DPQRS1=0
      DPQRS2=0
      REYNS1=0
      REYNS2=0
      QRATS1=0
      QRATS2=0
      TWS1=0
      TWS2=0
      FINSPC=S-Y
      LE=0.95
      KA=-8.487E-08*TA1*TA1+3.1923E-05*TA1+1.3005E-02
      PRA=1.047E-06*TA1*TA1-2.3187E-04*TA1+0.72307
      VISCA=-1.962E-07*TA1*TA1+8.2371E-05*TA1+3.9207E-02
      CPA=CPAD+0.45*WA1
      XCOMP=XSET+0.0001
```

```
      COEFFI=0.3
      PI=2.0*ATAN2(1.0,0.0)
      HRX=HR1
      X2=XSET
      TWEST=-100
      X1=(HR1-HF)/HFG
      CALL FLAREA(DO,Y,FINS,HC,DC,LENGTH,AHTTB,AHTFIN,
     #AO,DEQUIV,FHEQIV,PI,AFFLO,DH)
      ATBOUT=PI*DO*LENGTH
      TW=-100
      TFR=TW
      TA2=TA1-2.0
      WA2=WA1
      TAVI=(TA1+TA2)/2
      WAVI=(WA1+WA2)/2
C
C     CALCULATE FLOW AREAS.
C-----------------------------
      AFACKT=HC*LENGTH
      AX=PI*(DI*DI)/4.0
      AI=PI*DI*LENGTH
      GFLUXR=MFR/AX
      AFACKT=HC*LENGTH
      AFRFL=FACOIL-DO*WDTH*ROWH-12*(HT-DO*ROWH)*Y*FPI*WDTH
      GFLUXA=MFA/AFRFL
C
C     THE FRACTION OF THE COIL IN THE TWO PHASE REGION
C     IS ASSUMED.
C-------------------------------------------------------
      AFRCNI=0.5
    5 TA2SUP=0
      WA2SUP=0
      RH2SUP=0
      HA2SUP=0
      LENSUP=0
      QSUP=0
      TWSUP=0
      NFSUP=0
      HTASUP=0
      HTRSUP=0
      RESAS=0
      RESRS=0
      KFLAG=0
      MFASUP=0
      AMFSUP=0
      DEL2=0
      AFRCON=AFRCNI
      IF (AFRCON .LE. 0.01) AFRCON=0.01
      TWEST=TW
      TAV=TAVI
      WAV=WAVI
      HRX=HR1
```

```
C
C     RESET VARIABLES BETWEEN ITERATIONS.
C-------------------------------------------------------
   10 KK2=0
      X2=XSET
      X1=(HRX-HF)/HFG
      AFRCNI=0
      TFRI=0
      TWI=0
      TA2I=0
      WA2I=0
      RH2I=0
      MFA2PI=0
      HA2I=0
      CONDI=0
      AMF2I=0
      HTAI=0
      NFI=0
      HTRI=0
      RESAI=0
      Q2PI=0
      RESRI=0
C
C     HEAT TRANSFER AVAILABLE IN THE REGION UNDER
C     CONSIDERATION IS CALCULATED.
C-------------------------------------------------
   15 Q2PH=MFR*HFG*(X2-X1)*CKTS
      KK=0
      CALL FLAREA(DO,Y,FINS,HC,DC,LENGTH,AHTTB,AHTFIN,
     #AHTTOT,DEQUIV,FHEQIV,PI,AFFLO,DH)
      SIGMA=AFFLO/AFACKT
      ASAT=4*DC*HC*SIGMA/(DO*DH*PI)
C     KKOUNT INITIALIZED 92 AUG 11
      KKOUNT=0
C
C     PROPERTIES OF THE AIR AT THE AVERAGE AIR TEMPERATURE
C     ARE CALCULATED.
C-------------------------------------------------------------
   20 KA=-8.487E-08*TAV*TAV+3.1923E-05*TAV+1.3005E-02
      PRA=1.047E-06*TAV*TAV-2.3187E-04*TAV+0.72307
      VISCA=-1.962E-07*TAV*TAV+8.2371E-05*TAV+3.9207E-02
      CPA=CPAD+0.45*WAV
      Z(1)=TAV
      Z(4)=WAV
      CALL PSYC(Z,4)
      DENSDA=1.0/Z(9)
C
C     CALCULATE SLOPE OF PROCESS LINE.
C---------------------------------------
      TA2EST=TA2
      TAVEST=TAV
   25 IF (JFLAG .EQ. 0) GOTO 30
```

```
      Z(1)=TFR
      Z(3)=1.0
      CALL PSYC(Z,3)
      WFR=Z(4)
      C=(WAV-Z(4))/(TAV-TFR)
      IF (C .LT. 0) C=0
   30 CALL HEAT2(CPA,PRA,GFLUXA,VISCA,DO,ASAT,HTAD,
     #DC,ROWD)
      HTAW=HTAD*HFGW*C/(CPA*LE)
      HTA=HTAD+HTAW
      CALL FINEF3(HTA,KFIN,Y,DO,DEQUIV,FHEQIV,NF)
   35 KK=KK+1
      LEN2PH=LENGTH*AFRCON
      AI2PH=AI*AFRCON
      RESA=1.0/(HTA*AFRCON*(AHTTB+NF*AHTFIN)*CKTS)
      RESFM=1.0/(HTA*AFRCON*AHTTOT*CKTS)
      RESCON=1.0/(HCONT*AFRCON*ATBOUT*CKTS)
      RESFLI=1.0/(HFOULI*AFRCON*AI*CKTS)
      IF (X2 .GT. 1.0) X2=1.0
   40 CALL CLC2PH(JCR,GFLUXR,DI,AI,X2,X1,PR1,TR1,HTR,
     #RESR,LENGTH,AFRCON,CKTS,XX,XSET,PI)
C
C     DETERMINE TOTAL RESISTANCE TO HEAT TRANSFER,
C     AND HEAT TRANSFERED.
C-----------------------------------------------------
      SUMR=RESR+RESA+RESCON+RESFLI
      Q=(TAV-TR1)/SUMR
      DIFFQ=Q-Q2PH
      AA=5
      HR2=HRX+Q/(MFR*CKTS)
C
C     IF KFLAG=1 THERE IS NO SUPERHEATED REGION AND
C     EVAPORATOR OUTLET IS IN REGION UNDER CONSIDERATION
C-----------------------------------------------------
      IF (KFLAG .EQ. 1) THEN
          X2=(HR2-HF)/HFG
          DIFFX=X2-X1
          IF (ABS(X2-X2EST) .GT. 0.0001) THEN
             KK3=KK3+1
             X2EST=X2
             IF (KK3 .LT. 15) GOTO 40
             KK3=0
             GOTO 45
          ELSE
             KK3=0
             GOTO 45
          END IF
      END IF
C
C     CHECK CONVERGENCE ON HEAT TRANSFERRED IN A REGION.
C-----------------------------------------------------
      IF (ABS(DIFFQ) .LT. AA) THEN
```

```
        KK=0
        GOTO 45
       END IF
       IF (KK .GT. 30) THEN
        WRITE(3,*) '\CONVERGENCE NOT ATTAINED. KK=',KK
        WRITE(3,*) 'DIFFQ=',DIFFQ
        KK=0
        GOTO 45
       END IF
       IF (DIFFQ .LT. 0) THEN
         ALHS=AFRCON
         QLHS=Q
         J1=1
       ELSE
         ARHS=AFRCON
         QRHS=Q
         K1=1
       END IF
       IF ((J1 .EQ. 1) .AND. (K1 .EQ. 1)) THEN
         AFRCON=(Q2PH-QLHS)*((ARHS-ALHS)/(QRHS-QLHS))+ALHS
         GOTO 35
       END IF
       IF (DIFFQ .LT. 0) THEN
         AFRCON=ALHS+0.2*ALHS
       ELSE
         AFRCON=ARHS-0.2*ARHS
       END IF
       GOTO 35
C
   45  J1=0
       K1=0
       AMF2PH=AFFLO*AFRCON
       MFA2PH=MFA*AFRCON
       ATOT2P=AHTTOT*AFRCON
       ATL=AFRCON*AO
C
C      THE COIL SURFACE TEMPERATURES ARE CALCULATED.
C-----------------------------------------
       TFR=TAV-Q*RESFM
       TW=TAV-Q*RESFM
       HA2=HA1-Q/MFA2PH
       LL=LL+1
C
C      IF CONVERGENCE, WITHIN SPECIFIED TOLERANCE, IS NOT
C      ATTAINED ON THE COIL SURFACE TEMPERATURE, THE
C      SIMULATION IS TERMINATED.
C-------------------------------------------------------
       IF (LL .GT. 24) THEN
          WRITE(5,*) ' COIL SURFACE TEMP CONVERGENCE
      #  NOGO - LL = ',LL
          WRITE(3,*) ' COIL SURFACE TEMP CONVERGENCE
      #  NOGO - LL = ',LL
```

```
         GOTO 70
       END IF
       WRITE(5,*) ' LL, TW, TWEST ',LL,TW,TWEST
       IF (JFLAG .NE. 0) THEN
           IF (ABS(TW-TWEST) .GT. 0.01) THEN
               IF(LL.LE.16) THEN
                   TWEST=TW
               ELSE
                   TWEST=(TWEST+TW)/2
               END IF
               GOTO 25
           END IF
           GOTO 50
       END IF
C
C      COMPARE TWALL WITH THE DEW POINT.
C--------------------------------------
       IF (TW .LT. DPT1) THEN
          JFLAG=1
          TWEST=TW
          GOTO 25
       END IF
C
C      LEAVING AIR PROPERTIES ARE DETERMINED.
C---------------------------------------
   50 CALL TLEAV2(HA2,C,TFR,TA1,Z,WA1,HWALL)
C
C      CONVERGENCE ON AVERAGE TEMPERATURE IS MONITORED.
C      CONVERGENCE ON AVERAGE TEMPERATURE IS THE CRIETERIA
C      FOR COMPLETED ANALYSIS OF A PARTICULAR REGION.
C-------------------------------------------------------
       IF (Z(1) .LT. TR1) THEN
        Z(1)=TR1+2.0
        Z(3)=1.0
        CALL PSYC(Z,3)
       END IF
       DTLM=(TA1-Z(1))/ALOG((TA1-TR1)/(Z(1)-TR1))
       TAV=TR1+DTLM
       SAIR=(WA1-WFR)/(TA1-TFR)
       WAV=SAIR*(TAV-TFR)+WFR
       KKOUNT=KKOUNT+1
       IF (KKOUNT .GT. 30) THEN
          WRITE(3,*) '\KKOUNT=31 CFHZ CFMZ K',CFHZ,CFMZ,K
          GOTO 55
       END IF
       LL=0
       TA2=Z(1)
       IF (ABS(TAV-TAVEST) .GT. 0.005) THEN
           IF (KKOUNT .EQ. 1) TAVEST=TAV
           TAV=(0.75*TAVEST+0.25*TAV)
           WAV=SAIR*(TAV-TFR)+WFR
           GOTO 20
```

```
      END IF
   55 IF (HA2 .LT. HWALL) IWRN=1
      TA2=Z(1)
      RH2=Z(3)
      WA2=Z(4)
      PERC=AFRCON*100.0
      Z(1)=TFR
      Z(3)=1.0
      CALL PSYC(Z,3)
      WS2PH=Z(4)
C
C     CONDENSATION RATES ARE DETERMINED.
C-----------------------------------------
      IF (WA1 .GT. WA2) THEN
          COND=MFA2PH*(WA1-WA2)
          QLAT=COND*HFGW
      ELSE
          COND=0
          QLAT=0
      END IF
C
C     KKOUNT DE-INITIALIZED 92 AUG 11
C      KKOUNT=0
C
      AFRCNT=AFRCNI+AFRCON
      DXC=X2-XSET
      IF (DXC .LE. 0.0001) THEN
         TAVI=TAV
         WAVI=WAV
      END IF
C
C     RESULTS OBTAINED IN THE REGION X=X1 TO XSET
C     (IF X < XSET ) ARE STORED. THE REGION
C     X=XSET-1.0 IS THEN ANALYZED.
C-------------------------------------------------
      IF (ABS (X2-XSET) .LE. 0.0001) THEN
         IF (AFRCNT .GE. 1.0) THEN
             TCOND1=TCO1HD
             DPQRS1=DPQ1HD
             TWS1=TWS1HD
             REYNS1=REY1HD
             QRATS1=QR1HD
             GOTO 60
         END IF
         HRX=HF+XSET*HFG
         Q2PI=Q
         AFRCNI=AFRCON
         TFRI=TFR
         TWI=TW
         TFRI=TFR
         TA2I=TA2
         WA2I=WA2
```

```
            RH2I=RH2
            MFA2PI=MFA2PH
            HA2I=HA2
            CONDI=COND
            AMF2I=AMF2PH
            HTAI=HTA
            NFI=NF
            HTRI=HTR
            RESAI=RESA
            RESRI=RESR
            X2=1.0
            X1=XSET
            XX=(1.0+XSET)/2
            AFRCON=0.1
            Q2PH=MFR*HFG*CKTS*(X2-X1)
            GOTO 15
         END IF
         MFA2PT=MFA2PI+MFA2PH
         WA2=(WA2I*MFA2PI+WA2*MFA2PH)/MFA2PT
         HA2=(HA2I*MFA2PI+HA2*MFA2PH)/MFA2PT
         MFA2PH=MFA2PT
         IF (WA1 .GT. WA2) THEN
             QLAT=MFA2PH*(WA1-WA2)*HFGW
         ELSE
             QLAT=0
         END IF
         T2EST=TA2I
         IF (X2 .LE. XCOMP) T2EST=TA2
         CALL PROP1(HA2,WA2,T2EST,Z)
         TA2=Z(1)
         RH2=Z(3)
         PERC=AFRCNT*100.0
         Q=Q+Q2PI
         COND=COND+CONDI
         TW=(TWI*AFRCNI+TW*AFRCON)/AFRCNT
         TFR=(TFRI*AFRCNI+TFR*AFRCON)/AFRCNT
         AMF2PH=AMF2I+AMF2PH
         HTA=(HTAI*AFRCNI+HTA*AFRCON)/AFRCNT
         NF=(NFI*AFRCNI+NF*AFRCON)/AFRCNT
         HTR=(HTRI*AFRCNI+HTR*AFRCON)/AFRCNT
         RESA=(RESAI*AFRCNI+RESA*AFRCON)/AFRCNT
         RESR=(RESRI*AFRCNI+RESR*AFRCON)/AFRCNT
C
         IF (KFLAG .EQ. 1) GOTO 65
   60    IF (AFRCNT .GE. 1.0) THEN
            IF (X2 .GE. 1.0) THEN
               TCOND2=TCO2HD
               DPQRS2=DPQ2HD
               TWS2=TWS2HD
               REYNS2=REY2HD
               QRATS2=QR2HD
            END IF
```

```
            KFLAG=1
            AFRCON=1.0-AFRCNI
            X2=X1+((1.0-XSET)/(AFRCNT-AFRCNI))*AFRCON
            IF (X2 .LT. XSET) X2=XSET+0.01
            GOTO 15
          END IF
C*********************************************************
C THE SUPERHEATED REGION IS NOW ANALYSED, USING THE E-NTU
C METHOD. THE SUPERHEATED REGION IS ASSUMED DRY.
C*********************************************************
          CALLFLAREA(DO,Y,FINS,HC,DC,LENGTH,AHTTB,AHTFIN,AHTTOT,
         &DEQUIV,FHEQIV,PI,AFFLO,DH)
          SIGMA=AFFLO/AFACKT
          ASAT=4*DC*HC*SIGMA/(DO*DH*PI)
          AMFSUP=AFFLO*(1-AFRCNT)
          MFASUP=MFA-MFA2PH
          LSUP=LENGTH*(1.0-AFRCNT)
          AISUP=AI*(1.0-AFRCNT)
          C=0
          TR=TR1+1
          ITR=2
          CALL SPHT(ITR,TR,PR1,SV,CPR,GAMA,SONIC)
C
C         HEAT CAPACITIES OF THE HEAT EXCHANGING FLUIDS ARE
C         CALCULATED.
C-------------------------------------------------------
          CAIR=CPA*MFASUP
          CREF=CPR*MFR*CKTS
          IF (CREF .GT. CAIR) THEN
            CMAX=CREF
            CMIN=CAIR
          ELSE
            CMAX=CAIR
            CMIN=CREF
          END IF
          CALL HEAT2(CPA,PRA,GFLUXA,VISCA,DO,ASAT,HTAD,DC,ROWD)
          HTAW=HTAD*HFGW*C/CPA
          HTASUP=HTAD+HTAW
          CALL FINEF3(HTASUP,KFIN,Y,DO,DEQUIV,FHEQIV,NFSUP)
          CALL CLCSUP(TR,PR1,GFLUXR,HTRSUP,RESRS,AFRCNT,AI,
         #DI,CKTS)
          RESAS=1.0/(HTASUP*(1.0-AFRCNT)*(AHTTB+NFSUP*AHTFIN)
         #*CKTS)
          RESCON=1.0/(HCONT*(1.0-AFRCNT)*ATBOUT*CKTS)
          RESASF=1.0/(HTASUP*(1.0-AFRCNT)*AHTTOT*CKTS)
          RESFLI=1.0/(HFOULI*(1.0-AFRCNT)*AI*CKTS)
          UA=1.0/(RESAS+RESRS+RESCON+RESFLI)
          NTU=UA/CMIN
C
C         CROSS FLOW; BOTH FLUIDS MIXED.
C-----------------------------------
          DEN1=NTU/(1.0-EXP(-NTU))
```

```
      DEN2=(CMIN/CMAX)*NTU/(1.0-EXP(-NTU*CMIN/CMAX))
      EFF=NTU/(DEN1+DEN2-1.0)
      RA=CMIN/CMAX
      QSUP=EFF*CMIN*(TA1-TR1)
      TA2SUP=TA1-EFF*(CMIN/CAIR)*(TA1-TR1)
      DTSH=EFF*(CMIN/CREF)*(TA1-TR1)
      TR2=DTSH+TR1
      WA2SUP=WA1
      Z(1)=TA2SUP
      Z(4)=WA2SUP
      CALL PSYC(Z,4)
      RH2SUP=Z(3)
      HA2SUP=HA1-QSUP/MFASUP
C
C     AN ESTIMATE OF AN AVERAGE WALL TEMP IN SUPERHEATED
C     REGION IS MADE.
C-------------------------------------------------------------
      TAVSUP=(TA1+TA2SUP)/2
      TWSUP=TAVSUP-QSUP*RESASF
C
   65 T2EST=AFRCNT*TA2+(1-AFRCNT)*TA2SUP
      QTOT=QSUP+Q
      QSEN=QTOT-QLAT
      SHF=QSEN/QTOT
      Q2PH=Q
      WA2MIX=(MFA2PH*WA2+MFASUP*WA2SUP)/MFA
      HA2MIX=(MFA2PH*HA2+MFASUP*HA2SUP)/MFA
      CALL PROP1(HA2MIX,WA2MIX,T2EST,Z)
      TA2MIX=Z(1)
      RH2MIX=Z(3)
      TWMIX=AFRCNT*TW+(1.0-AFRCNT)*TWSUP
      TSMIX=AFRCNT*TFR+(1.0-AFRCNT)*TWSUP
      CALL PSYC(Z,3)
      SVA2=Z(9)
      Z(1)=TWSUP
      Z(3)=1.0
      CALL PSYC(Z,3)
      WSSUP=Z(4)
      WSMIX=(MFA2PH*WS2PH+MFASUP*WSSUP)/MFA
      WINMIX=WA1
   70 CONTINUE
C
      IF (X2 .LE. 0.9999) THEN
         TR2=TR1
         DTSH=0
      END IF
C
      HE2=HR1+QTOT/(MFR*CKTS)
      HRLVG=HRLVG+HE2
      QESEN=QESEN+QSEN
      QEVAP=QEVAP+QTOT
      QAIR=QAIR+MFA*(HA1-HA2MIX)
```

```
      TA1=TA2MIX
      RH1=RH2MIX
      TMEAN=TMEAN+TAV
      WMEAN=WMEAN+WAV
   75 CONTINUE
      TA1=TA10
      RH1=RH10
      SHF=QESEN/QEVAP
      HRLVG=HRLVG/NCKTS
      TMEAN=TMEAN/NCKTS
      WMEAN=WMEAN/NCKTS
      HR3=HR1+QEVAP/PPHR
      IF(HR3.LT.HG) THEN
          EDTSH3=0
          EX3=(HR3-HF)/HFG
      ELSE
          CALL TVAP(0,PR1,HR3,TR1,TR3,V3,S3)
          EDTSH3=TR3-TR1
          EX3=1
      ENDIF
C
C     DETERMINE THE APPARATUS DEW POINT, AND
C     THE CORRESPONDING ENTHALPY.
C-----------------------------------------
      CALL ADPSUB(TA10,WA10,TA2MIX,WA2MIX,ADPMIX,AHMIX,
     #ASHMIX,ADSMIX,ADRHMIX,TR1)
      ETEMP1=(TA10-TA2MIX)/(TA10-TR1)
      EHOV1=(HA10-HA2MIX)/(HA10-AHMIX)
      CCOV1=(ADPMIX-TR1)/(HA10-AHMIX)
C
C     PRESSURE DROP ACROSS EVAPORATOR
C-------------------------------------
      TAV=TMEAN
      WAV=WMEAN
      KA=-8.487E-08*TAV*TAV+3.1923E-05*TAV+1.3005E-02
      PRA=1.047E-06*TAV*TAV-2.3187E-04*TAV+0.72307
      VISCA=-1.962E-07*TAV*TAV+8.2371E-05*TAV+3.9207E-02
      CPA=CPAD+0.45*WAV
      Z(1)=TAV
      Z(4)=WAV
      CALL PSYC(Z,4)
      DENSDA=1.0/Z(9)
      CALL PDROP(DO,PI,Y,FPI,HC,DC,VFACEC,WDTH,HT,
     &GFLUXA,VISCA,DENSDA,S,DPAIR,ROWDT,ROWH)
      DP=DPAIR
C
      RETURN
      END
```

APPENDIX III

SAMPLE COMPUTER OUTPUT FILE

O1.DAT

```
  PROGRAM VERSION: ACSYSE2-1993 MAY 07
    INPUT FILE NAME:      AECFHFM.DAT
    OUTPUT FILE 2 NAME:   O1.DAT
    OUTPUT FILE 3 NAME:   O2.DAT
    OUTPUT FILE 4 NAME:   O3.DAT
           ICALC
             1

   TSRC  DTSRC  RHSRC  DRHSRC   TSNK  NEVP  NCPR NTSRC NRHSRC
   68.0    4.0   .450    .050   88.0     5     5     1      1

COMPRESSOR
  DCFH0     DDCFH        CL     REFLO     VERMD       IVE
  430.0      85.0      .028     400.0     .7600         1

  EFFI0     DEFFI      QCO0      DQCO       EE0       DEE
  .5800     .0000     .6400     .0000     .7500     .5000

CONDENSER
   DTSC     CHTE0     CHTE1    CHTCAP      ITC0       ICD      PCD
   5.20  .600000  .000000    1250.0         0         1     170.

EVAPORATOR
   NREF      XSET      CPAD      HFGW      IMIX      ITE0
     12      .700      .240   1068.37         1        40

   WDTH        HT      DPTH      CKTS      ROWH      ROWD
 1.5000    1.5000     .2887      4.00     18.00      4.00

     DO        DI         Y      KFIN       FPI
 .03125    .02542    .00050    128.00     10.00

  HCONT    HFOULI      CFM0      DCFM
  2000. 9999999.     600.0     200.0

HEAT EXCHANGER
 HTEI1D    HTEI2D    HTEI1W
   .200      .350      .250

THROTTLING DEVICE
    DTSH
 28.000

DATA FOR SYSTEM PERFORMANCE COEFFICIENT
  CFANW    EFANW0
     0.       70.
```

CFM	DCFH	TSRC	RHSRC	VFACE	K	
1000.0	600.0	68.0	.45	444.4	4	

QEVP	QCOND	POWER	QI1SS	QI1LS	QI2SS	QI2LS
22382.	30883.	8501.	691.	691.	1245.	1245.

PPHR	DCFH	CFH CI	EPOWER	CMPWR	EFPWR	CFPWR
419.5	600.0	427.9	11795.4	10689.3	1106.1	.0

XCHTE	VERX	XEAS	XCC	COPC	EHOV1	CCOV1
.6000	.760	.38032	3.77602	1.8975	.72071	1.70187

QEVAP	QSEN	QLAT	SHF	QCD	CHTCAP	
22375.	18654.	2615.	.8831	30883.	1664.	

EDTSH3	EX3	PPHDA
17.2	1.000	4463.4

T11	T8		TCLD	TSRC
113.7	225.0		49.8	68.0

TSNK	THOT		TE	T3
88.0	106.6		30.9	48.2

TA1	RH1	WA1	HA1	SVA1
68.00	.450	.006208	19.6236	13.0718

TA2	RH2	WA2	HA2	SVA2
49.85	.790	.005974	18.4331	12.9688

ADP	ADRH	ASH	AH	ADS
42.73	1.000	.005775	16.4935	12.7837

XHTEI1	XHTEI2
.200	.350

EFFI	QCO	EE	XQCO
.580	.640	.795	.640

PT	P	T	TS	H	X	V	T - TS
1	43.9	30.9	30.9	29.837	.223	.2109	.0
3	43.9	48.2	30.9	83.188	1.000	.9477	17.3
4	43.9	58.9	30.9	84.835	1.000	.9739	28.0
5	43.9	78.1	30.9	87.804	1.000	1.0199	47.2
6	43.9	160.6	30.9	100.772	1.000	1.2079	129.7
8	170.0	225.0	118.9	108.067	1.000	.3185	106.1
11	170.0	113.7	118.9	34.453	.000	.0130	-5.2
12	158.8	113.7	113.7	34.453	.000	.0130	.0
13	158.8	101.6	113.7	31.485	.000	.0127	-12.1
14	158.8	94.7	113.7	29.837	.000	.0126	-19.0

PT	P	T	TS	H	X	V	T - TS
2	43.9	30.9	30.9	80.513	1.000	.9042	.0
7	170.0	177.6	118.9	99.556	1.000	.2849	58.6
9	170.0	118.9	118.9	88.532	1.000	.2367	.0
10	170.0	118.9	118.9	35.747	.000	.0131	.0

O2.DAT

```
\ ICALC      1
\  QTOTX      SHFX     QSENX     QLATX      CFHX      CFMX      COPX
  16117.      .859   13612.7    2265.6     430.0     600.0    1.6140
  16828.      .921   14925.0    1337.0     430.0     800.0    1.6908
  17423.      .969   15778.1     538.9     430.0    1000.0    1.6928
  17925.      .993   15880.6     133.3     430.0    1200.0    1.6078
  18362.     1.000   15326.8        .0     430.0    1400.0    1.4984
  18314.      .822   14806.6    3268.4     515.0     600.0    1.7049
  19270.      .874   16282.7    2421.3     515.0     800.0    1.7399
  19980.      .925   17369.7    1504.0     515.0    1000.0    1.8027
  20504.      .964   17853.5     739.2     515.0    1200.0    1.7044
  20995.      .987   17685.8     274.3     515.0    1400.0    1.6083
  20300.      .796   15913.5    4147.6     600.0     600.0    1.7667
  21504.      .840   17499.2    3439.0     600.0     800.0    1.8204
  22375.      .883   18653.6    2614.9     600.0    1000.0    1.8975
  23039.      .926   19432.0    1695.4     600.0    1200.0    1.8227
  23554.      .957   19516.4    1002.7     600.0    1400.0    1.7177
  22108.      .778   16955.8    4913.4     685.0     600.0    1.8065
  23559.      .814   18610.2    4382.3     685.0     800.0    1.8907
  24593.      .851   19833.3    3653.4     685.0    1000.0    1.9783
  25400.      .889   20668.3    2820.3     685.0    1200.0    1.9103
  26014.      .923   20972.5    2006.1     685.0    1400.0    1.8165
  23774.      .765   17941.1    5594.1     770.0     600.0    1.8318
  25453.      .795   19676.1    5210.7     770.0     800.0    1.9491
  26681.      .827   20967.3    4608.1     770.0    1000.0    1.9999
  27614.      .861   21857.5    3845.1     770.0    1200.0    1.9931
  28349.      .892   22265.0    3049.4     770.0    1400.0    1.9066
  16117.      .859   13612.7    2265.6     430.0     600.0    1.6140
  18314.      .822   14806.6    3268.4     515.0     600.0    1.7049
  20300.      .796   15913.5    4147.6     600.0     600.0    1.7667
  22108.      .778   16955.8    4913.4     685.0     600.0    1.8065
  23774.      .765   17941.1    5594.1     770.0     600.0    1.8318
  16828.      .921   14925.0    1337.0     430.0     800.0    1.6908
  19270.      .874   16282.7    2421.3     515.0     800.0    1.7399
  21504.      .840   17499.2    3439.0     600.0     800.0    1.8204
  23559.      .814   18610.2    4382.3     685.0     800.0    1.8907
  25453.      .795   19676.1    5210.7     770.0     800.0    1.9491
  17423.      .969   15778.1     538.9     430.0    1000.0    1.6928
  19980.      .925   17369.7    1504.0     515.0    1000.0    1.8027
  22375.      .883   18653.6    2614.9     600.0    1000.0    1.8975
  24593.      .851   19833.3    3653.4     685.0    1000.0    1.9783
  26681.      .827   20967.3    4608.1     770.0    1000.0    1.9999
  17925.      .993   15880.6     133.3     430.0    1200.0    1.6078
  20504.      .964   17853.5     739.2     515.0    1200.0    1.7044
  23039.      .926   19432.0    1695.4     600.0    1200.0    1.8227
  25400.      .889   20668.3    2820.3     685.0    1200.0    1.9103
  27614.      .861   21857.5    3845.1     770.0    1200.0    1.9931
  18362.     1.000   15326.8        .0     430.0    1400.0    1.4984
  20995.      .987   17685.8     274.3     515.0    1400.0    1.6083
  23554.      .957   19516.4    1002.7     600.0    1400.0    1.7177
  26014.      .923   20972.5    2006.1     685.0    1400.0    1.8165
  28349.      .892   22265.0    3049.4     770.0    1400.0    1.9066
```

O3.DAT

```
\ICALC      1
\VFACE   PPHR    EH     CC    X1     TE    TA1 RH1  SHF DTSH    X3    CFM  CFH
    25   13
 266.7  301.9  .806  1.415  .223  31.13  68.0 .45  .859 17.4  1.00   600. 430.
 355.6  313.9  .741  1.704  .219  33.13  68.0 .45  .921 17.8  1.00   800. 430.
 444.4  326.3  .686  1.793  .216  35.13  68.0 .45  .969 18.2  1.00  1000. 430.
 533.3  335.1  .615  1.709  .213  36.52  68.0 .45  .993 18.4  1.00  1200. 430.
 622.2  341.9  .548  1.566  .211  37.58  68.0 .45  .999 18.7  1.00  1400. 430.
 266.7  343.2  .815  1.340  .228  28.47  68.0 .45  .822 16.8  1.00   600. 515.
 355.6  360.3  .755  1.604  .223  30.94  68.0 .45  .874 17.3  1.00   800. 515.
 444.4  374.6  .712  1.778  .220  32.94  68.0 .45  .925 17.7  1.00  1000. 515.
 533.3  383.3  .663  1.902  .218  34.13  68.0 .45  .964 18.0  1.00  1200. 515.
 622.2  392.0  .614  1.908  .215  35.30  68.0 .45  .987 18.2  1.00  1400. 515.
 266.7  381.9  .822  1.266  .232  26.18  68.0 .45  .796 16.4  1.00   600. 600.
 355.6  403.3  .764  1.512  .227  28.92  68.0 .45  .840 16.9  1.00   800. 600.
 444.4  419.5  .721  1.702  .223  30.92  68.0 .45  .883 17.3  1.00  1000. 600.
 533.3  432.6  .688  1.873  .221  32.49  68.0 .45  .926 17.6  1.00  1200. 600.
 622.2  440.9  .647  1.989  .219  33.47  68.0 .45  .957 17.8  1.00  1400. 600.
 266.7  417.6  .827  1.211  .236  24.05  68.0 .45  .778 16.0  1.00   600. 685.
 355.6  443.2  .764  1.412  .230  27.00  68.0 .45  .814 16.5  1.00   800. 685.
 444.4  461.2  .721  1.609  .227  29.00  68.0 .45  .851 16.9  1.00  1000. 685.
 533.3  477.1  .694  1.795  .224  30.72  68.0 .45  .889 17.3  1.00  1200. 685.
 622.2  487.6  .659  1.934  .222  31.83  68.0 .45  .923 17.5  1.00  1400. 685.
 266.7  452.1  .836  1.169  .239  22.21  68.0 .45  .765 15.6  1.00   600. 770.
 355.6  480.0  .769  1.362  .234  25.15  68.0 .45  .795 16.2  1.00   800. 770.
 444.4  501.8  .725  1.537  .230  27.36  68.0 .45  .827 16.6  1.00  1000. 770.
 533.3  519.6  .698  1.724  .227  29.11  68.0 .45  .861 17.0  1.00  1200. 770.
 622.2  532.1  .668  1.879  .224  30.32  68.0 .45  .892 17.2  1.00  1400. 770.
```